5-1998

Quaternary Amino Acid Geochronology of the Lahontan Basin, Nevada, and the Chewaucan Basin, Oregon

Jeffrey Bigelow
Utah State University

Recommended Citation

Bigelow, Jeffrey, "Quaternary Amino Acid Geochronology of the Lahontan Basin, Nevada, and the Chewaucan Basin, Oregon" (1998). *All Graduate Theses and Dissertations*. 3587.
https://digitalcommons.usu.edu/etd/3587

QUATERNARY AMINO ACID GEOCHRONOLGY OF THE LAHONTAN BASIN, NEVADA, AND THE CHEWAUCAN BASIN, OREGON

by

Jeffrey Bigelow

A thesis submitted in partial fulfillment
of the requirements for the degree

of

MASTER OF SCIENCE

in

Geology

Approved:

UTAH STATE UNIVERSITY
Logan, Utah

1998

ABSTRACT

Quaternary Amino Acid Geochronology of the Lahontan Basin, Nevada,
and the Chewaucan Basin, Oregon

by

Jeffrey Bigelow, Master of Science
Utah State University, 1998

Major Professor: Dr. Darrell S. Kaufman
Department: Geology

Amino acid geochronology based on fossil molluscs provides a useful approach to determining the Quaternary history of Great Basin lakes. The Lahontan basin, Nevada, and the Chewaucan basin, Oregon, in the northwest corner of the Great Basin, both contained lakes during the Quaternary. The aim of this study is to improve the Quaternary geochronology in these two basins by measuring time-dependent changes in amino acids preserved in fossil molluscan shells. The abundance of D-alloisoleucine relative to L-isoleucine (A/I) characterizes the extent of racemization, which increases with age and forms the basis of relative and correlated ages. An age-calibration curve for *Vorticifex* was developed using A/I ratios in shells from layers with radiocarbon-dated shells and with one thermoluminescence date in the Chewaucan basin. The A/I ratios from non-dated deposits were assigned ages from this calibration curve.

The A/I ratios in 77 samples (~350 shells) of mainly *Vorticifex* were analyzed to improve the lake chronology in the Lahontan and Chewaucan basins. From the stratigraphic position, A/I ratios in the shells, and previously published radiometric ages, at least five and possibly six lake cycles were inferred in the Lahontan basin for the Quaternary period. Shells with highest A/I ratios (~0.8) might correlate with the Rye Patch

Alloformation, named for deep-lake sediments deposited in the Lahontan basin ~630 ka. The next younger lake deposits are ascribed to the Eetza Alloformation. On the basis of the amino acid data, two and possibly three distinct lake expansions took place during the Eetza lacustrine episode, which lasted from ~385 to 145 ka. Deposits of the Sehoo Alloformation (~35 to 12 ka) can be differentiated from older deposits on the basis of A/I ratios in mollusc shells. Finally, a few shells with low A/I ratios near Pyramid Lake may indicate a minor lake expansion during the Holocene. Only two lake cycles were inferred from the amino acid data in the Chewaucan basin for the Quaternary period. Shells with the highest ratios correlated with the Eetza Alloformation and the shells with lowest ratios correlate with the Sehoo Alloformation. The amino acid data suggest that Lake Lahontan and Lake Bonneville experienced similar lake-level histories during the past ~660 ka. The Sehoo Alloformation in the Lahontan basin broadly correlates with Bonneville Alloformation in the Bonneville basin based on A/I ratios and radiocarbon dates. The late and early aminozones within the Eetza Alloformation might correlate, respectively, with the Little Valley and Pokes Point Alloformations in the Bonneville basin.

(144 pages)

ACKNOWLEDGMENTS

I thank all those who have provided me with assistance in completing this task. Special thanks goes to my parents for instilling the ambition and drive to finish this project. Your encouragement, love, and support were invaluable when things were tough.

I received guidance from Kurt Cupp, Peter Wigand, Martha Hemphill, Larry Benson, Rich Hum, Roger Morrison, Bill McCoy, Jerry Miller and Darrell Kaufman. I also benefitted from lab support by Rich Hum, Jordan Bright, Bill Manley, and Darrell Kaufman. This project would not have been possible without assistance from: Peter Hovingh for collecting modern shells used in this study; Bob Oaks and Janis Boettinger for their suggestions and guidance; and my friends and officemates for their advice and support.

Finally, I would like to thank my advisor, Darrell Kaufman, for his support, suggestions, and drive, which made this project possible. This project was funded by a grant from Utah State University, obtained by Darrell Kaufman.

Jeffrey Bigelow

CONTENTS

LIST OF TABLES

LIST OF FIGURES

CHAPTER 1

INTRODUCTION

SCOPE AND OBJECTIVES

During the Quaternary period (roughly the last 2 million years), large freshwater lakes filled many hydrographic basins within the Great Basin (Figure 1). Many researchers have recognized the evidence for expanded lakes in the Great Basin during the Quaternary and have attempted to determine the ages of these lakes and the types of climate changes that caused them to expand and contract. Although the history of the last deep-lake cycle within the major basins is rather well defined, little is known about the earlier lake cycles. The aim of this study is to improve the Quaternary geochronology in two basins in the northwest corner of the Great Basin by measuring time-dependent changes in amino acids preserved in fossil molluscan shells.

Amino acid geochronology based on fossil molluscs provides a useful approach to determining the Quaternary history of Great Basin lakes. The abundance of D-alloisoleucine relative to L-isoleucine (A/I) increases with age, and forms the basis of assessing relative and correlated ages. The A/I ratios can be used directly as relative-age indices, and, with suitable calibration, can provide reasonable estimates of absolute age. The history of Great Basin lakes older than the range of radiocarbon dating (ca. > 30 ka) can be addressed with amino acid geochronology where other age controls are not available. Previous studies of earlier lake levels have relied on U-Th ages of shells, K-Ar and Ar-Ar ages of tephra layers, and estimates of duration of soil development to estimate the chronology of older lake levels (e.g., Morrison, 1991). These estimates can be improved with amino acid geochronology. An accurate and firmly established lake-level chronology is pivotal to correlating between basins, to determine if the growth and ablation of the lakes were caused by regional or global climate change, and to assess leads and lags in the past climate system.

The specific objectives of this work are to:

1) Determine the chronology of lake-level changes older than the range of radiocarbon dating in the Lahontan and Chewaucan basins;

2) Determine A/I ratios from previously named stratigraphic units and then correlate unknown units to these known stratigraphic units by means of A/I ratios in fossil molluscs; and

3) Correlate A/I ratios in fossil molluscs from stratigraphic units in the Lahontan basin with previously determined A/I ratios in fossil molluscs from lake units in the Bonneville basin;

STUDY AREAS

The Great Basin is the largest section of the Basin and Range physiographic province (Fenneman, 1930). It includes most of Nevada and western Utah, with fringes extending into Oregon, Idaho, and California (Figure 1). The Great Basin drains inward with no modern outlet to any ocean. Its climate is chiefly semiarid to arid. Mountain ranges to the west, especially the Sierra Nevada, remove much of the moisture from the generally eastward-moving airmasses from the Pacific Ocean, producing a strong rain shadow in the western Great Basin. The Rocky Mountains to the east block moisture-laden air masses from the Gulf of Mexico. Precipitation is also strongly influenced by local orography (Morrison, 1991). Increased hydrologic balance in the past caused large lakes to form in the Great Basin.

The name Lake Lahontan refers to the most recent deep-lake cycle in the Lahontan basin of northwestern Nevada (Figure 2). Samples collected in this study were mostly from the northern subbasins of the Lahontan basin. Pluvial Lake Chewaucan was a four lobed body of water that occupied the confluent structural basins of modern Summer Lake, Upper Chewaucan Marsh, Lower Chewaucan Marsh, and Lake Abert in south central Oregon (Figure 3). Samples were collected in each of these subbasins, plus one site in Surprise Valley, in northeastern California between the Chewaucan and Lahontan lake basins (Figure 1).

PREVIOUS WORK

Lake Lahontan

During the late Pleistocene, Lake Lahontan was the second largest lake in the Great Basin (Morrison, 1991). During its highstand, Lake Lahontan covered a huge area (~22,000 km^2) of northwestern Nevada and adjacent northeastern California (Figure 2). The Lahontan basin consists of seven major subbasins and a number of minor subbasins separated by sills of varying altitude (Benson and Thompson, 1987). The major subbasins include the Carson Desert, Pyramid-Winnemuca Lake, Smoke Creek-Black Rock Deserts, Humboldt Valley, Walker Lake, Honey Lake, and Buena Vista valley.

Considerable research has been done in the Lahontan basin. Russell (1885) made the first comprehensive study of the stratigraphic record of Lake Lahontan. He identified two zones of clay and silt separated by alluvial and lacustrine gravel and sand. He inferred two deep-lake periods separated by a long interval of complete desiccation.

In the mid-1960's, deposits of Lake Lahontan were correlated with the Wisconsin glacial interval by Morrison (1965a) and Morrison and Frye (1965). The existing framework of Lahontan stratigraphy evolved from detailed stratigraphic mapping in Lake Lahontan's northern basins by Morrison and his co-workers. Only the Walker Lake terminal basin has a significantly different stratigraphic record and requires a partly separate stratigraphic classification (Morrison, 1991). This is because the Walker River, the only important inflow to the Walker Lake subbasin, changed course several times, with its terminus in either Walker Lake or Carson Desert (Morrison, 1991). Davis (1978, 1983) revised Morrison and Frye's stratigraphy and history of Lake Lahontan, based on tephrochronology at new and previously described sites. Morrison (1991) then revised the ages of several of his units with data from Davis's tephrochronologic studies and other chronologic information (Figure 4). The geologic history of Lake Lahontan, summarized most recently by Morrison (1991), includes four lake episodes that are represented by exposed lacustrine sediments. From oldest to youngest these are (1) a lowermost unnamed unit, (2) Rye Patch Alloformation, (3) Eetza Alloformation, and (4) Sehoo Alloformation.

Although the geochronology of the last lake cycle of Lake Lahontan has been thoroughly studied with radiocarbon dating, the timing of older lake-level changes is still poorly understood. The following overview of lake cycles draws from a summary by Morrison (1991), who has developed a crude chronology of these older lake units from correlated tephra deposits and U-Th dates on snail shells.

The oldest known exposed Lake Lahontan deposits are in the Walker River badlands from ~3 km south to 6 km north of Weber Dam (Figure 2), between 1280 and 1310 m in altitude. Here the Glass Mountain G tephra layer (1.0 Ma) lies near the middle of the upper unit. In the northern basins, four lake episodes are represented by exposed lacustrine sediments. The lowermost unnamed unit is poorly studied, and may be a deltaic deposit (Morrison, 1991). The Rye Patch Alloformation records a major lake episode with two principal lake cycles, represented by lower and upper members of this alloformation. It consists of lacustrine sediments and tephra (Morrison, 1991). Unnamed sediments below Rye Patch Dam and south of Nixon, Nevada, have received only perfunctory stratigraphic and sedimentologic study. These possible lacustrine (deltaic?) sediments have been tentatively correlated with the unnamed pre-Lovelock lacustrine unit (Figure 4). The only age control for this lake cycle is in the lower member, which contains the Rye Patch tephra layer (~630 ka).

The Eetza Alloformation represents the longest of the Lahontan basin's lake episodes and has its thickest deposits. The ~150 to 200 ka age for the Wadsworth tephra layer in the upper part of the Eetza Alloformation in the Pyramid Lake subbasin correlates this part with deep-ocean isotope stage 6. A few U-series dates on snail shells from deposits in the Carson Desert subbasin support this interpretation.

The Sehoo Alloformation records the Lahontan basin's last major lake episode. It is divided into lower, middle, and upper members on the basis of two major lake recessions (Figure 4). The lower member dates from ~35 to 18 ka, and records the strongest wave action of Sehoo time. The following recession reached its lowest level at ~17.5 ka. The middle member of the Sehoo Alloformation, from ~17 to 11.5 ka, records the highest Sehoo lake at 1332 m at ~13 ka. The last Sehoo lake cycle, recorded by the upper member of the Sehoo Alloformation, rose only to ~1216 m in the nonconnecting Carson Desert and Pyramid-Winnemuca lake subbasins. This minor lake cycle probably lasted until ~10 to ~8 ka.

All the lacustrine alloformations are separated by interlacustrine alloformations that represent long periods when the terminal basins were dry or held temporarily shallow lakes (Morrison, 1991). These interlacustrine alloformations usually consist of alluvium and eolian sediments with many geosols. The Lovelock Alloformation (Figure 4) represents a long interlacustrine episode when terminal basins were dry or held shallow lakes. It separates the lowermost unnamed unit from the Rye Patch Alloformation. Its upper part contains a tephra layer stratigraphically below the Brunhes-Matuyama geomagnetic boundary. Although compositionally similar to the Bishop Ash, this tephra must be older because it is paleomagnetically reversed. A thick, essentially non-lacustrine unit, the Pauite Alloformation, overlies the Rye Patch Alloformation. The ~510 ka Dibekulewe tephra layer is in the lower part of the Pauite Alloformation, and the ~435 Rockland tephra layer is in the upper part, indicating that the Pauite Alloformation correlates with deep-sea oxygen-isotope stages 15 through 13. The Wyemaha Alloformation and Churchill geosol represent a ~100 ka interlacustrine episode between the Eetza and Sehoo lake episodes (Figure 4). Inception of the Wyemaha Alloformation dates from the beginning of the last interglaciation, ~130 to 35 ka. Finally, during most of Holocene time, terminal basins, such as the Carson Desert, were dry or held shallow lakes. Middle Holocene (~8 to 3.5 ka) time is represented by the Turapah Alloformation, whereas the late Holocene (3.5 ka to present) is represented by the Fallon Alloformation.

Along with stratigraphic studies, detailed radiometric studies have attempted to determine the ages of Quaternary deposits in the Lahontan basin. Broecker and his co-workers (Broecker and Orr, 1958; Broecker and Walton, 1959; Broecker and Kaufman, 1965) were the first to attempt to date deposits of the Lahontan basin by coupling radiocarbon measurements with measurements of U-series isotopes of tufas, and shells of ostracodes and gastropods. Their results suggested that lake occupying the Lahontan basin was relatively high four times during the late Wisconsin, near 17, 14.5, 12, and 9.5 ka. Later work by Benson (1978, 1993), Benson and Thompson (1987), and Benson and others (1990) revised Broecker's geochronology of the lakes in the Lahontan basin. They compiled new and previously published radiocarbon ages and U-series ages from the Lahontan basin, improved sample-selection procedures to avoid uncertainty caused by the introduction of secondary carbon, and proposed a new and improved chronology of lake-level variations.

The lake-level history of the last rise and fall of Lake Lahontan has been studied in great detail by Benson and his co-workers (Figure 5). The rise of Lake Lahontan was gradual but not continuous, in part because of topographic constraints such as intrabasin spill (Benson and others, 1990). A moderate-size lake connected three western Lahontan subbasins from ~45 to 16.5 ka (Benson and Thompson, 1987). By 20 ka, lake level in the western Lahontan subbasins had risen to about 1265 m above sea level, where it remained for 3.5 ka (Benson and Thompson, 1987). By 16 ka, lake level in the western Lahontan subbasins had fallen to 1240 m. Radiocarbon ages of Lake Lahontan carbonates reported by Benson (1993) indicate that Lake Lahontan reached its highstand of 1330 m by 13.8 ka and then receded to 1310 m by 13.7 ka. In addition to this highstand, Lake Lahontan experienced large and abrupt rises at ~23.5 and 15.5 ka (Benson and others, 1995). The recession of Lake Lahontan that commenced ~13.5 ka was interrupted at ~11.5 ka by a relatively large rise in lake level that persisted for ~2 ka (Benson and others, 1992). During the Holocene, the Lahontan basin contained shallow lakes (Benson and Thompson, 1987).

McCoy (1981) applied aminostratigraphy to the deposits of Lakes Bonneville and Lahontan in an attempt to define the sequence and magnitude of Quaternary lake-level fluctuations. Although his emphasis was on the Bonneville basin, McCoy also collected and analyzed 15 gastropod samples from the Lahontan basin for his dissertation (McCoy, 1981). McCoy (1981) also analyzed amino acids in ostracodes and tufas from the Lahontan basin and dated several gastropods, ostracodes, tufa, marl, wood, and other material with radiocarbon. From their relative stratigraphic positions, amino acid compositions in carbonate fossils, radiometric ages, and tephrochronology, the deposits of at least five Quaternary lake episodes were recognized in the Lahontan basin, although only three of these were characterized by amino acid analyses of included gastropod shells. No stratigraphic proof of the major intra-Sehoo regression suggested by Morrison (1964) was found by McCoy (1981). However, at least three pre-Eetza lake cycles were recognized, rather than just two reported by Morrison (1964). McCoy (1981) also determined from amino acid geochronology and radiometric ages that Lakes Bonneville and Lahontan may have had similar histories and were responding to similar climatic trends.

Recent research by Reheis and Morrison (1997) provides evidence of old, very high lake levels in the Lahontan basin from the Walker Lake basin and to a lesser extent in the Black Rock-Smoke Creek Desert. Fine-grained beds in the Walker Lake basin locally contain tephra layers, such as the ~790 ka Bishop Ash, and the age of the units is further constrained by magnetostratigraphy and by identification of vertebrate fossils. Shoreline evidence from sites in the Smoke Creek Desert indicates high stands at elevations of about 1370 and 1400 m. The Walker Lake basin and other southern Nevada basins show abundant stratigraphic and geomorphic evidence of old pluvial lakes during the Pliocene to early middle Pleistocene that were much larger, and had significantly higher shorelines, than the late middle and late Pleistocene lakes. Reheis and Morrison (1997) suggested that the reasons for these older, higher lake levels may include: (1) increasing rain shadow through time due to the uplift of the Sierra Nevada; (2) changes in position of the jet stream; and (3) drainage captures that have changed the size of the Lahontan drainage basin.

Lake Chewaucan

The Chewaucan basin lies in the northwestern portion of the Great Basin in south-central Oregon (Figure 3). Lake Chewaucan was a four-lobed body of water that occupied about 800 km^2 in the confluent structural basins of modern Summer Lake, Upper Chewaucan Marsh, Lower Chewaucan Marsh, and Lake Abert (Allison, 1982). The Chewaucan basin is separated into two subbasins by a large alluvial fan at Paisley. The northern subbasin is the Summer Lake basin, and the southern subbasin consists of the Chewaucan Marshes and Lake Abert (Freidel, 1993). The water that accumulated in these basins rose sufficiently during the Pleistocene to join these detached lakes into one large lake (Allison, 1982). The Pleistocene water level reached a maximum elevation of 1378 m, so the maximum depth of water in Summer Lake basin, the lowest subbasin, was about 114 m (Allison, 1982).

Unlike the Lahontan basin, little research has been done on the succession of Quaternary lakes in the Chewaucan basin. Allison (1982) was the first to publish an extensive Quaternary geology of Lake Chewaucan. He determined a sequence of at least six distinct stages in the history of Lake Chewaucan and its successors, Winter Lake and ZX Lake. These are (1) a high level shown by shore features near Paisley; (2) a sustained stand at 1367 m marked by pronounced beach development; (3) an erosional stage that produced the Paisley flat at Paisley; (4) a stand at ~1330 m represented by a baymouth bar north of the Ana River; (5) an overflow stage when water southeast of Paisley Flat (ZX Lake) reached an elevation of about 1338 m and cut a channel across Paisley Flat, while Winter Lake, on the Summer Lake side of the divide, was near 1323 m; and (6) later independent stages in Winter Lake and ZX Lake. These six stages were not to be interpreted as separate cycles, because Allison (1982) could not find evidence of multiple lake cycles separated by periods of low-water levels. Also, the chronology of these lake-level fluctuations is poorly known.

An improved lake-level chronology of Lake Chewaucan was proposed by Freidel (1993). Using Allison's previous dates and her own, Freidel constructed a discontinuous lake-level chronology for the Chewaucan basin. The chronology was combined with two other basins just north of the Chewaucan basin (Fort Rock and Alkali) to form a composite radiocarbon lake-level chronology for the region of south-central Oregon (Figure 6). The combined chronology suggests that the lakes were high sometime before 34 ka and then dropped between ~27.4 and 23.2 ka, rose to almost half full, then dropped again between 21.7 and 20.9 ka. Beginning ~20.9 ka, the lakes rose to their high stands, and peaked sometime before 18 to 16.4 ka. The lakes began to regress before 16.4 ka.

Considerable work has been done on a thick section of lacustrine deposits exposed near the mouth of the Ana River (Figure 3) in the northern Summer Lake basin (Davis, 1985; Negrini and Davis, 1992; Negrini and others, 1994; Roberts and others, 1994). These sediments of Lake Chewaucan contain 54 tephra beds of Quaternary age, and record lake-level fluctuations that may reach back farther than 335 ka (Davis, 1985). The section's numerous tephra beds and fossiliferous sediment layers are important for correlating tephras with other dated paleolake sequences in the Great Basin (Davis, 1985; Negrini and Davis, 1992). Davis (1985) determined the major-element chemistry of tephra glasses from some of the younger tephra beds, and thereby correlated them with those from the Lahontan basin. Davis determined that the section at Ana River represents nearly continuous deposition from ~335 to 16 ka and that the long lacustrine record suggests that a larger lake in the Summer Lake basin persisted through the last interpluvial interval, which correlates with marine oxygen-isotope stage 5 (130 to 75 ka). Lake Chewaucan may have dried up at the end of the Pleistocene due to diversion of the Chewaucan River into Lake Abert. However, if the Chewaucan River flowed into Summer Lake during marine oxygen-isotope stage 5, then a permanent lake seems to have persisted there during that episode.

The Ana River section is also an important reference section for correlation of paleosecular variation of the earth's magnetic field with other dated paleolake sediment sequences in the Great Basin (Negrini and Davis, 1992; Negrini and others, 1994; Roberts and others, 1994). Negrini and Davis (1992) used paleomagnetic records to correlate sedimentary sequences from pluvial Lakes Chewaucan and Russell in the western Great Basin. This correlation is the basis of age control in the rather poorly dated sequence from Lake Chewaucan. The resulting chronology suggests a lack of sedimentation in Lake Chewaucan during the interval 27.4 to 23.2 ka, which is consistent with Freidel's (1993) composite hydrograph (Figure 6). The Lake Chewaucan lowstand is the same age as the lowstand accompanying the Wizard's Beach Recession, previously interpreted from the Lahontan basin (Benson and others, 1997). This suggests strong similarities in the responses to regional climate change by Lakes Chewaucan and Lahontan.

Surprise Valley

Surprise Valley basin is in northeastern California and northwestern Nevada, and lies near the westernmost edge of the Great Basin (Figure 1). Surprise Valley is about 80 km long and 20 km wide, and trends north-south (Ingraham and Taylor, 1989). It is bounded by the Warner Mountains in the west and the Hays Canyon Range in the east. The basin is hydrologically closed, and contains three shallow lakes. These playa lakes, Upper Alkali, Middle Alkali, and Lower Alkali, form terminal basins. However, during the Pleistocene, these lakes were much deeper, and coalesced to form Lake Surprise (Snyder and others, 1964). Davis (1978) suggested that the Lower Member of the Sehoo Alloformation in Lake Lahontan correlated with the deepest phase of Lake Surprise. The Trego Hot Springs tephra was discovered in the lake deposits by Davis (1978).

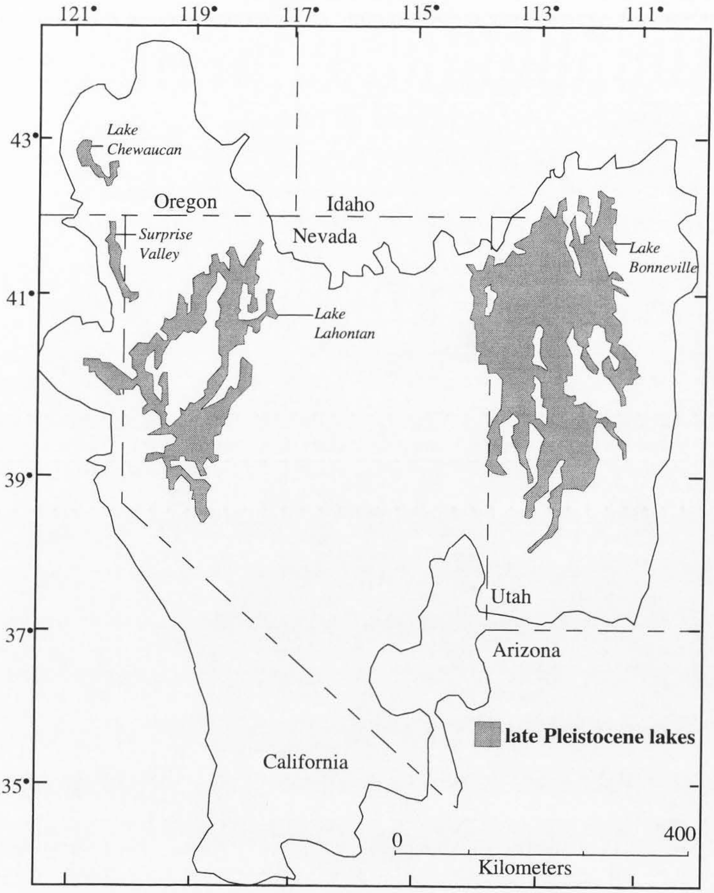

Figure 1. Map showing the physiographic extent of the Great Basin (solid line) and Pleistocene lakes discussed in this thesis (modified from Morrison, 1991).

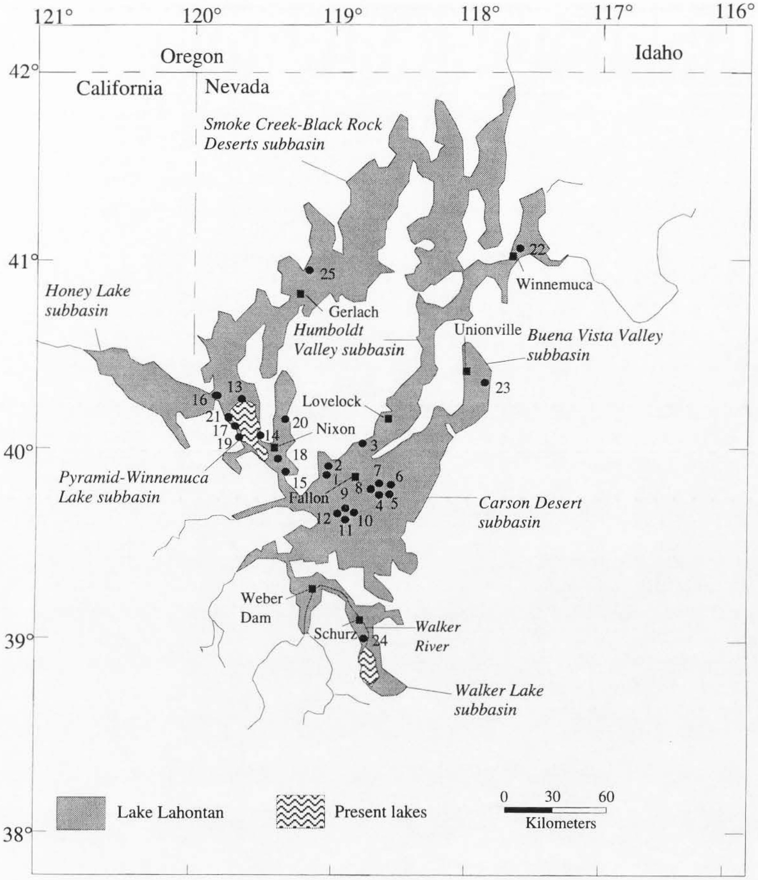

Figure 2. Lake Lahontan, major subbasins, and present lakes. Circles with numbers represent sample sites where shells were collected for this study (modified from Benson and Thompson, 1987).

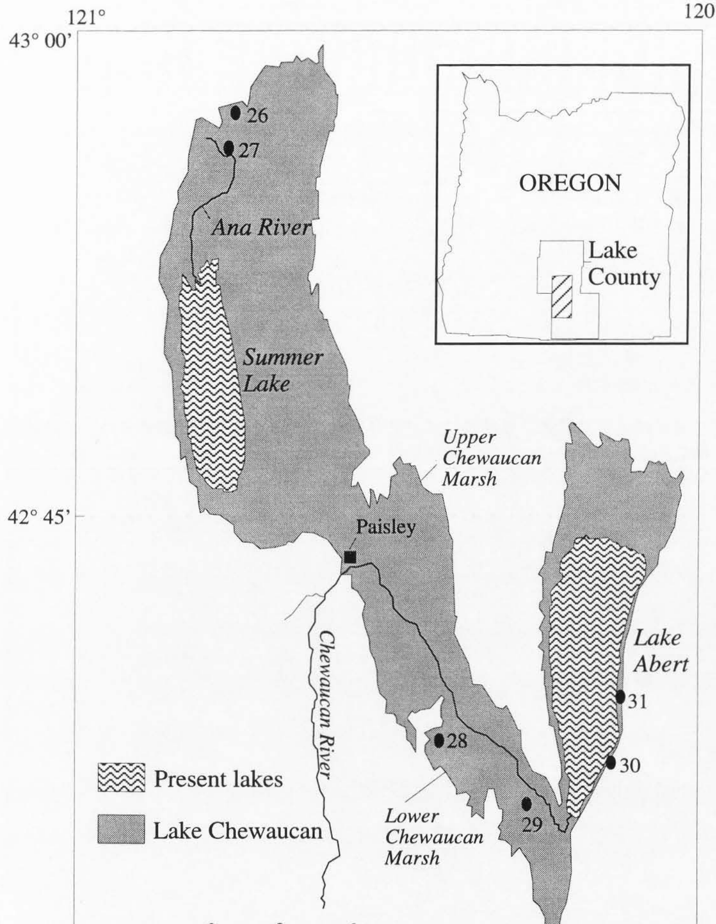

Figure 3. Lake Chewaucan, major subbasins, and present lakes. Circles with numbers represent sample sites where shells were collected for this study (modified from Allison, 1982).

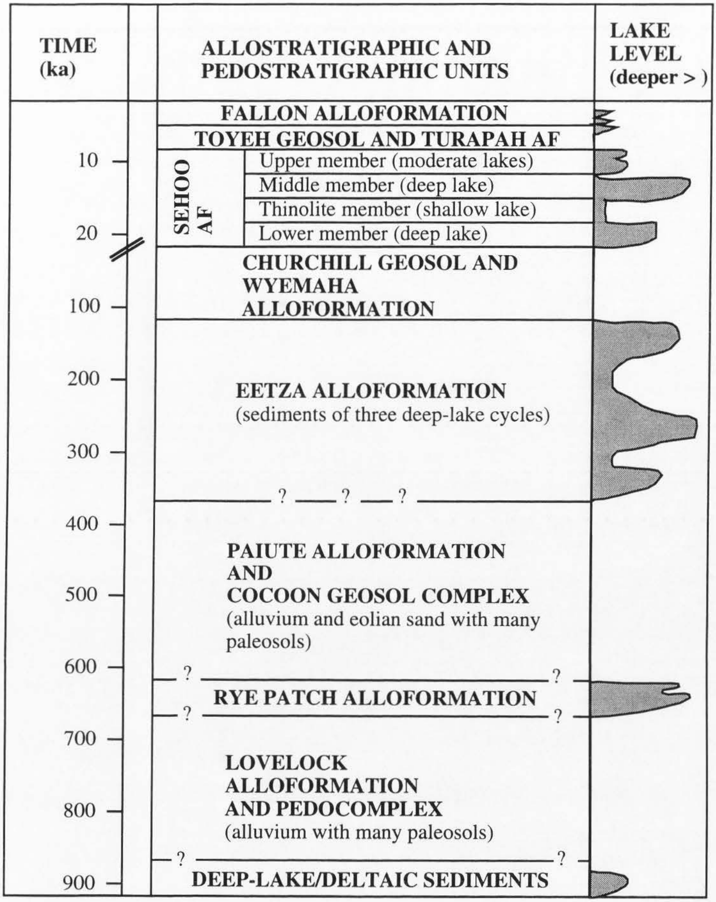

Figure 4. Principal exposed allostratigraphic and pedostratigraphic units in the Lahontan basin and inferred fluctuations in lake level (modified from Morrison, 1991).

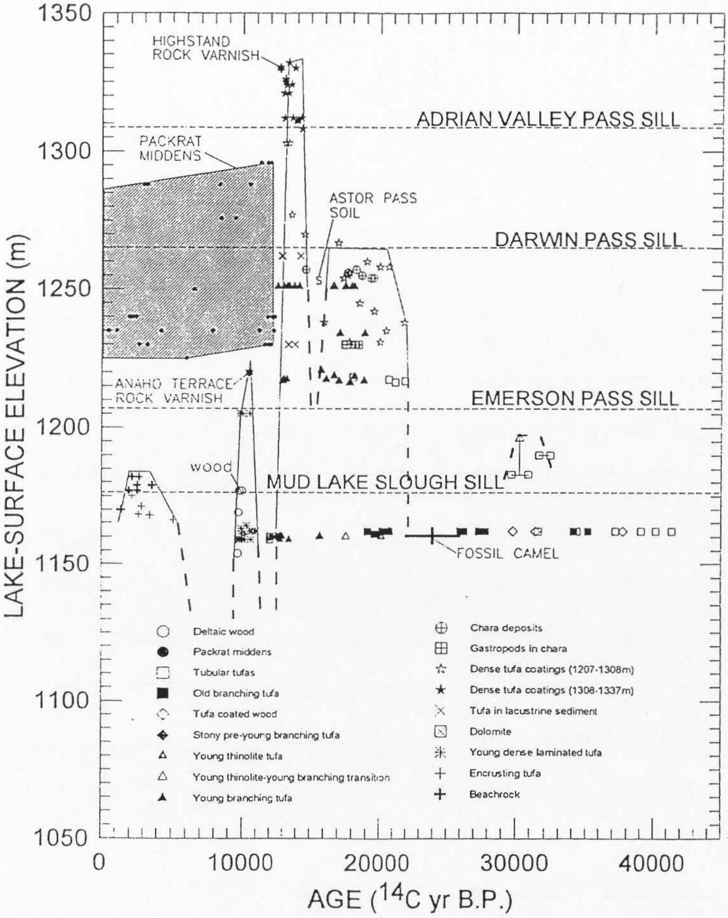

Figure 5. Lahontan lake-level record (Benson and others, 1995).

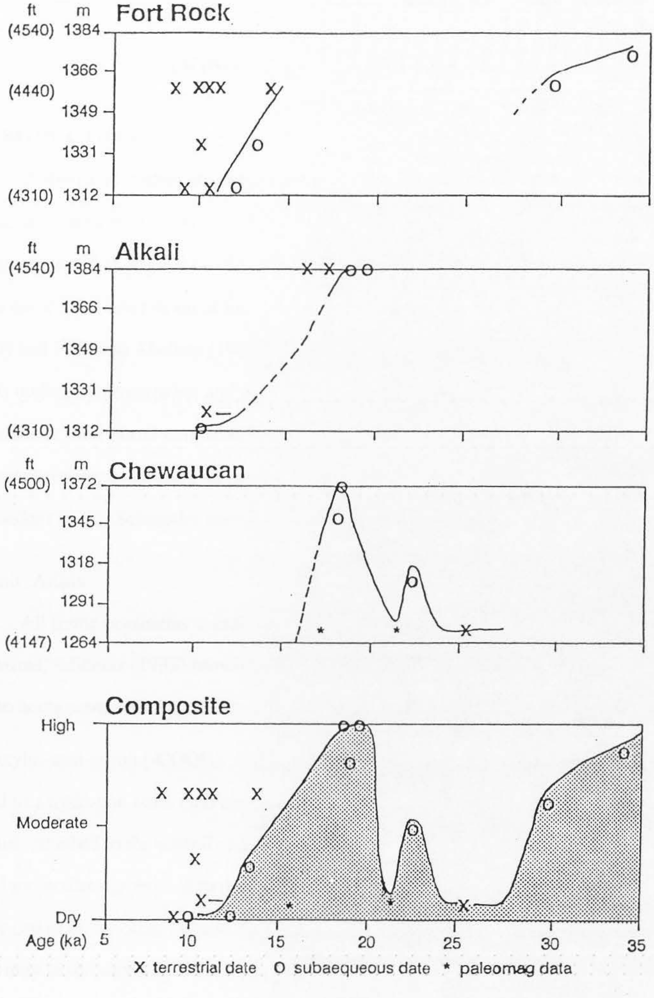

Figure 6. Lake-level chronologies of lakes Fort Rock, Alkali, and Chewaucan, and a composite of the three chronologies (Freidel, 1993).

CHAPTER 2

AMINO ACID GEOCHRONOLOGY

INTRODUCTION

Amino acid studies are one of the most important chronological tools in Quaternary research. Abelson's (1954) discovery of amino acids in fossil shells was the first demonstration that original biochemical constituents of organisms were preserved intact millions of years after death of the animal (Mitterer, 1993). Hare and Mitterer (1967, 1969) and Hare and Abelson (1968) subsequently discovered that amino acids in fossil shells undergo epimerization and racemization reactions that can be used to estimate the age of fossils or their burial temperature (Mitterer, 1993). Later research, with emphasis on the geochemistry of amino acid racemization reactions, has been summarized by Bada and Schroeder (1975), Schroeder and Bada (1976), and Bada (1982).

Amino Acids

All living organisms contain amino acids. There are 20 common amino acids in organisms. Mitterer (1993) provided an overview of the basic structure of amino acids. Amino acids contain in their molecular structure at least one amino group ($-NH_2$) and a carboxylic-acid group (-COOH). These are attached to a central carbon atom, which is also linked to a hydrogen atom (-H) and a hydrocarbon group (-R). If all the atoms or groups of atoms attached to the central carbon are different, then the molecule is said to be chiral. Chiral molecules can exist in two optically different forms (stereoisomers), each being the mirror image of the other (Figure 7). Enantiomers have the same physical properties, and differ only in the way they rotate plane-polarized light. The relative configuration of enantiomers is designated, by convention, D or L (dextro or levo). Virtually all amino acids in living organisms occur in the L configuration. The interconversion to the D configuration takes place by a process known as racemization. The abundance of D-forms relative to L-forms (D/L) of a specific amino acid defines the extent of racemization. Several amino acids contain two chiral atoms, which means they can exist as four stereoisomers: a set of mirror image isomers (enantiomers) and a set of non-mirror image isomers (diastereomers). The interconversion of only one of the two chiral atoms takes place by a process known as epimerization. Epimerization is analogous to racemization, and the two reactions are usually considered simply as "racemization" in the geochemical literature (Mitterer, 1993). An example of epimerization occurs in the diastereomers of isoleucine and alloisoleucine (Figure 7b). In isoleucine, only one of the two chiral atoms undergoes interconversion, thereby producing only one other isomer (D-alloisoleucine, a diastereomer) (Mitterer, 1993). Because the initial abundance of D-amino acids is negligible, the D/L ratio increases with time from 0.0 (living samples) to some equilibrium value (usually 1.0) in samples of "infinite" age (Wehmiller, 1993).

Protein Diagenesis

This discussion of protein diagenesis draws mostly from a summary by Mitterer (1993). Three common diagenetic processes affecting amino acids are attrition, hydrolysis, and racemization/epimerization (Figure 8). Attrition, which includes decomposition, leaching, and microbial metabolism, results in a net loss of amino acids after the organism dies. Although as much as 50% of the modern amino acid population is lost from some fossils during early diagenesis, the portion that remains is quite stable (Wehmiller, 1993). Decomposition or defunctionalization involves the loss of amino acid functional groups by decarboxylation, deamination, and other reactions. Initial products of amino acid defunctionalization are probably organic acids and amines (Hoering, 1980). In some cases, partial defunctionalization leads to other amino acids. Leaching is used here to include physical transport as well as diffusion of amino acids out of organic matter.

Penetration of water into the shells may cause leaching of original organic components and introduction of contaminants. Therefore, leaching causes a decrease in amino acid concentration, while contamination introduces additional compounds. Finally, microbial metabolism involves the consumption of proteins by microbes after the organism has died. The microbes selectively tend to consume L-amino acids, and probably concentrate on the exposed surfaces of shells (Sejrup and Haugen, 1994).

Hydrolysis breaks peptide bonds and converts the original protein initially to a mixture of large and small peptides and ultimately to free amino acids (Mitterer, 1993). It therefore transfers amino acids from an internal configuration to a terminal configuration and finally to a free amino acid. Because free amino acids are smaller and more easily leached than complex molecules, hydrolysis and subsequent leaching lead to preferential loss of free amino acids and a decrease in the concentration of amino acids in fossils through time (Muller, 1984). This also might result in a decrease in the D/L ratio of the shell because free amino acids have higher D/L ratios than bound amino acids.

Other controls on the rate of racemization include: the extent of hydrolysis, temperature, type of amino acid, and taxonomy. As previously mentioned, hydrolysis breaks peptide bond and converts the original protein initially to a mixture of large and small peptides and ultimately to free amino acids. While both internally bound amino acids and free amino acids racemize slowly, terminally bound amino acids racemize quickly (Mitterer, 1993). Therefore, the longer an amino acid remains as a terminal amino acid, the more likely it is to racemize, and the higher the D/L ratio will be. If hydrolysis occurs rapidly, then amino acids will remain at terminal positions for a relatively short length of time, and the resulting D/L ratios for free amino acids will be relatively low. If hydrolysis occurs slowly, then amino acids will remain at terminal positions for longer periods of time, and the resulting D/L ratios for free amino acids will be relatively high. Measuring the D/L ratios for total amino acids (free and bound) for the sample dampens the effect that hydrolysis has on the D/L ratio of the sample (Mitterer, 1993).

By far the most significant factor affecting the rate of racemization is temperature, specifically the integrated temperature of the sample since deposition, or the "effective diagenetic temperature" (EDT) (Miller and Hare, 1980). The racemization rate doubles for every 4°C increase in temperature (Miller and Brigham-Grette, 1989). The temperature dependence of racemization for a species buried since death may be put to advantage if the sample age is known independently. In such cases, the extent of racemization can indicate mean temperature of the sample since deposition, or the extent of a step-change in temperature where there are two samples of known age (e.g., McCoy 1981).

Another important control on racemization rate is the type of amino acid that is racemizing. Those most suitable for geochronological applications include valine, leucine, and isoleucine. Aspartic acid and proline have also been used (Miller and Brigham-Grette, 1989). Each amino acid has a characteristic racemization rate in a given environment (Miller and Brigham-Grette, 1989). While isoleucine racemizes rather slowly, aspartic acid racemizes relatively quickly.

Finally, the rate of racemization is dependent on the taxonomy of the organism. Subtle differences in D/L ratios occur between different mollusc genera. These differences are probably due to the original protein structure and differential preservation effects of the environment in which the fossil resides. The taxonomic effect relates to the way the amino acids are ordered in a protein (which is taxon-dependent). The rate of hydrolysis depends on which two amino acids form the peptide bond. If a certain amino acid in a certain taxon is preferentially linked to a strong bond, then its hydrolysis will be slow, and therefore its D/L ratio will be low. The observed differences in D/L values among different genera are referred to as intergeneric differences in apparent rates of racemization (Wehmiller, 1993).

Taxonomic-dependent variables include the reproducibility of D/L ratios within and between individuals of the same age.

Field Methods

My goal was to collect shells from classic sites of exposed multiple lake deposits and other sites that had some independent chronology from the Lahontan and Chewaucan basins. I also collected shells from sites that did not have any independent chronology. To find these sites, I relied primarily on previous work. I collected shells at 32 sites where either tephras have been previously identified and correlated, where shells have been previously dated by radiocarbon, or where important stratigraphic relationships were present. From these sites I collected 77 samples consisting of ~350 individual shells (~5 shells per sample).

Wherever possible, specimens of both molluscs and ostracodes for amino acid analysis were collected from each stratigraphic unit (ostracodes were not analyzed for this study). Wherever possible, samples were taken from greater than 1 to 2 m below the present surface. This was to minimize diurnal and annual temperature fluctuations that subsequently affected the samples. The most prevalent genus collected from the strata of Pleistocene Lake Lahontan and Lake Chewaucan deposits was *Vorticifex*. Other genera, including *Lymnaea*, *Physa*, *Psidium*, *Amnicola*, *Spherium*, and *Planorbella*, were also collected. These names are the conventional names used in the geologic literature of the Great Basin (e.g., Oviatt and others, 1992). Because the taxonomy of freshwater molluscs from the Great Basin has received little scientific attention in the past 60 years and is presently being revised, I use the older names for these genera.

Analytical Methods

To prepare shells for amino acid analysis, I used the standard procedure of the Amino Acid Geochronology Laboratory at Utah State University. Samples were first assigned a laboratory number (UAL). Each sample (UAL#) was composed of 1-5 subsamples, each comprising one and sometimes two shells of a single genus with a weight of > 5 mg. Distinguishing characteristics of each specimen were noted. For most shells, the inner whorl was broken off, and only the remaining outer shell was cleaned and used for analysis. This was done because the inner whorls frequently contained sediment and discoloration that were difficult to remove during the cleaning processes.

The first step in the cleaning procedure was to physically clean the shells with ultrasound. After the inner whorls of the shell were removed, each shell was sonicated in purified water 3 to 5 times for 15 to 30 seconds each, or until silt and clay was removed from the shell surface. The shell was rinsed in pure water between each sonication. The second step in the cleaning procedure was to chemically clean the shell. Most shells were cleaned with dilute hydrogen peroxide. However, some dirtier shells were also leached with dilute HCl.

Shells cleaned with hydrogen-peroxide were immersed in a 30% hydrogen peroxide solution and placed in a centrifuge for 1 hour. The shell was then rinsed 3 to 4 times in purified water. In the acid-leach method, the shell was submerged in purified water and 1 drop of 2M HCl was added for every 10 mg of shell. Once the reaction was completed (usually around 15 minutes) the shell was rinsed again 3 to 4 times in purified water. The cleaned shells were air dried, weighed to the nearest 0.1 mg, and transferred to a sterile glass vial. The shell was then dissolved by adding 7M HCl in the proportion of 0.2 ml per 10 mg of shell. After the shell was dissolved, each vial was flushed with N_2 and placed in the oven at 110°C for 22 hours. Following hydrolysis, the sample was dried in a desiccator, then rehydrated with acidified water and injected into the amino acid analyzer.

The separation and detection of amino acids was accomplished by high-pressure ion-exchange liquid chromatography (HPLC). The following overview of this analytical technique draws from a summary by Miller and Brigham-Grette (1989). HPLC is based on movement of a mobile phase through a stationary bed. Within this bed or column, amino acids undergo a continuous series of interactions with the stationary phase. These interactions exploit differences in physical and chemical properties of each amino acid. These differences affect the rate at which each species of amino acid migrates through the column. Each amino acid has a different residence time, which allows successful resolution of each amino acid. In ion-exchange HPLC, cation-exchange sites on the resin in the column form temporary bonds with the amino acids. Differences in polarity, pH, and ionic strength of the amino acids affect the retention time on the column. After the amino acids are separated, they are derivitized with an optically active reagent (OPA) and detected by fluorescence. This method separates diastereomers well, such as the D-alloisoleucine/L-isoleucine pair, but is not selective enough to separate enantiomers. D/L ratios were calculated from peak heights based on the electronically integrated signal.

Each subsample was analyzed at least two times, unless the standard deviation of the D/L values between runs was high [coefficient of variation ([C.V. = x/σ] > 5%). In this case, another injection was made until at least two D/L ratios clustered within acceptable limits, or the subsample was used up. D/L ratios and standard deviations are reported to the nearest 0.01, commensurate with the accuracy of the amino acid analyzer. To monitor the amount of drift in D/L measured by the amino acid analyzer, the Utah State University Amino Acid Laboratory runs interlaboratory comparative standards (ILC; Wehmiller, 1984) several times each month. The results show little or no systematic variation through time. D/L ratios represented in this thesis are the mean values of 3 to 5 subsamples that make up a sample. The standard deviations of the mean represents inter-shell variation within a sample. The possible cause of this variability is discussed later.

In this study, I evaluated the extent of epimerization of L-isoleucine in fossil shells. Therefore, instead of determining D/L ratios *per se*, I measured the ratio of D-alloisoleucine to L-isoleucine, designated as A/I.

HEATING EXPERIMENTS AND CALIBRATION

Wehmiller (1980) suggested that intergeneric variation in racemization rates results from genus-dependent rates of protein hydrolysis, which in turn influences the rate of racemization. The rate of hydrolysis depends on the taxon-dependent sequence of amino acids in a peptide of protein. *Lymnaea* was chosen because its rate of racemization has been well documented, so that more data are presently available for *Lymnaea* than for any other freshwater mollusc. *Vorticifex* was chosen because it is the most widely found mollusc in the lacustrine deposits of the Lahontan and Chewaucan basins. The difference in the rate of racemization of *Lymnaea* and *Vorticifex* must be known to compare A/I ratios in *Vorticifex* shells collected in the Lahontan basin with *Lymnaea* shells previously collected in the Bonneville basin. This difference can be evaluated where fossils of *Vorticifex* and *Lymnaea* are found in the same stratigraphic horizon or by laboratory-heating experiments in which modern shells of *Vorticifex* and *Lymnaea* are heated simultaneously.

For the laboratory-heating experiments, modern *Lymnaea* and *Vorticifex* were supplied by Peter Hovingh (University of Utah Veteran's Hospital, Salt Lake City). The preparation for laboratory-heating experiments was similar to that of fossil shells, but with some minor adjustments. The shells were first boiled for 5 minutes to remove the soft body inside the shell. The shells were then sonicated in the same manner as the fossil shells. After the shells were sonicated and dried, they were centrifuged twice in 30% hydrogen peroxide. First they were centrifuged for 1 hour, then rinsed and centrifuged for 2 hours.

Once the shells were cleaned, the two genera were separated into five groups, each consisting of about six shells per group. One group of *Vorticifex* shells and one group of *Lymnaea* shells were prepared following standard procedure. The remaining groups of shells were each placed in a glass ampule, covered with sterilized quartz sand, and moistened with purified water. The ampules were flame-sealed and placed in a temperature-stable oven for 5, 12, 23, and 37 days at 120°C. One group of *Vorticifex* shells and one group of *Lymnaea* shells were removed at each of these time steps. These time steps were chosen based on previous heating experiments and in an attempt to attain certain A/I ratios. Upon removal from the oven, laboratory shells were prepared for amino acid analysis following standard procedure.

Laboratory Sample Data

The laboratory-heating data for *Lymnaea* and *Vorticifex* (Table 1, A1) demonstrate that the rate of racemization under isothermal conditions at 120°C for these two genera is similar (Figures 9 and 10). Because racemization is a reversible, first-order reaction (L-amino acid ⇔ D-amino acid), its rate under isothermal conditions can be expressed by the relationship (Schroeder and Bada, 1976):

$$\text{Time} \approx \ln[(1+A/I)/(1-0.77*A/I)] \qquad (1)$$

This equation assumes that there is no loss or gain of reactants and that the equilibrium constant is 1.3. Graphs of $\ln[(1+A/I)/(1-0.77*A/I)]$ versus time at 120°C (Figure 9) show that first-order kinetics is followed for *Vorticifex* and *Lymnaea* up to an A/I of ~0.4.

I compared the forward rate constants (k = slope of regression line in Figure 9) for the different genera at 120°C to determine whether the racemization rates of these genera are significantly different. A *t* test (Zar, 1984) using a significance level of 0.10 α indicates that there is not enough evidence to accept the null hypothesis that the slopes of these two regression lines are different ($t_{cal} = 0.612$, df = 6, P = 0.561). Therefore, the racemization rates for *Vorticifex* and *Lymnaea* are indistinguishable for shells heated at 120°C.

This trend is also seen in the A/I data from the fossil snails (Figure 10). In two stratigraphic beds where *Lymnaea* and *Vorticifex* shells co-occurred, the A/I ratios overlapped at ± 1 SD. At West Sehoo Mountain, one unit yielded A/I ratios of 0.429 ± 0.022 (UAL-1937) for *Lymnaea* and 0.446 ± 0.049 (UAL-1938) for *Vorticifex.* A lower unit yielded A/I ratios of 0.480 ± 0.032 (UAL-2183) for *Lymnaea* and 0.460 ± 0.019 (UAL-2182) for *Vorticifex.* Therefore, the A/I ratios in fossils support the laboratory-heating experiments that the rates of racemization for *Vorticifex* and *Lymnaea* are indistinguishable.

Calculating Ages

The following overview of age estimates based on amino acid ratios draws from a summary by Bradley (1985). Three basic approaches are used in amino acid geochronology. While the uncalibrated and calibrated methods aim at producing an estimate of absolute age, relative dating simply uses A/I ratios as a stratigraphic tool. For this study I primarily use A/I ratios as a relative-age index to subdivide and correlate lake units. I use the calibrated method to assign an absolute age to several lake units that are too old for radiocarbon dating. The calibrated method uses rate constants derived empirically by the measurements of A/I ratios in fossils of known ages. Other samples can then be dated by interpolation, under the assumption that they have experienced essentially the same thermal history as the fossils used for calibration. Where samples from a limited geographical area are analyzed, this assumption is probably valid.

TABLE 1. A/I DATA FOR MOLLUSCS HEATED AT 120°C. TABLE A1 GIVES FURTHER SAMPLE INFORMATION

Time (days)	Genus	Lab# (UAL)	A/I	± 1 SD	N
0	*Lymnaea*	2067	0.008	0.001	4
5	*Lymnaea*	2068	0.094	0.005	6
12	*Lymnaea*	2069	0.187	0.017	5
23	*Lymnaea*	2070	0.280	0.012	5
37	*Lymnaea*	2071	0.453	0.022	4
0	*Vorticifex*	2062	0.008	0.001	7
5	*Vorticifex*	2063	0.083	0.015	5
12	*Vorticifex*	2064	0.165	0.005	4
23	*Vorticifex*	2065	0.283	0.007	4
37	*Vorticifex*	2066	0.406	0.034	5

* N = number of shells used to calculate mean A/I and standard deviation (SD)

(a) Enantiomers

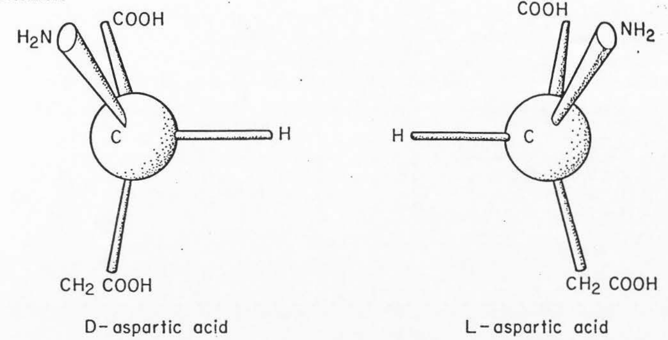

(b) Disastereomers

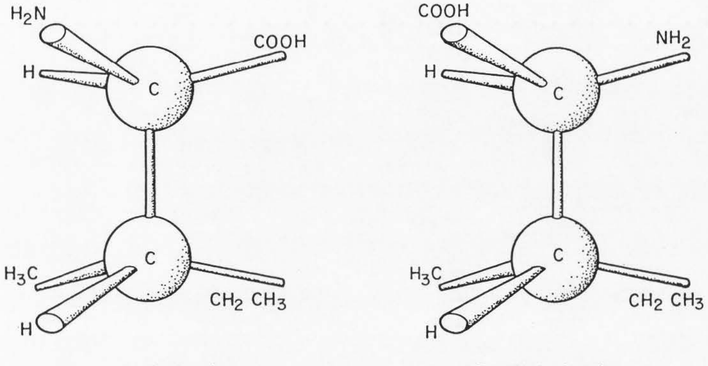

Figure 7. An example of (a) enantiomers (D-aspartic acid and L-aspartic acid); and (b) diastereomers (L-isoleucine and D-alloisoleucine) (Bradley, 1985).

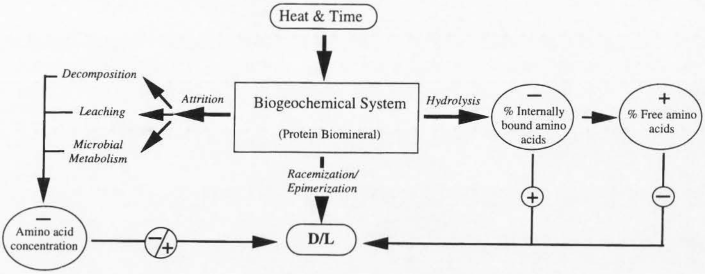

Figure 8. Simplified model of factors that affect the extent of racemization (D/L) in a fossil (Kaufman, unpublished).

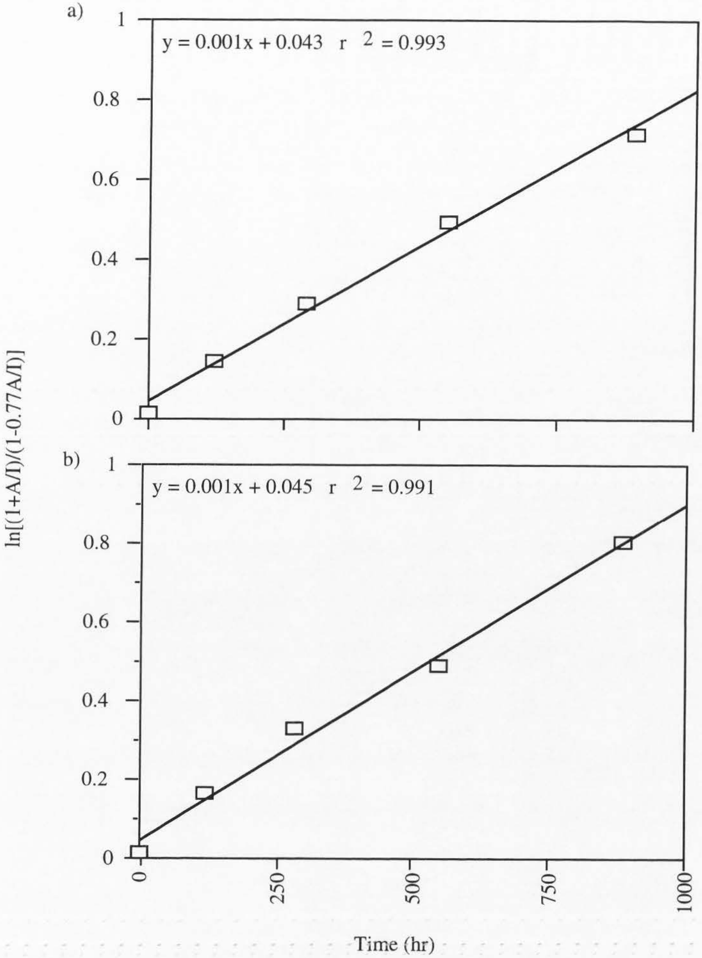

Figure 9. First-order reversible reaction for modern (a) *Vorticifex*; and (b) *Lymnaea* heated at 120°C. Data are listed in Table 1. Lines are linear regressions.

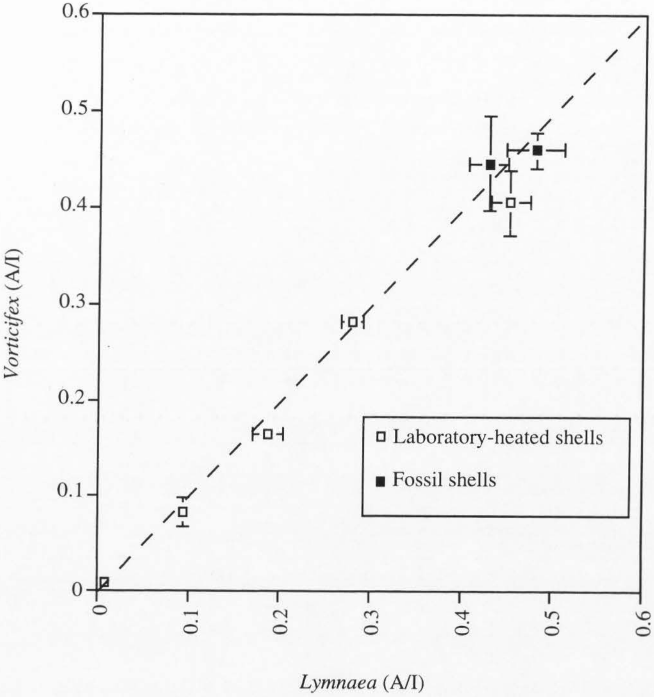

Figure 10. Relationship between A/I measured in *Lymnaea* and *Vorticifex* fossil shells and those heated simultaneously at 120°C (Table 1). Error bars are ± 1 SD and dashed line shows 1:1 relationship.

CHAPTER 3

AMINO ACID AND STRATIGRAPHIC DATA

INTRODUCTION

Stratigraphic columns were measured and described, and shells were collected at 25 sites in the Lahontan basin and seven sites in the Chewaucan and Surprise Valley basins. These sites were chosen because they: (1) contained shells, (2) exposed lake deposits including classic sites of Morrison and of others, (3) were recommended by previous workers, and (4) were accessible. Unless otherwise indicated, the sites are described for the first time in this thesis. Stratigraphic columns are included only for sites where at least two distinctly different stratigraphic units were exposed (Figures 11-35). Site numbers refer to locations in Figures 2 and 3.

I measured stratigraphic sections at each site. Altitudes were taken from estimates by previous workers or estimated from U.S.G.S. topographic maps of the base of the outcrop. At each site, sediments were described and bed thicknesses were measured to the nearest decimeter. Primary sedimentary features and structures were noted, and evidence of pre-Holocene soil development was recorded. Although tephra was not analyzed for this study, it was used for age control where the age of the tephra had been determined by previous studies. Radiocarbon dates on shells were also used for age control, including one new analysis obtained for this study (Table 2). Fossil gastropods were collected, and their genus, distribution, elevation, and condition were recorded. From these descriptions and amino acid analysis (Tables 3, 4, 5, and A2), I have attempted to correlate my units with those of Morrison (1991) while recognizing that his stratigraphic sequence may need to be revised.

I used grain size, rounding, sorting, fossils, pedogenic features, tephra, and other sedimentary features and structures to interpret the depositional environments of the outcrops. Lake deposits were distinguished from colluvium by rounder grains, better sorting, and the presence of bedding, fossils, tephra, or tufa. Sediments deposited in a beach environment consisted of well-rounded gravel in a sand matrix possibly containing gastropods. Sediments deposited in a nearshore environment consisted mainly of sand. Sediments deposited in a nearshore environment usually contained gastropods, and occasionally contained tephra and tufa. Sediment deposited in a deep lake consisted of silt or clay, was usually finely laminated, and contained few gastropods. Colluvium was distinguished from lake deposits by the presence of angular grains and the absence of bedding. Geosols were distinguished by the presence of pedogenic features. These features include blocky textures, root traces, carbonate accumulations, and oxidation features. The following sites are separated into basins and listed according to subbasins.

LAHONTAN BASIN

Sand Ramp (Site 1).
39°40'00'' N, 119°04'43'' W

I was directed to this site by Kurt Cupp (University of Nevada), who recently completed his dissertation in this area (Cupp, 1997). This outcrop (Figure 12) is a laterally continuous, ~15-m-high exposure at an elevation of 1265 m. It includes two units: (1) Coarse to very fine sand; horizontal beds 3 mm to 35 cm thick; poorly to well cemented, with lenses of abundant lacustrine gastropods (*Vorticifex*). The sand is well-cemented with lenses of coarse subangular to rounded gravel, 10 to 25 cm thick. Gastropods (*Vorticifex*) within this unit have been AMS radiocarbon dated at ~13 ka (Table 2). (2) Rounded gravel with some sand- and shell-rich beds 4 mm to 6 cm thick, dipping 20° to 40°, and moderately to well cemented. The sequence is interpreted as Sehoo beach gravel overlain by Sehoo nearshore sand and gravel.

Corral (Site 2).
39°36'16'' N, 119°05'56'' W

I was directed to this site by Kurt Cupp (University of Nevada). It is ~5 km south of Site 1 at an elevation of 1250 m. It consists entirely of coarse rounded gravel with sand- and shell-rich beds. Fossil gastropods (*Vorticifex*) were collected ~0.5 m below the surface, so they may have experienced excessive near-surface heating. The sediment is interpreted as Sehoo nearshore sand and gravel.

Jessup (Site 3).
39°55'12'' N, 118°49'48'' W

This site is ~2 km north of I-80 from the Jessup exit, and about 50 km southwest of Lovelock, Nevada. I was directed to this site by Ken Adams (University of Nevada), who recently completed his dissertation in this area (Adams, 1997). This outcrop (Figure 13) exposes a large, laterally continuous progradational barrier complex composed of multiple, closely spaced barrier ridges. The stratigraphy is described in detail by Adams (1997). I collected gastropods (*Vorticifex*) at two levels in the outcrop. One sample (UAL-1941) was collected at 1331 m in sand and gravel where shells had been dated by AMS radiocarbon at ~13.1 ka (Table 2). The other sample (UAL-1942) was collected at 1327 m in subrounded gravel and sand, where shells had been dated at ~13.3 ka (Table 2).

Wyemaha Valley (Site 4).
39°23'27'' N, 118°36'31'' W

This is one of five outcrops in the Wyemaha Valley gravel pit ~10 km east of Fallon, Nevada. Outcrops in this area have been studied by Broecker and Kaufman (1965), Morrison (1964), and McCoy (1981). However, the previously studied sites have been destroyed by gravel-pit operations. I found new outcrops that may correlate with previously measured outcrops. Site 4 is at an elevation of ~1244 m. It is composed of a ~1-m-high exposure in the gravel pit (Figure 14a). It includes three units: (1) Cobbly imbricated gravel and medium sand; (2) light brown sand containing fossil gastropods (*Vorticifex*) collected ~0.5 m below the surface; and (3) dark brown silt. The sequence is interpreted as late Eetza nearshore sand and silt overlain by colluvium.

West Wyemaha Valley (Site 5).
39°23'23'' N, 118°36'31'' W

This is another outcrop in the Wyemaha Valley gravel-pit area. It is ~100 m west of Site 4, at an elevation of ~1219 m (Figure 14b), and is a ~1-m-high gravel pit-exposure. This may be the same location as Broecker and Kaufman's (1965) shell sample L-773L, which gave a U-Th age of 110 ± 15 ka. It includes three units: (1) Light brown sand and cobbly angular gravel; (2) light brown laminated sand and pebbly rounded gravel, containing fossil gastropods (*Vorticifex*) that were collected ~1 m below the surface; and (3) light brown, well-sorted sand. The sequence is interpreted as late Eetza nearshore sand overlain by colluvium.

West Sehoo Mountain (Site 6).
39°25'00'' N, 118°36'17'' W

This outcrop (Figure 15) is ~1 km northeast of Site 5 in the Wyemaha Valley gravel pit at an elevation ~1283 m. It is a ~1-m-high outcrop, and is laterally continuous. It includes five units: (1) Angular basaltic cobbles in a white silt matrix; (2) white laminated silt exhibiting northward-dipping cross-strata containing fossil gastropods (*Vorticifex* and *Lymnaea*) (Figure 16); (3) subrounded basaltic boulders in a white silt matrix with *Vorticifex* shells; (4) interbedded white silt and brown sand containing shells of *Lymnaea*; and (5) subrounded boulders with very little matrix. The sequence is interpreted as early Eetza nearshore gravel overlain and underlain by colluvium.

Southwest Sehoo Mountain (Site 7).
39°24'40'' N, 118°36'29'' W

This outcrop (Figures 17 and 18) is ~500 m west of Site 6 at an elevation of ~1256 m. It is a ~5 m high and laterally discontinuous. This may be the same location as Broecker and Kaufman's (1965) shell sample L-773B, which gave two U-Th ages, 330 + 110/-50 ka and 400 +200/-70 ka. This may also be McCoy's (1981) site AAL-1740. It includes nine units: (1) Cobbly angular gravel in a light brown sand matrix; (2) cobbly, well-rounded gravel in a light brown sand matrix; (3) distinctly finer gravel in a grey sand matrix; (4) crossbedded black to grey coarse sand with gastropods (*Amnicola* and *Physa*); (5) medium-sand with a blocky structure and containing of burrows, carbonate accumulations, and other pedogenic features. It also contained gastropod shells that were too scarce and fragile to collect; (6) cross-laminated black to grey coarse sand containing lenses of light brown fine sand with fossil gastropods (*Physa*); (7) laminated, light brown medium sand; (8) light brown sand supporting well-rounded cobbles; and (9) dark brown coarse sand grading downward into sandy gravel, both containing fossil gastropods (*Physa*). The sequence is interpreted as pre-Eetza beach deposits overlain by possible Eetza beach deposits and colluvium.

South Sehoo Mountain (Site 8).
39°24'35'' N, 118°36'10'' W

This is the fifth of five outcrops in the Wyemaha Valley gravel-pit area. It is ~275 m east of Site 7 at an elevation of ~1219 m. This 1.6-m-high, laterally discontinuous outcrop consists entirely of sandy rounded gravel in a dark brown, medium-sand matrix containing fossil gastropods shells (*Vorticifex*) collected about 1 m below the surface. This section is interpreted as early Eetza nearshore deposits.

Lower Fallon Pit (Site 9).
39°15'31'' N, 118°46'44'' W

This is McCoy's (1981) site AAL-1742. This outcrop (Figure 19) is in an abandoned gravel pit about 25 km south of Fallon, Nevada, at an elevation of 1273 m and is a ~4-m-high laterally continuous exposure. It includes three units: (1) Rounded cobbles in light brown, medium sand; (2) laminated light brown, medium sand containing fossil gastropod shells (*Vorticifex*); and (3) subrounded cobbles in light brown sand. This sequence is interpreted as Sehoo beach gravel overlain by Sehoo nearshore deposits and colluvium.

Upper Fallon Pit 1 (Site 10).
39°15'20'' N, 118°47'04'' W

This site is McCoy's (1981) site AAL-1746. It is 20 m higher and about 100 m west of Site 9 and is a ~7-m-high laterally discontinuous outcrop (Figure 20) in an abandoned gravel pit at an elevation of 1293 m. It includes four units: (1) Subangular boulders grading downward to subangular cobbles; (2) sandy, subrounded cobbles; (3) sandy, subrounded cobbles containing a tufa mound with fossil gastropod shells (*Vorticifex*); and (4) laminated light brown sand with abundant fossil gastropod shells (*Vorticifex*). This sequence is interpreted as Sehoo nearshore deposits overlain by Sehoo beach deposits and colluvium.

Upper Fallon Pit 2 (Site 11).
39°15'15'' N, 118°47'10'' W

This laterally discontinuous outcrop is ~ 50 m east of Site 10 at an elevation of ~1303 m. It consists entirely of parallel laminated, light-brown medium sand with abundant fossil gastropod shells (*Vorticifex*) collected ~1 m below the surface. This section is interpreted as a Sehoo nearshore deposit.

Upper Fallon Pit 3 (Site 12).
39°15'10'' N, 118°46'44'' W

This laterally continuous outcrop (Figure 21) is ~20 m east of Site 11 at an elevation of ~1310 m. It is a ~9-m-high exposure in an active gravel pit. It includes four units: (1) Subrounded boulders interbedded with yellow sand; (2) subrounded pebbles in dark-brown sand containing sand lenses with fossil gastropod shells (*Vorticifex*) to the west; (3) tufa-coated cobbles in brown, coarse sand which pinches out to the west; and (4) cross-laminated, subrounded cobbles in fine sand containing fossil gastropod shells (*Vorticifex*). This sequence is interpreted as Sehoo nearshore deposits overlain by Sehoo beach deposits.

North Pyramid Lake (Site 13).
40°12'14'' N, 119°38'52'' W

This site consists of tufa carbonate coatings on basaltic boulders near the north shore of Pyramid Lake (Figure 22) at an elevation of ~1260 m. The fossil gastropod shells (*Vorticifex*) collected were cemented in the tufa coatings. This is interpreted as a Holocene beach deposit.

Pyramid Island (Site 14).
39°59'00'' N, 199°29'54'' W

This is Davis' (1978) site JOD 11. It lies about 500 m southeast of Pyramid Island on the east shore of Pyramid Lake. The Trego Hot Springs, Wono, Timber Lake, and Marble Bluff tephras are exposed in a wave-cut scarp interbedded with clay layers of the lower member of the Sehoo Alloformation at an elevation of 1158 m. No stratigraphic section was included for this outcrop because the gastropod shells (*Amnicola*) collected near the level of the present lake are believed to have been reworked, as evidenced by their low A/I ratios and the absence of shells farther back in the outcrop.

Railroad Cut (Site 15).
39°44'44'' N, 119°19'42'' W

This outcrop (Figures 23 and 24) is Morrison's Stop 5-3 in the 1965 INQUA Guidebook (Morrison, 1965c). This laterally continuous exposure is a railroad cut ~10 km south of Nixon, Nevada, at an elevation of 1265 m (Figure 24). It includes four units: (1) Dendritic member of the Sehoo Alloformation, which consists of brown, medium sand, sparse dendritic tufas at the base of the unit, and fossil gastropod shells (*Vorticifex*); (2) lower member of the Sehoo Alloformation, which consists of brown medium sand, gravel at the base of the unit, and fossil gastropod shells (*Vorticifex*); (3) Wyemaha Alloformation, which consists of highly oxidized sand and gravel with abundant roots, burrows, and other pedogenic features; and (4) Eetza Alloformation, which consists mostly of pebbles coated by tufa deposits and a few sand interbeds with fossil gastropod shells (*Vorticifex*). This sequence has already been interpreted by Morrison (1965c). My data and observations agree with his.

Astor Pass (Site 16).
40°12'00'' N, 119°48'21'' W

This may be site L-364CQ, L-772K, or L-772NA of Broecker and Kaufman (1965). Fossil gastropod shells (*Vorticifex*) collected at ~1225 m were eroding out of marl and tufa mounds in an outcrop ~ 5 km southwest of Pyramid Lake. These shells were radiocarbon dated by Broecker and Kaufman (1965) at ~16 to ~19 ka (Table 2). This is interpreted as Sehoo nearshore deposits.

Blanc Tetons (Site 17).
40°05'28'' N, 119°41'22'' W

This site is on the west shore of Pyramid Lake. Two tufa mounds at an elevation of 1169 m were described by Benson (1994), who directed me to this site (Figure 25a). I collected fossil gastropod shells (*Vorticifex*) from a poorly cemented carbonate sand layer at the bottom of the northern tufa mound (Figure 25b). This layer was radiocarbon dated at ~10 ka (Benson, 1994). This is interpreted as a Holocene beach deposited near the base of an older tufa mound.

Agency Bridge (Site 18).
39°49'05'' N, 119°21'06'' W

This is Davis's (1978) site JOD 44 locateed 2 km south of Nixon, Nevada. I examined a laterally continuous bulldozer exposure (Figure 26a) on the west side of the Truckee River at an elevation of 1207 m. It consists of four units: (1) Finely laminated silt and tufa containing the Trego Hot Springs tephra (5 mm thick) determined by Benson and others (1997) to be ~23 ka; (2) brown silt containing the Wono tephra, determined by Benson and others (1997) to be ~27 ka. Directly under the Wono tephra, abundant fossil gastropod shells (*Vorticifex*) were collected; (3) finely laminated brown clay; and (4) brown silt. The sequence is interpreted as Sehoo deep-lake deposits.

Pelican Point (Site 19).
39°59'12'' N, 119°37'14'' W

This site is on the west shore of Pyramid Lake. Two tufa mounds at an elevation of 1162 m were described by Benson (1994), who directed me to this site. I collected fossil gastropod shells (*Vorticifex*) that were encrusted in the outer portions of the northernmost tufa mound. The tufa was radiocarbon dated at ~35 to 20 ka (Benson, 1994). However, the age relation of the shells encrusted on the mounds to the tufa is unknown. If the A/I ratios are age-diagnostic, then this is interpreted as a Holocene beach deposit.

Winnemuca Dry Lake (Site 20).
40°08'09'' N, 119°18'01'' W

This laterally continuous outcrop (Figure 26b) is on the eastern margin of Winnemuca Dry Lake at an elevation of ~1274 m. This outcrop has been exposed by an ephemeral stream draining into the Winnemuca basin. It consists of two units: (1)

Medium, laminated silt heavily burrowed and containing fossil gastropod shells (*Vorticifex*); and (2) gravel in brown sand. This sequence is interpreted as colluvium overlain by Sehoo nearshore deposits.

Wizards Beach (Site 21).
40°05'55'' N, 119°42'30'' W

This laterally continuous outcrop (Figure 27) is on the northwestern shore of Pyramid Lake in a small gravel pit at an elevation of ~1183 m. It consists of two units: (1) Well-rounded, well-sorted gravel in brown coarse sand containing abundant fossil gastropod shells (*Vorticifex*, *Physa*, and *Amnicola*); and (2) brown sand with few pebbles and abundant fossil gastropod shells (*Vorticifex*, *Physa*, and *Amnicola*). This sequence is interpreted as Sehoo nearshore deposits overlain by Sehoo beach deposits.

Winnemuca Pit (Site 22).
40°58'09'' N, 117°46'12'' W

This is McCoy's (1981) site AAL-1738 and Davis's (1978) site JOD 43. The laterally continuous outcrop (Figure 28) is 3 km northwest of Winnemuca, Nevada, in an abandoned gravel pit at an elevation of 1317 m. It consists of four units: (1) Pebbly gravel lenses in a light brown sand; (2) angular pebbles in a light brown medium sand; (3) light brown medium sand containing red oxidation features and 10-cm-thick unidentified white tephra; and (4) pebbly, subrounded gravel in a light brown medium sand containing some cross-laminae, fossil gastropod shells (*Vorticifex*), and increased evidence of oxidation farther down the outcrop. The sequence is interpreted as Sehoo nearshore and beach deposits overlain by colluvium.

American Canyon (Site 23).
40°20'27'' N, 118°03'34'' W

This site is ~5 km south of Unionville, Nevada. This outcrop is a pit dug into a beach terrace at ~1200 m elevation. The exposure consists of brown, fine sand and fossil gastropod shells (*Vorticifex*). These shells were collected at 0.5 and 1 m below the surface and radiocarbon dated at ~12 ka by Jerry Miller (Table 2). This is interpreted as Sehoo nearshore deposits.

Schurz (Site 24).
38°53'54'' N, 118°47'47'' W

This site is ~7 km south of Schurz, Nevada. The outcrop (Figure 29) is a small gravel pit on the west side of Route 95, at an elevation of ~1250 m. It consists of two units: (1) Bouldery tufa-cemented gravel in a brown, coarse sand matrix containing fossil gastropod shells (*Amnicola*) with a sand lens also containing fossil gastropod shells (*Vorticifex*); and (2) interbedded dark brown, coarse sand and subrounded gravel. This sequence is interpreted as Sehoo beach deposits.

Black Rock (Site 25).
41°01'22'' N, 118°54'38'' W

Although I never visited this site, I was given shells from it by Peter Wigand (Desert Research Institute). This site is ~10 km north of Gerlock, Nevada, at an elevation of ~1250 m. The gastropods (*Lymnaea* and *Planorbella*) were radiocarbon dated at ~15 ka (Table 2). This is interpreted as Sehoo lacustrine deposits.

CHEWAUCAN AND SURPRISE BASINS

Burrow Pit (Site 26).
43°00'24'' N, 120°46'10'' W

This site was first described by Allison (1982) who radiocarbon dated gastropods at ~22 ka (Table 2). This laterally discontinuous outcrop is ~1 km northeast of Ana River, Oregon, at an elevation of 1367 m. It is composed entirely of northwest-dipping parallel laminated, maroon silt and sand with fossil gastropod shells (*Vorticifex*). This is interpreted as an older lacustrine deposit.

Ana River (Site 27).
42°59'24'' N, 120°44'35'' W

I was directed to this site by Rob Negrini (California State University, Bakersfield), who is currently studying paleomagnetic secular variations in the exposed sediments at this outcrop. The outcrop (Figure 30) is~1 km southwest of Ana River, Oregon, at ~1280 m elevation. Allison (1982), Davis (1985), and Negrini and Davis (1992) described the ~13-m-thick section in detail. It contains clay, silt, sand, numerous tephra, and ostracode shells. Allison (1982) radiocarbon dated fossil gastropod shells from a layer ~6 m below the surface at ~25.5 ka and ~30.7 ka from ostracode shells and oolites a few meters above this layer. I collected fossil gastropod shells (*Vorticifex*) ~7 m below the surface. From a previous thermoluminescence (TL) date (Berger, 1991), these gastropods should be ~165 ka (Table 2). This is interpreted as a deep lacustrine deposit from Summer Lake.

Tucker Hill (Site 28).
42°36'11'' N, 120°24'49'' W

I was directed to this site by Dorothy Freidel (Sonoma State University). This site is ~18 km northwest of Valley Falls, Oregon, in an abandoned gravel pit, at an elevation of ~1310 m (Figure 31). It consist of three units: (1) Subangular cobbles in coarse sand consisting of two distinct layers of concentrated shells. The top layer contains shells of *Vorticifex, Psidium,* and *Amnicola*, whereas the bottom layer contains shells of *Vorticifex, Psidium,* and *Spherium* (Figure 32a). These shells were AMS radiocarbon dated at ~12.2 ka (Table 2); (2) discontinuous layer of rounded cobbles and laminated sand; and (3) coarse sand containing large-scale cross-laminae and cobbles (Figure 32b). This section is interpreted as younger nearshore deposits overlain by reworked beach deposits.

Willow Creek (Site 29).
42°30'47'' N, 120°19'47'' W

I was directed to this site by Peter Clark (Oregon State University). This site is ~4 km northwest of Valley Falls, Oregon, at an elevation of 1325 m. The outcrop (Figure 33) is on the south bank of Willow Creek. It consists of three units: (1) Angular cobbles in coarse sand; (2) well-laminated interbedded silt and fine sand containing red oxidation layers and fossil shells (*Vorticifex* and *Spherium*) determined to be ~11.9 ka (Table 2); and (3) dark brown clay. This sequence is interpreted as younger deep lake deposits overlain by younger nearshore deposits and colluvium.

Southeast Abert Lake (Site 30).
42°32'06'' N, 120°13'42'' W

I was directed to this site by Peter Clark (Oregon State University). This site is on the east side of Lake Abert ~8 km northeast of Valley Falls, Oregon, at an elevation of 1311 m. This exposure (Figure 34) is a roadcut. It consists of three units: (1) Loosely cemented, rounded cobbles in black medium sand and silt containing fossil shells (*Vorticifex* and *Spherium*) determined to be 11.5 ka (Table 2); (2) finely laminated dark tan medium sand with some discontinuous fine-gravel layers; and (3) finely laminated light tan coarse sand with abundant gravel layers. This section is interpreted as younger nearshore deposits overlain by reworked beach deposits.

Northeast Abert Lake (Site 31).
42°35'47'' N, 120°11'03'' W

I was directed to this site by Peter Clark (Oregon State University). This site is also on the east side of Lake Abert ~17 km northeast of Valley Falls, Oregon, at an elevation of 1312 m. This section (Figure 35a) is a roadcut. It consists of two units: (1) Angular cobbles; and (2) interbedded subrounded pebbles and dark brown sand containing two distinct layers of concentrated fossil shells (*Vorticifex, Amnicola,* and *Psidium*). Two radiocarbon ages from this site, one from Peter Clark and one for this study, both determined the shells to be ~11.7 ka (Table 2). This sequence is interpreted as younger nearshore deposits overlain by wave-induced colluvium.

Surprise Valley (Site 32).
41°13'09'' N, 120°03'53'' W

This roadcut (Figure 35b) is Davis's (1978) site JOD 15. It is on the southwest corner of Surprise Valley, California, at an elevation of 1378 m. It consists of three units: (1) Boulders and sandy gravel; (2) well-cemented, sandy cobbles; and (3) brown, medium sand containing the Trego Hot Springs tephra determined by Benson and others (1997) to be ~23 ka. I collected fossil gastropod shells (*Vorticifex*) about 10 cm above the tephra. This sequence is interpreted as younger nearshore deposits overlain by beach deposits.

TABLE 2. RADIOCARBON DATES AND A/I RATIOS FOR DATED SITES. SEE TABLES 3-5 FOR COMPLETE A/I AND SITE DATA

Lab # (UAL)	Site Name	Site #	Field ID	Genus	A/I	Radiocarbon Age (yr B.P.)	Lab #	Source of Date
Lahontan basin								
1968/2167	Sand Ramp	1	JB96-1C	*Vorticifex*	0.196	12,800 ± 60	HSM-SR-30	Kurt Cupp (1997)
1967	Sand Ramp	1	JB96-1D	*Vorticifex*	0.252	12,950 ± 60	HSM-SR-10	Kurt Cupp (1997)
1966	Sand Ramp	1	JB96-1E	*Vorticifex*	0.190	13,130 ± 60	HSM-SR-20	Kurt Cupp (1997)
1941	Jessup	3	JB96-3C	*Vorticifex*	0.123	13,110 ± 110	ETH12798	Adams (1997)
1942	Jessup	3	JB96-3A	*Vorticifex*	0.117	13,280 ± 110	ETH12799	Adams (1997)
1961†	Astor Pass	16	JB96-16A	*Vorticifex*	0.167	16,500 ± 300	L-64CQ	Broecker and Kaufman (1965)
1961†	Astor Pass	16	JB96-16A	*Vorticifex*	0.167	17,900 ± 800	L-772K	Broecker and Kaufman (1965)
1961†	Astor Pass	16	JB96-16A	*Vorticifex*	0.167	19,100 ± 700	L-772NA	Broecker and Kaufman (1965)
1977	America Canyon	23	JB96-23B	*Vorticifex*	0.207	12,050 ± 170	Not Available	Jerry Miller (pers. commun.)
2091	America Canyon	23	JB96-23A	*Vorticifex*	0.192	12,050 ± 170	Not Available	Jerry Miller (pers. commun.)
1976	Black Rock	25	JB96-25A	*Lymnaea*	0.223	15,000 ± 100	BRD250988FN1	Peter Wigand (pers. commun.)
2092	Black Rock	25	JB96-25A	*Planorbella*	0.088	15,000 ± 100	BRD250988FN1	Peter Wigand (pers. commun.)
Chewaucan and Surprise basins								
1933	Burrow Pit	26	JB96-26A	*Vorticifex*	0.403	22,000	Not Available	Allison (1982)
1935§	Ana River	27	JB96-27A	*Vorticifex*	0.270	165,000 ± 19,000*	SML-1a	Berger (1991)
1714§	Tucker Hill	28	JB96-28A	*Vorticifex*	0.134	12,170 ± 115	AA-20142	Dorothy Freidel (pers. commun.)
1715	Tucker Hill	28	JB96-28A	*Psidium*	0.130	12,170 ± 115	AA-20142	Dorothy Freidel (pers. commun.)
1717	Tucker Hill	28	JB96-28B	*Amnicola*	0.173	12,340 ± 80	AA-20143	Dorothy Freidel (pers. commun.)
1718§	Tucker Hill	28	JB96-28B	*Vorticifex*	0.125	12,340 ± 80	AA-20143	Dorothy Freidel (pers. commun.)
1719	Tucker Hill	28	JB96-28B	*Psidium*	0.119	12,340 ± 80	AA-20143	Dorothy Freidel (pers. commun.)
1720	Tucker Hill	28	JB96-28B	*Spherium*	0.086	12,340 ± 80	AA-20143	Dorothy Freidel (pers. commun.)
1936§	Willow Creek	29	JB96-29A	*Vorticifex*	0.072	11,934 ± 94	Not Available	Peter Clark (pers. commun.)
2094	Willow Creek	29	JB96-29A	*Spherium*	0.073	11,934 ± 94	Not Available	Peter Clark (pers. commun.)
1930§	SE Abert Lake	30	JB96-30A	*Vorticifex*	0.105	11,546 ± 15	Not Available	Peter Clark (pers. commun.)
1931	SE Abert Lake	30	JB96-30A	*Spherium*	0.121	11,546 ± 15	Not Available	Peter Clark (pers. commun.)
1922§	NE Abert Lake	31	JB96-31B	*Vorticifex*	0.152	11,673 ± 94	Not Available	Peter Clark (pers. commun.)
1923	NE Abert Lake	31	JB96-31B	*Amnicola*	0.245	11,673 ± 94	Not Available	Peter Clark (pers. commun.)
1924	NE Abert Lake	31	JB96-31B	*Psidium*	0.299	11,673 ± 94	Not Available	Peter Clark (pers. commun.)
1923	NE Abert Lake	31	JB96-31B	*Amnicola*	0.245	11,970 ± 80	NSRL-3491	This study

* Thermoluminescence age

† Site JB96-16A might correspond to any of Broecker and Kaufman's three ages

§ Used for calibration curve

TABLE 3. RESULTS OF AMINO ACID ANALYSIS FROM THE CARSON DESERT SUBBASIN OF LAKE LAHONTAN, NEVADA. APPENDIX B GIVES FURTHER SAMPLE INFORMATION

Lab # (UAL)	Site Name	Site #	Field ID	Elevation (m)	A/I	± 1 SD	N*	Genus	Lake Cycle
1968/2167	Sand Ramp	1	JB96-1C	1277	0.196	0.020	9	*Vorticifex*	Sehoo
1967	Sand Ramp	1	JB96-1D	1273	0.252	0.031	4	*Vorticifex*	Sehoo
1966	Sand Ramp	1	JB96-1E	1268	0.190	0.025	5	*Vorticifex*	Sehoo
1962/1864/1927/2166	Sand Ramp	1	JB96-1B/JB97-1C	1265	0.160	0.019	17	*Vorticifex*	Sehoo
1975/2165	Sand Ramp	1	JB96-1A/JB97-1A	1263	0.136	0.042	8	*Vorticifex*	Sehoo
1865	Corral site	2	JB96-2A	~1250	0.185	0.028	3	*Vorticifex*	Sehoo
1941	Jessup	3	JB96-3C	1331	0.123	0.010	5	*Vorticifex*	Sehoo
1942	Jessup	3	JB96-3A	1327	0.117	0.010	4	*Vorticifex*	Sehoo
2093	Wyemaha Valley	4	JB97-4A	~1244	0.321	0.011	5	*Vorticifex*	Late Eetza
2195	West Wyemaha Valley	5	JB97-5A	~1219	0.298	0.013	5	*Vorticifex*	Late Eetza
1937	West Sehoo Mtn	6	JB96-6C	~1280	0.429	0.022	2	*Lymnaea*	Early Eetza
1939	West Sehoo Mtn	6	JB96-6B	~1280	0.471	0.027	4	*Vorticifex*	Early Eetza
2182	West Sehoo Mtn	6	JB97-6B	1282	0.460	0.019	4	*Vorticifex*	Early Eetza
2183	West Sehoo Mtn	6	JB97-6B	1282	0.480	0.032	3	*Lymnaea*	Early Eetza
2181/1938	West Sehoo Mtn	6	JB97-6A/JB96-6C	1281	0.453	0.009	10	*Vorticifex*	Early Eetza
2184	West Sehoo Mtn	6	JB97-6C	1280	0.464	0.045	5	*Lymnaea*	Early Eetza
2185	SW Sehoo Mtn	7	JB97-7A	1256	0.548	0.113	3	*Amnicola*	Pre-Eetza
2189	SW Sehoo Mtn	7	JB97-7A	1256	0.768	0.057	4	*Physa*	Pre-Eetza
2190/1869	SW Sehoo Mtn	7	JB97-7E/JB96-7A	1254	0.839	0.026	8	*Physa*	Pre-Eetza
2180	SW Sehoo Mtn	7	JB97-7H	1252	0.807	0.099	3	*Physa*	Pre-Eetza
2196	South Sehoo Mtn	8	JB97-8A	~1219	0.461	0.114	3	*Vorticifex*	Early Eetza
2202	Lower Fallon Pit	9	JB97-9A	1273	0.179	0.011	5	*Vorticifex*	Sehoo
2197	Upper Fallon Pit 1	10	JB97-10A	1293	0.105	0.047	5	*Vorticifex*	Sehoo
2198	Upper Fallon Pit 1	10	JB97-10B	1291	0.127	0.015	5	*Vorticifex*	Sehoo
2191	Upper Fallon Pit 2	11	JB97-11A	~1303	0.126	0.003	5	*Vorticifex*	Sehoo
2192	Upper Fallon Pit 3	12	JB97-12A	1310	0.177	0.010	5	*Vorticifex*	Sehoo
2193	Upper Fallon Pit 3	12	JB97-12B	1307	0.141	0.010	5	*Vorticifex*	Sehoo

Average: ILC-A (UAL-1999) = 0.161 ± 0.008 , ILC-B (UAL-1742) = 0.489 ± 0.025 , ILC-C (UAL-1743) = 1.045 ± 0.068

* N = number of shells (subsamples) used to calculate mean A/I ratios and standard deviations (SD)

TABLE 4. RESULTS OF AMINO ACID ANALYSIS FROM THE PYRAMID-WINNEMUCA LAKE VALLEY, HUMBOLDT VALLEY, BUENA VISTA, WALKER LAKE, AND BLACK ROCK-SMOKE CREEK DESERTS SUBBASINS IN THE LAHONTAN BASIN, NEVADA. TABLE A2 GIVES FURTHER SAMPLE INFORMATION

Lab # (UAL)	Site Name	Site #	Field ID	Elevation (m)	A/I	± 1 SD	N*	Genus	Lake Cycle
Pyramid-Winnemuca Lake Valley subbasin									
1848	North Pyramid Lake	13	JB96-13A	~1260	0.024	0.003	4	*Vorticifex*	Holocene
1978	Pyramid Island	14	JB96-14A	1158	0.077	0.030	5	*Amnicola*	Holocene
2177/1866	Railroad Cut	15	JB97-15C/JB96-15A	1265	0.140	0.018	8	*Vorticifex*	Dendritic Sehoo
2168	Railroad Cut	15	JB97-15A	1264	0.115	0.021	3	*Vorticifex*	Early Sehoo
2169	Railroad Cut	15	JB97-15B	1264	0.113	0.012	5	*Vorticifex*	Early Sehoo
2178	Railroad Cut	15	JB97-15D	1260	0.278	0.047	3	*Vorticifex*	Late Eetza
2179/1867	Railroad Cut	15	JB97-15E/JB96-15D	1259	0.379	0.016	10	*Vorticifex*	Middle Eetza
1961	Astor Pass	16	JB96-16A	~1225	0.167	0.009	3	*Vorticifex*	Sehoo
1960	Blanc Tetons	17	JB96-17A	1169	0.068	0.012	4	*Vorticifex*	Holocene
1958	Agency Bridge	18	JB96-18A	1207	0.110	0.024	2	*Vorticifex*	Sehoo
1956	Pelican Point	19	JB96-19A	1162	0.069	0.017	5	*Amnicola*	Holocene
1957	Pelican Point	19	JB96-19A	1162	0.059	0.029	5	*Vorticifex*	Holocene
1955	Winnemuca Lake	20	JB96-20A	~1274	0.113	0.019	5	*Vorticifex*	Sehoo
2203	Wizards Beach	21	JB97-21A	1183	0.113	0.003	5	*Vorticifex*	Sehoo
2204	Wizards Beach	21	JB97-21A	1183	0.084	0.013	5	*Physa*	Sehoo
2205	Wizards Beach	21	JB97-21A	1183	0.127	0.010	5	*Amnicola*	Sehoo
2200	Wizards Beach	21	JB97-21B	1182	0.083	0.014	5	*Vorticifex*	Sehoo
2206	Wizards Beach	21	JB97-21B	1182	0.071	0.009	5	*Physa*	Sehoo
2207	Wizards Beach	21	JB97-21B	1182	0.158	0.033	5	*Amnicola*	Sehoo
Humboldt Valley subbasin									
2194	Winnemuca Pit	22	JB97-22A	1317	0.118	0.012	5	*Vorticifex*	Sehoo
Buena Vista subbasin									
1977	America Canyon	23	JB96-23B	1200	0.207	0.019	5	*Vorticifex*	Sehoo
2091	America Canyon	23	JB96-23A	1199	0.192	0.013	5	*Vorticifex*	Sehoo
Walker Lake subbasin									
2201	Schurz	24	JB97-24A	1250	0.102	0.012	5	*Amnicola*	Sehoo
2199	Schurz	24	JB97-24C	1249	0.127	0.015	5	*Vorticifex*	Sehoo
2208	Schurz	24	JB97-24B	1248	0.132	0.012	4	*Vorticifex*	Sehoo
Black Rock - Smoke Creek Deserts subbasin									
1976	Black Rock	25	JB96-25C	~1250	0.223	0.029	5	*Lymnaea*	Sehoo
2092	Black Rock	25	JB96-25B	~1250	0.088	0.011	4	*Planorbella*	Sehoo

Average: ILC-A (UAL-1999) = 0.161 ± 0.008 , ILC-B (UAL-1742) = 0.489 ± 0.025 , ILC-C (UAL-1743) = 1.045 ± 0.068

* N = number of shells (subsamples) used to calculate mean A/I ratios and standard deviations (SD)

TABLE 5. RESULTS OF AMINO ACID ANALYSES FROM THE CHEWAUCAN BASIN, OREGON AND THE SURPRISE BASIN, CALIFORNIA. TABLE A2 GIVES FURTHER SAMPLE INFORMATION

Lab # (UAL)	Site Name	Site #	Field ID	Elevation (m)	A/I	± 1 SD	N*	Genus
Summer Lake subbasin								
1933	Burrow Pit	26	JB96-26A	1367	0.403	0.036	5	*Vorticifex*
1935	Ana River	27	JB96-27A	~1280	0.270	0.021	5	*Vorticifex*
Lower Chewaucan Marsh subbasin								
1714	Tucker Hill	28	JB96-28A	1310	0.134	0.006	4	*Vorticifex*
1715	Tucker Hill	28	JB96-28A	1310	0.130	0.001	2	*Psidium*
1717	Tucker Hill	28	JB96-28B	1309	0.173	0.010	5	*Amnicola*
1718	Tucker Hill	28	JB96-28B	1309	0.125	0.003	5	*Vorticifex*
1719	Tucker Hill	28	JB96-28B	1309	0.119	0.005	5	*Psidium*
1720	Tucker Hill	28	JB96-28B	1309	0.086	0.006	5	*Spherium*
1936	Willow Creek	29	JB96-29A	1325	0.072	0.003	3	*Vorticifex*
2094	Willow Creek	29	JB97-29A	1325	0.073	0.026	4	*Spherium*
Lake Abert subbasin								
1930	SE Abert Lake	30	JB96-30A	1311	0.105	0.011	4	*Vorticifex*
1931	SE Abert Lake	30	JB96-30A	1311	0.121	0.008	5	*Spherium*
1928	NE Abert Lake	31	JB96-31A	1312	0.273	0.014	5	*Vorticifex*
1922	NE Abert Lake	31	JB96-31B	1311	0.152	0.021	4	*Vorticifex*
1923	NE Abert Lake	31	JB96-31B	1311	0.245	0.010	4	*Amnicola*
1924	NE Abert Lake	31	JB96-31B	1311	0.299	0.013	5	*Psidium*
Surprise basin								
1921	Surprise Valley	32	JB96-32A	1378	0.233	0.015	5	*Vorticifex*

Average: ILC-A (UAL-1999) = 0.161 ± 0.008 , ILC-B (UAL-1742) = 0.489 ± 0.025 , ILC-C (UAL-1743) = 1.045 ± 0.068

* N = number of shells (subbsamples) used to calculate mean A/I ratios and standard deviations (SD)

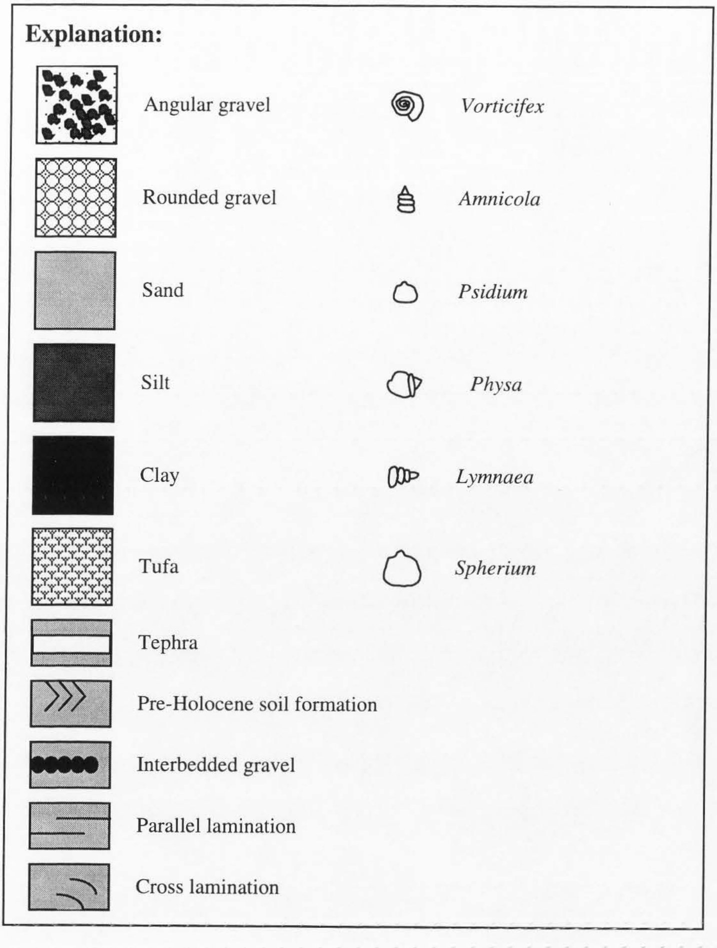

Figure 11. Explanation of symbols for stratigraphic columns in Figures 12-35.

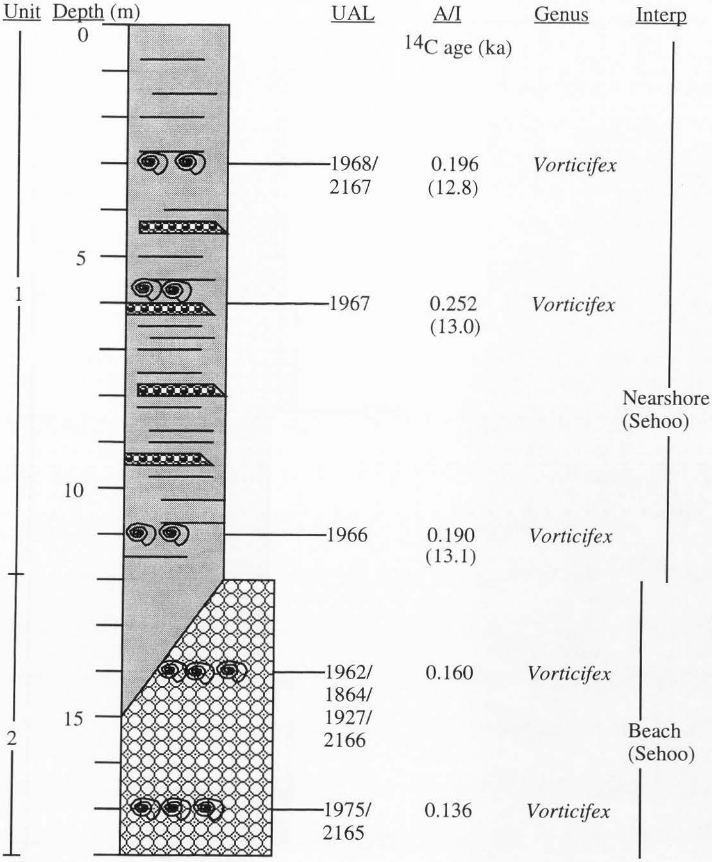

Figure 12. Stratigraphic section for Sand Ramp (Site 1), Nevada. Information on radiocarbon ages in Table 2.

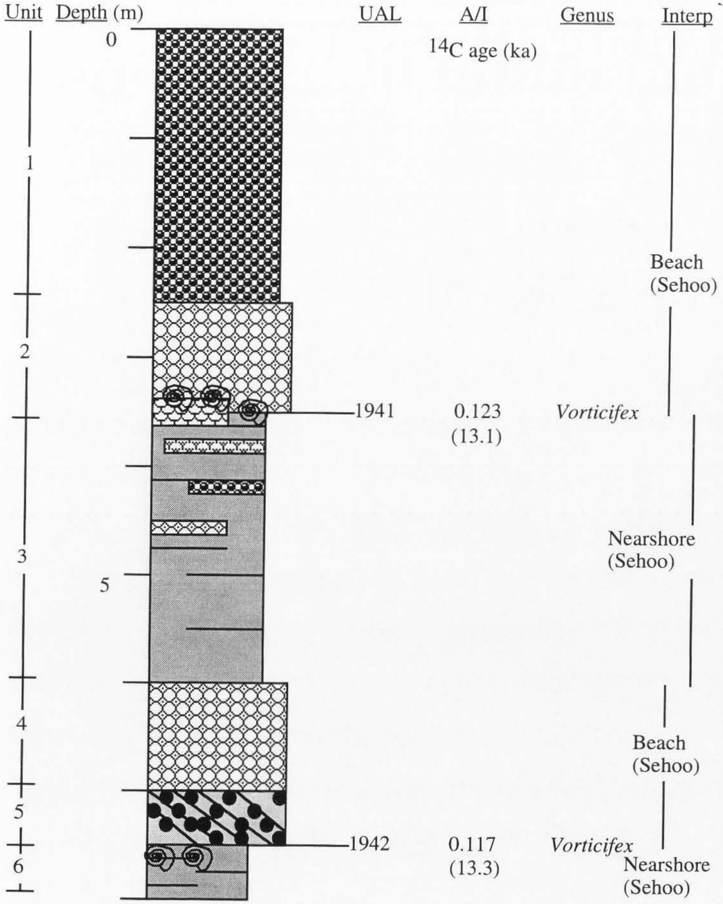

Figure 13. Stratigraphic section for Jessup (Site 3), Nevada. Information on radiocarbon ages in Table 2.

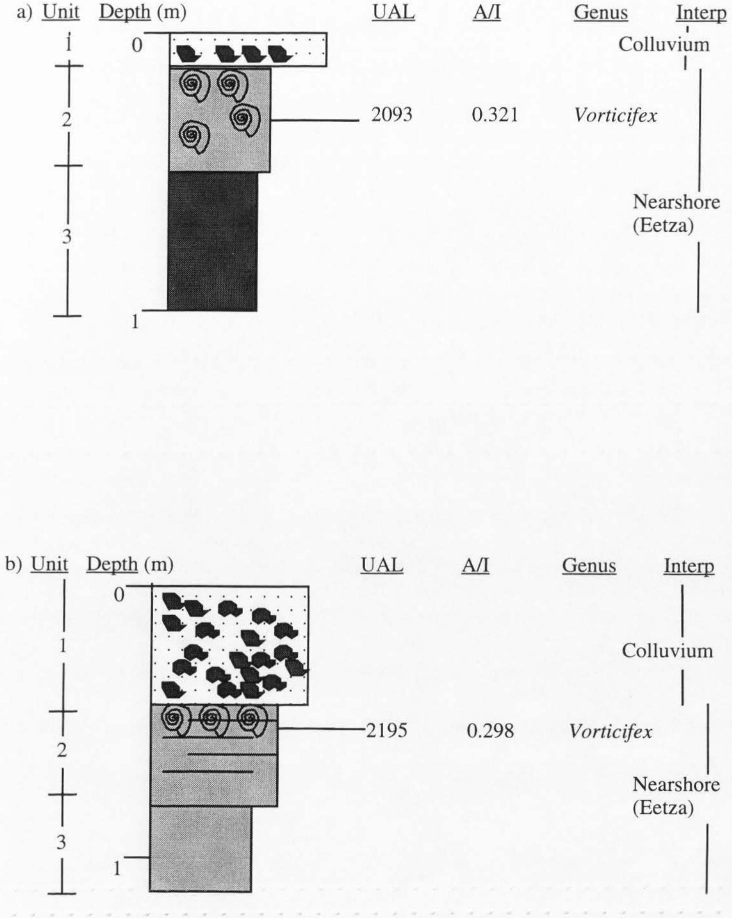

Figure 14. **Stratigraphic section for (a) Wyemaha Valley (Site 4), Nevada; and (b) West Wyemaha Valley (Site 5), Nevada.**

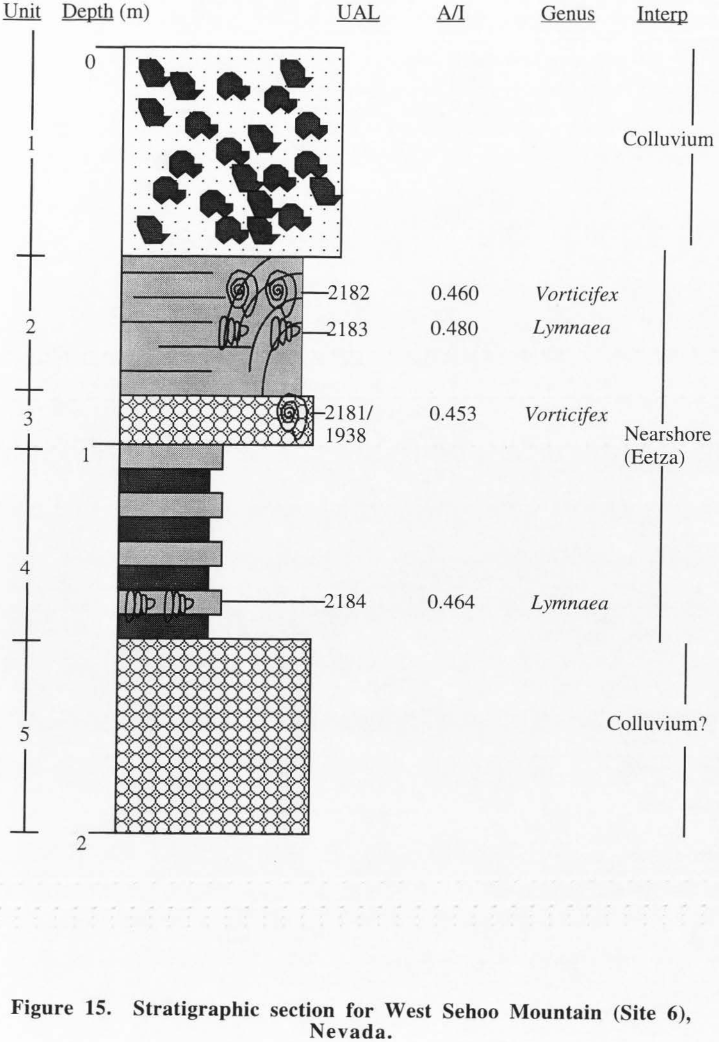

Figure 15. Stratigraphic section for West Sehoo Mountain (Site 6), Nevada.

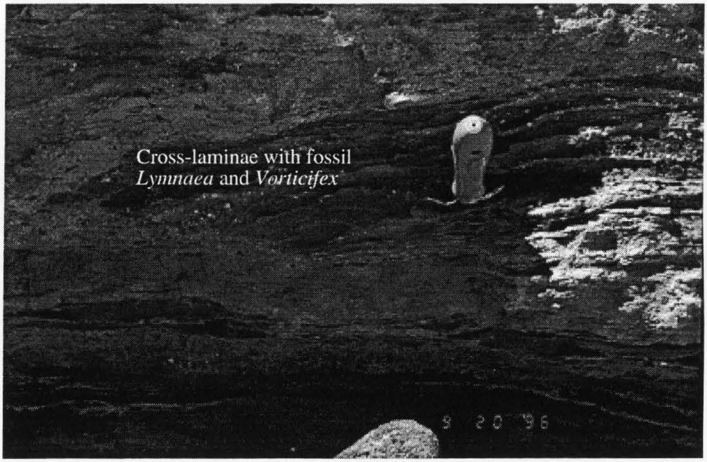

Figure 16. Cross-laminated silt and sand containing fossil *Lymnaea* and *Vorticifex* at West Sehoo Mountain (Site 6), Nevada. Trowel handle is 12 cm long.

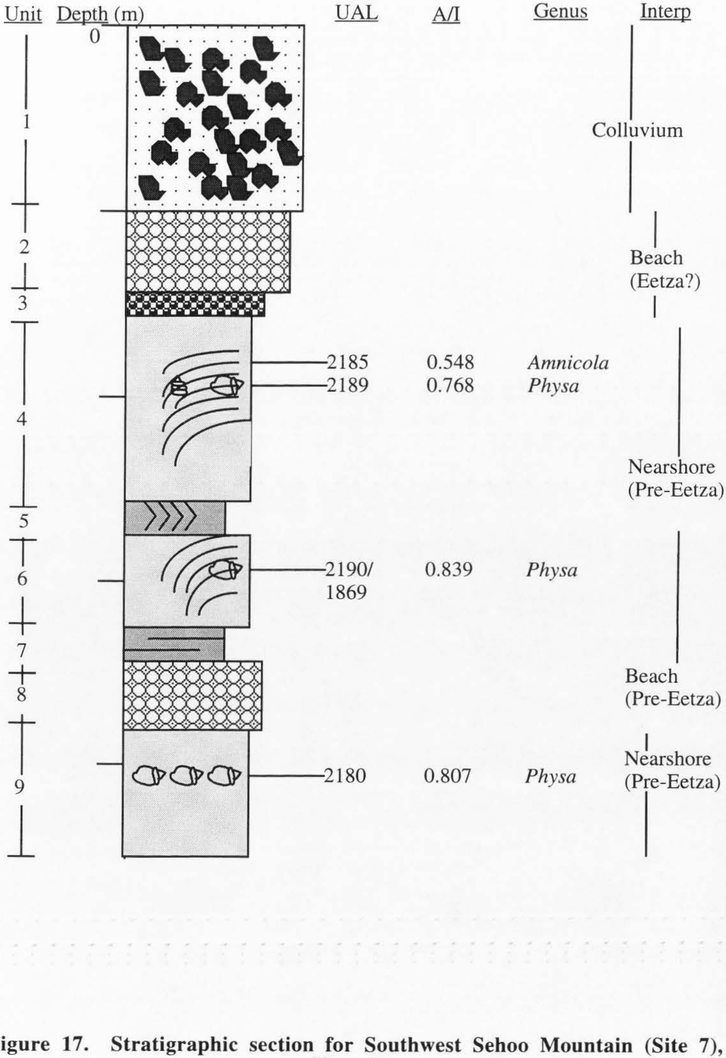

Figure 17. Stratigraphic section for Southwest Sehoo Mountain (Site 7), Nevada.

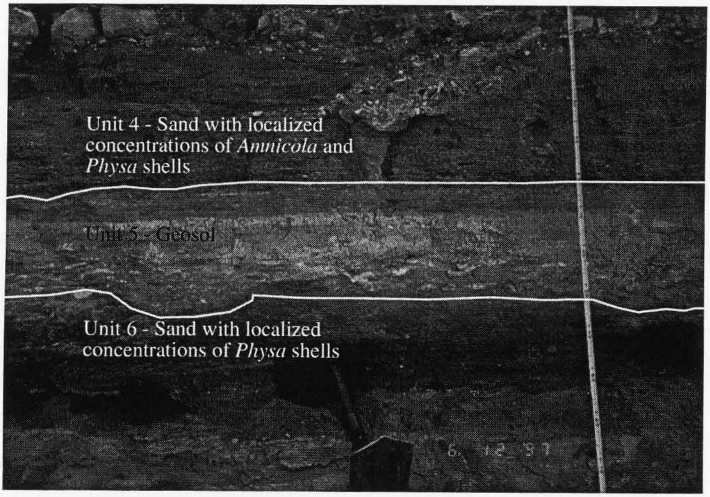

Figure 18. Units 4 to 6 (Figure 17) at Southwest Sehoo Mountain (Site 7), Nevada. This sequence is interpreted as a geosol between two lake units. The shovel handle is 30 cm long.

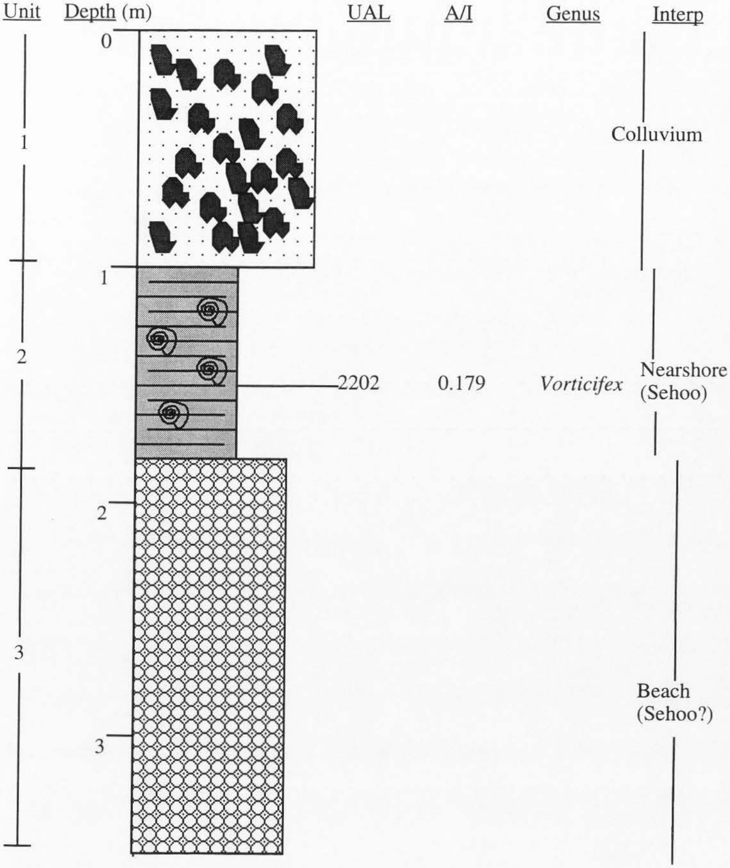

Figure 19. Stratigraphic section for Lower Fallon Pit (Site 9), Nevada.

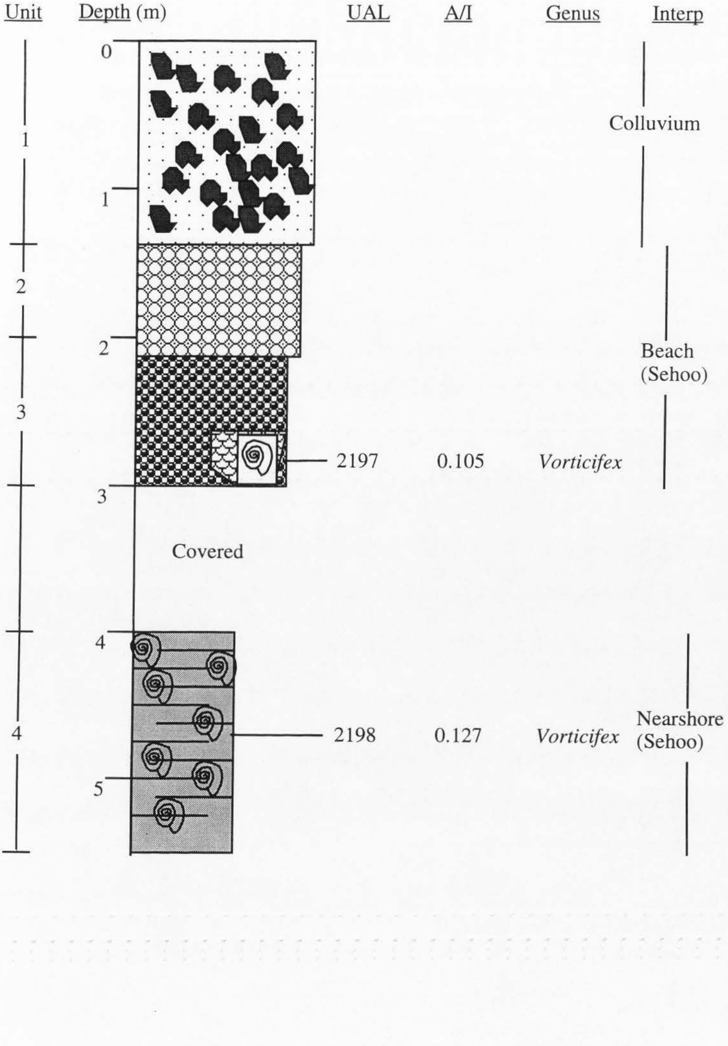

Figure 20. Stratigraphic section for Upper Fallon Pit 1 (Site 10), Nevada.

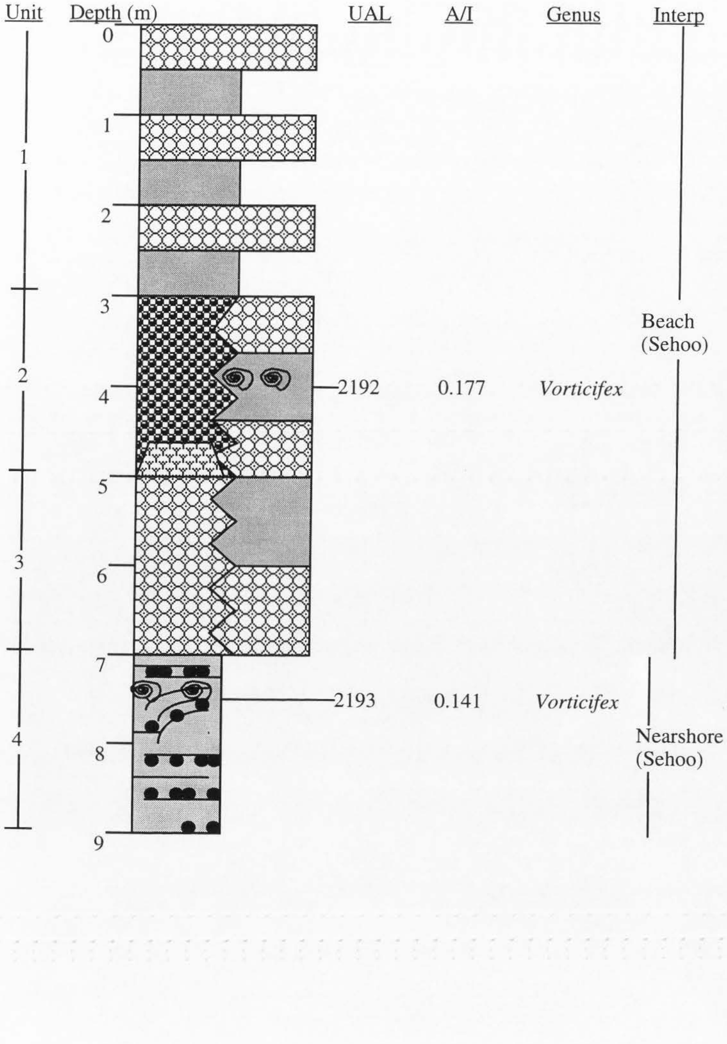

Figure 21. Stratigraphic section for Upper Fallon Pit 3 (Site 12), Nevada.

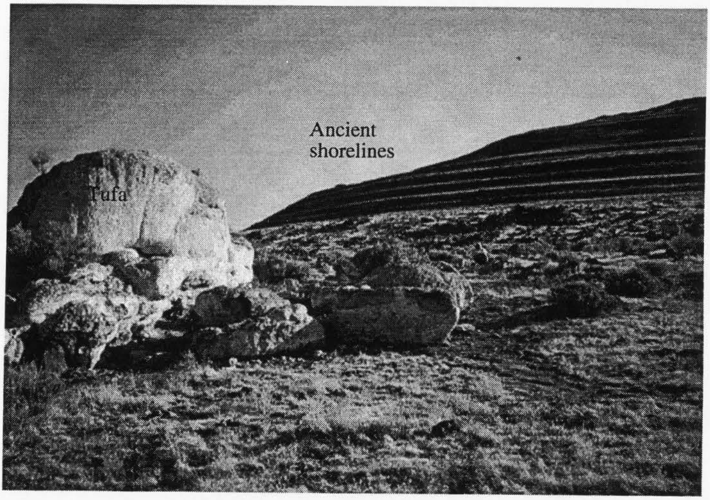

Figure 22. Tufa at North Pyramid Lake (Site 13), Nevada, with shoreline features in background. Largest mound is ~2 m high.

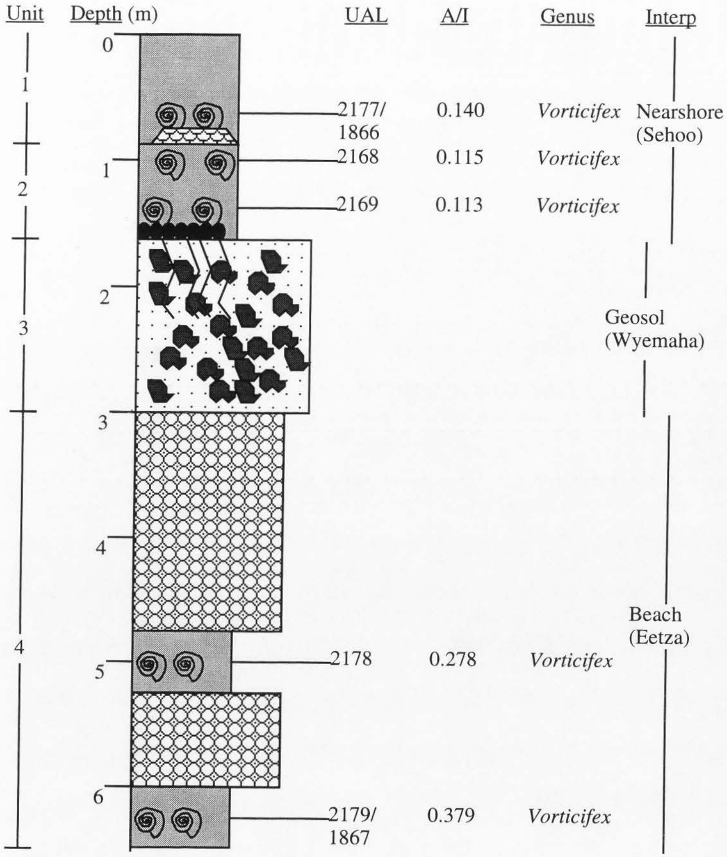

Figure 23. Stratigraphic section for Railroad Cut (Site 15), Nevada.

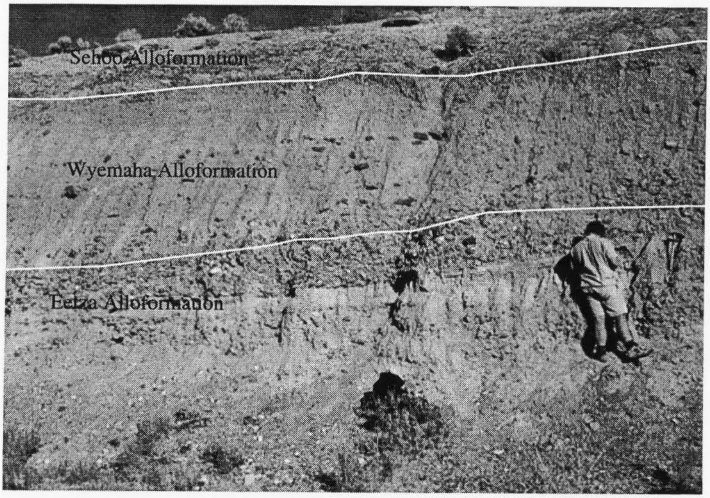

Figure 24. Railroad Cut (Site 15), Nevada.

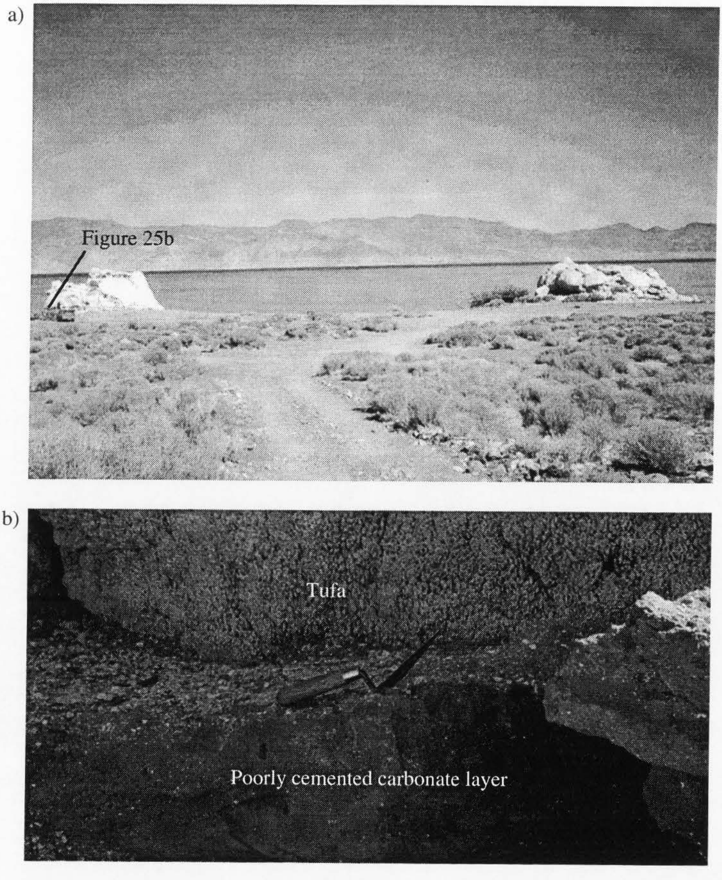

Figure 25. (a) Tufa mounds at Blanc Tetons (Site 17) on west shore of Pyramid Lake, Nevada. (b) Shell layer in poorly cemented carbonate layer below tufa mound at Blanc Tetons (Site 17), Nevada. Trowel is 12 cm long.

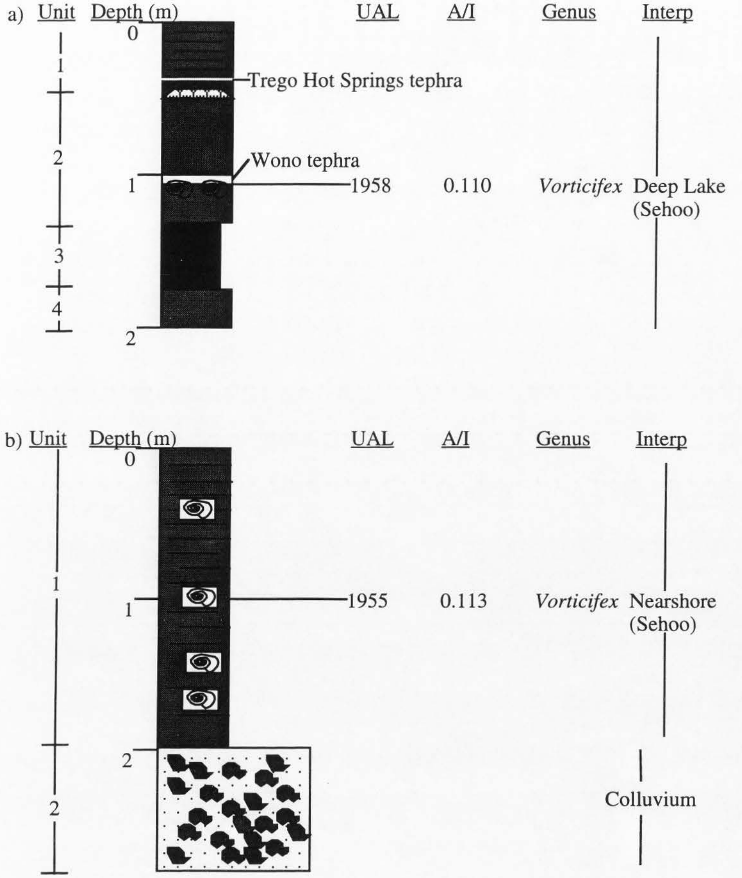

Figure 26. Stratigraphic section for (a) Agency Bridge (Site 18), Nevada, and (b) Winnemuca Dry Lake (Site 20), Nevada.

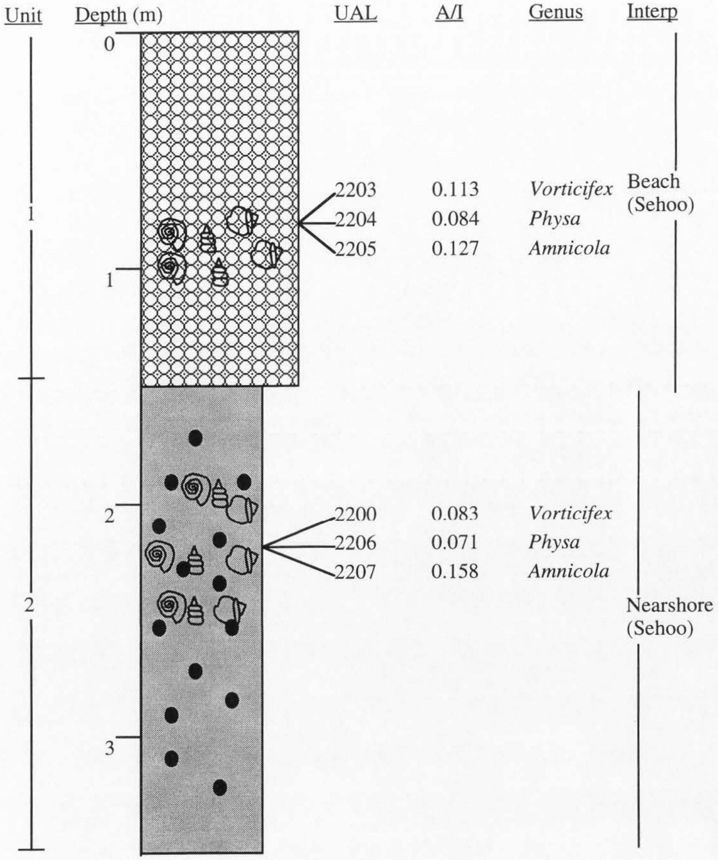

Figure 27. Stratigraphic section for Wizards Beach (Site 21), Nevada.

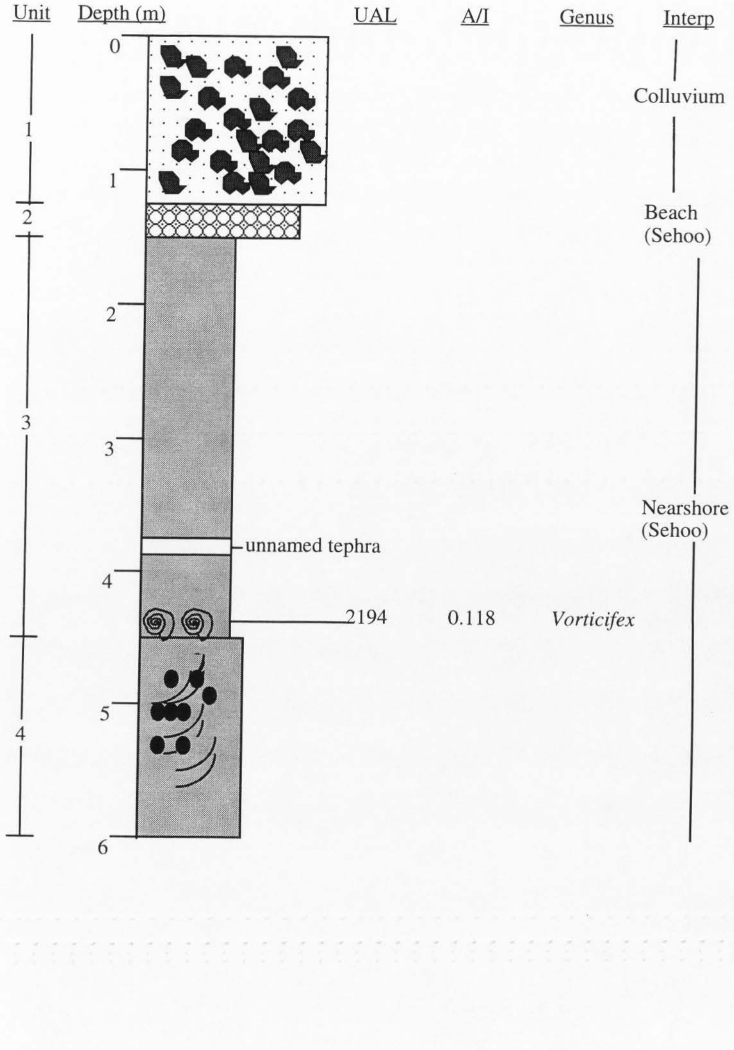

Figure 28. Stratigraphic section for Winnemuca Pit (Site 22), Nevada.

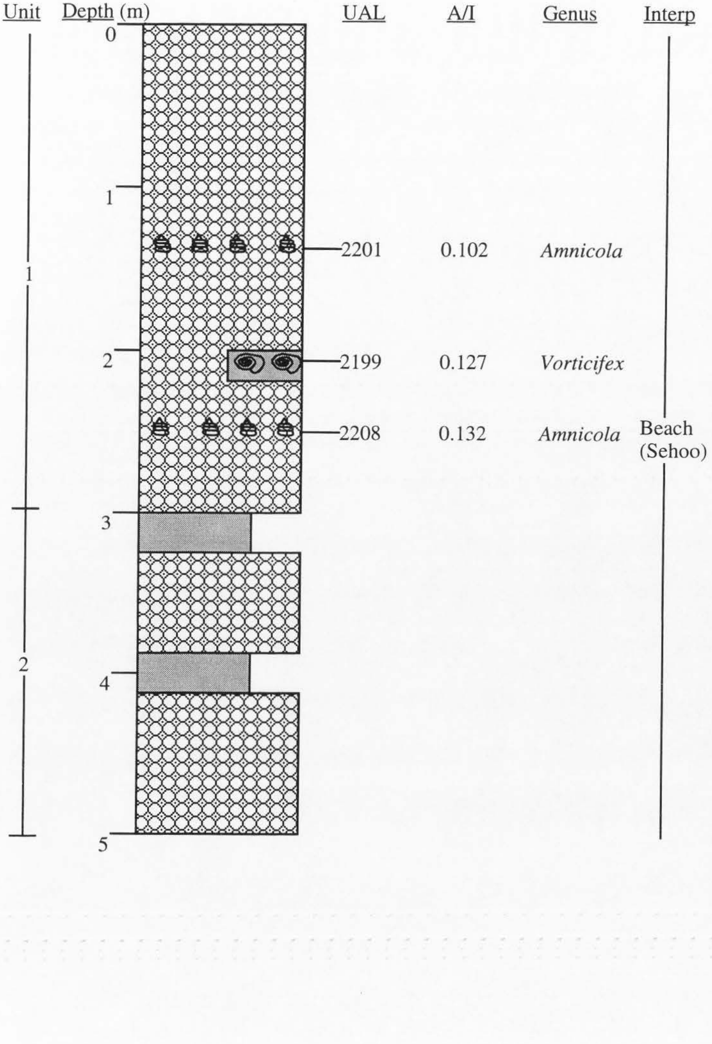

Figure 29. Stratigraphic section for Schurz (Site 24), Nevada.

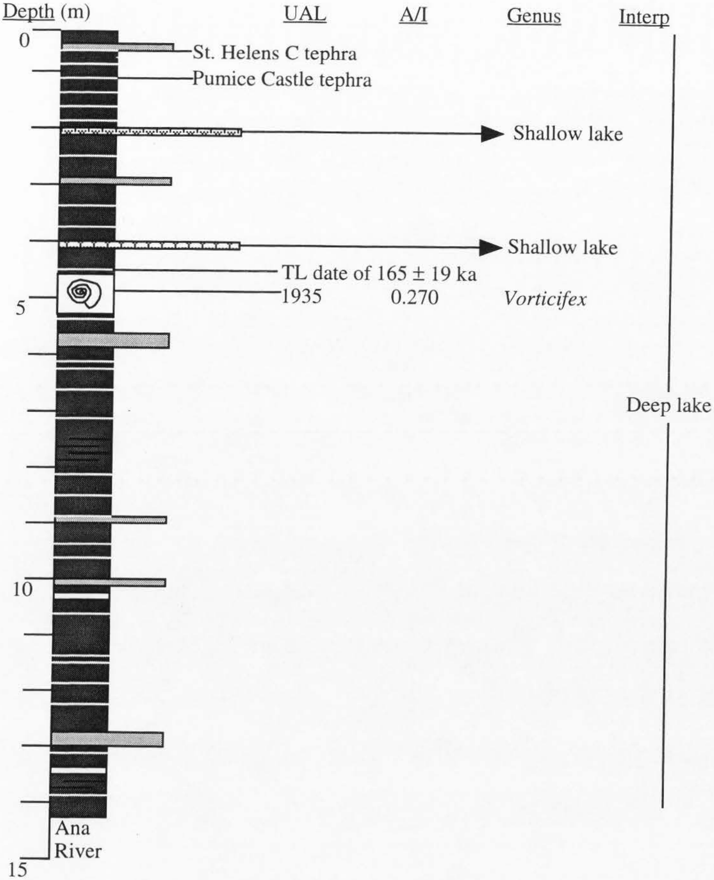

Figure 30. Stratigraphic Section for Ana River (Site 27), Oregon from Negrini and Davis (1992).

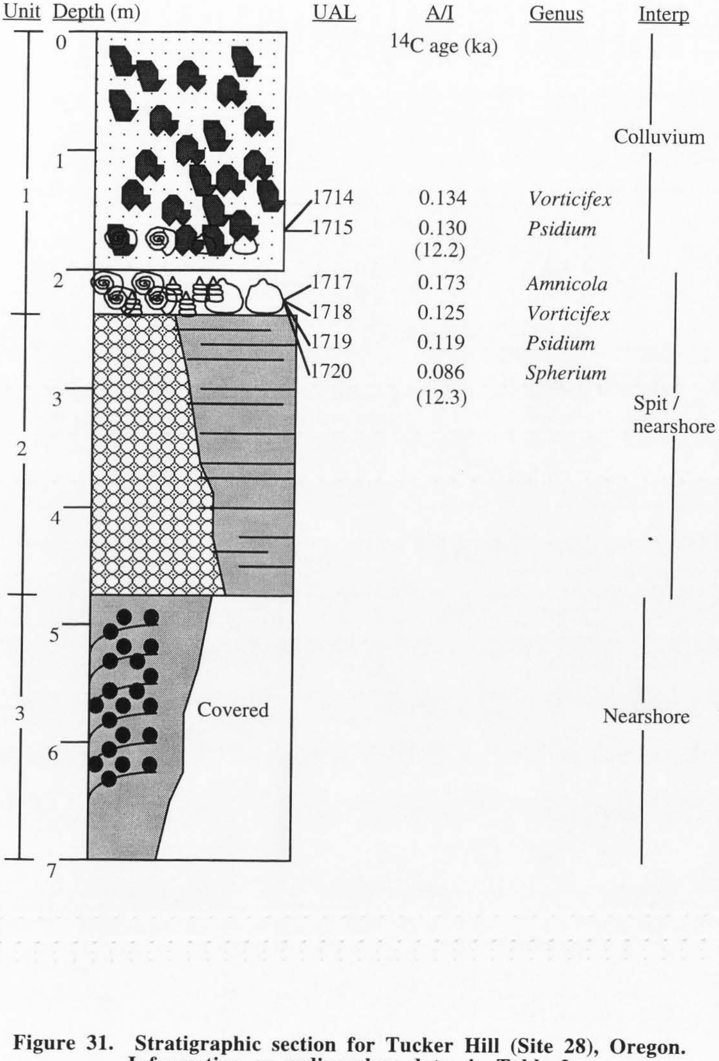

Figure 31. Stratigraphic section for Tucker Hill (Site 28), Oregon. Information on radiocarbon dates in Table 2.

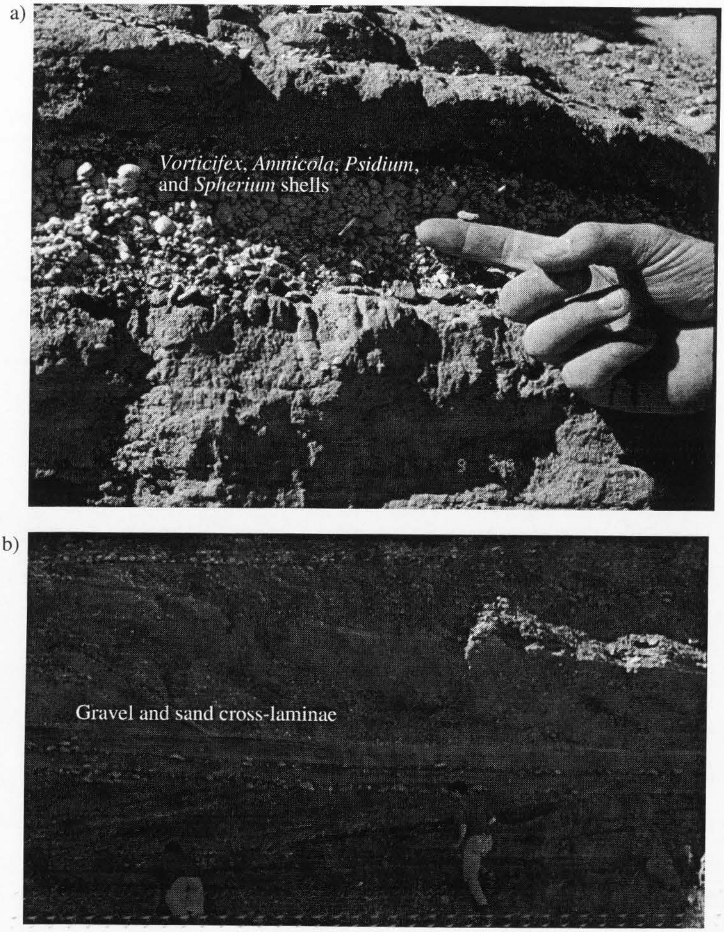

Figure 32. Tucker Hill site (Site 28): (a) Lower shell layer; (b) large-scale gravel and sand cross-laminae.

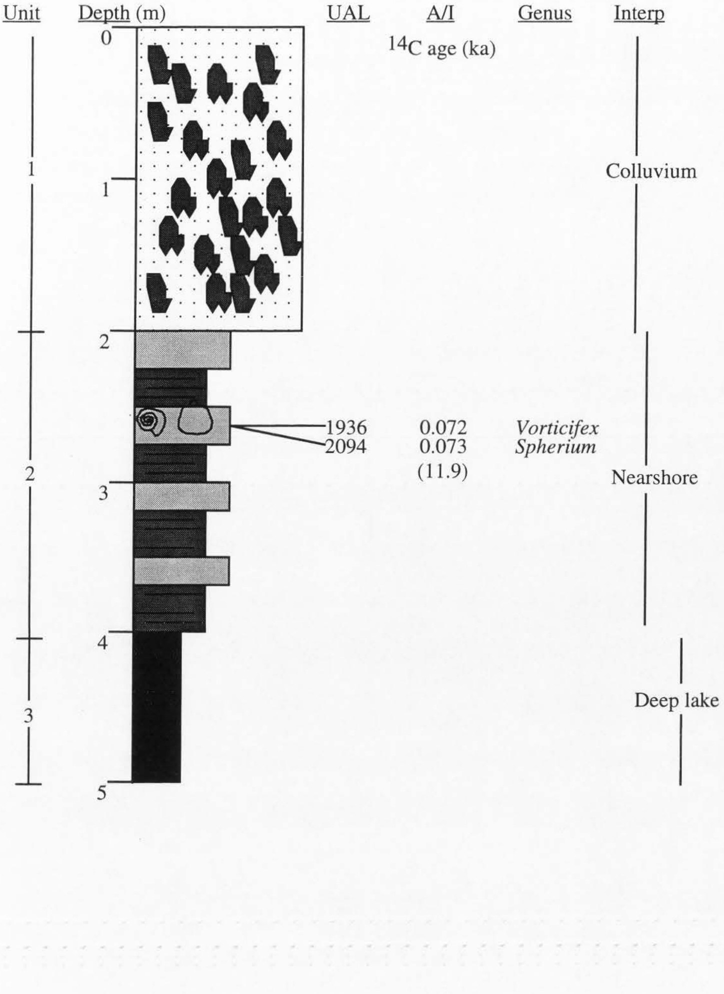

Figure 33. Stratigraphic section for Willow Creek (Site 29), Oregon. Information on radiocarbon dates in Table 2.

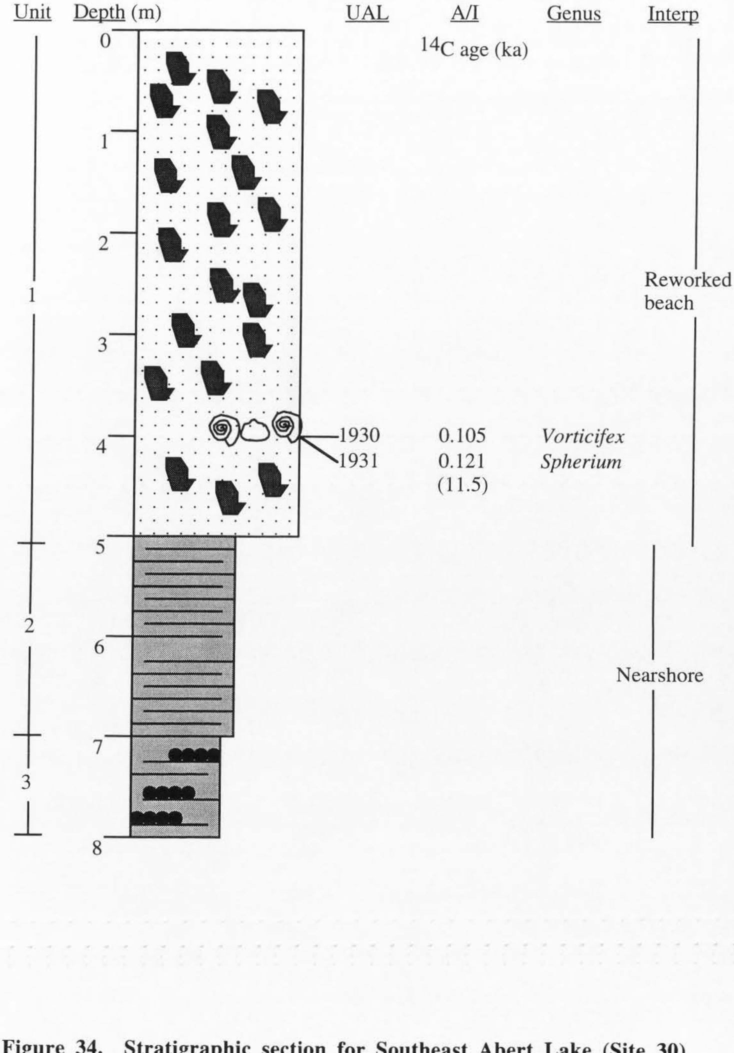

Figure 34. Stratigraphic section for Southeast Abert Lake (Site 30), Oregon. Information on radiocarbon dates in Table 2.

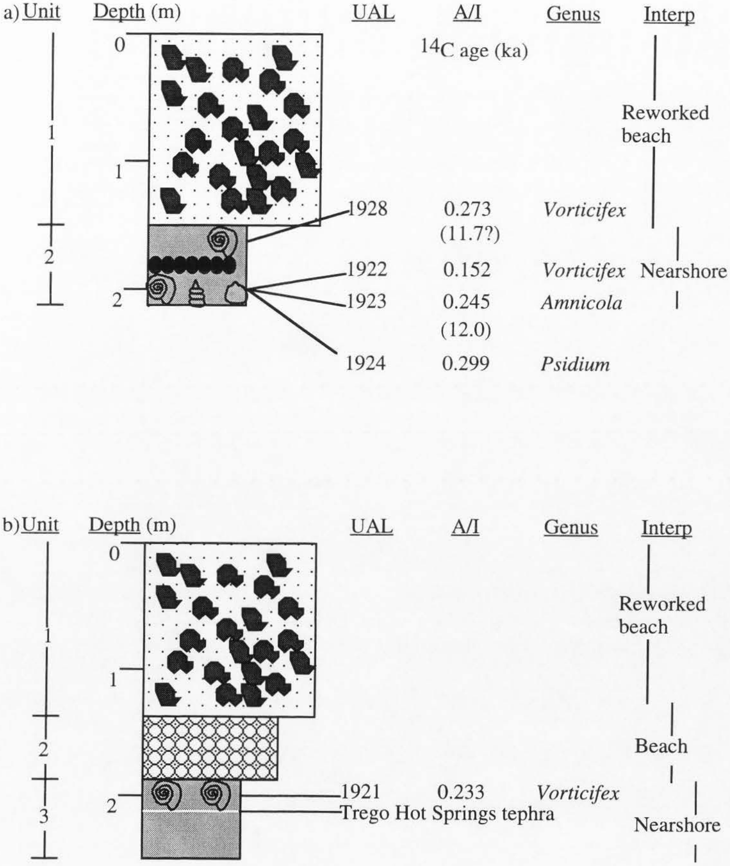

Figure 35. Stratigraphic section for (a) Northeast Abert Lake (Site 31), Oregon; and (b) Surprise Valley (Site 32), California. Information on radiocarbon dates in Table 2.

CHAPTER 4

DISCUSSION

SOURCES OF VARIATION

This section discusses possible sources of variation in the A/I data. This variation affects the determination of the age of lake episodes in both the Lahontan and Chewaucan basins. The two main types of variation exhibited in my data are: (1) the variation in A/I ratios among shells collected from the same bed, and (2) the variation among shells of the same genus determined to be approximately the same age by radiocarbon dating, but with markedly different A/I ratios (Table 2). The latter variation is the most difficult to reconcile and an example of this variation is in the samples from Sand Ramp (Site 1) and from Jessup (Site 3). The *Vorticifex* shells at each of these outcrops have been radiocarbon dated at ~12 to 13 ka, but their A/I ratios are significantly different (Table 3). These variations may be due to a number of factors discussed below.

Analytical Variation

Amino Acid Analyzer. To monitor the amount of drift in the A/I measured by the amino acid analyzer, the Utah State University Amino Acid Laboratory analyzes inter-laboratory calibration standards (ILC, Wehmiller, 1984) several times a month. The data (not included in this thesis) show little systematic variation through time. Given the reproducibility of analytical results and the lack of machine drift, I conclude that the amino acid analyzer is not responsible for differences in A/I between shells in one bed, or for differences among shells of different beds.

Sample Preparation. Although caution is taken (shells are not touched with hands, and sterile equipment is used), some contamination may enter during shell preparation in the laboratory. Usually, it is possible to identify modern contamination by high concentrations of serine and glycine, or by just a few shells having much lower ratios than the other shells. Because my data do not show this, I conclude that contamination in the laboratory is not responsible for the variability obtained in this study.

Geologic Variation

Diagenesis. Protein diagenesis is discussed in Chapter 2. It is possible that different sites had different diagenetic histories. Shells from some sites may have been affected by the introduction of contaminants or microbial metabolism, leading to aberrant A/I ratios. Ellis and others (1996) attempted to assess variation in racemization rates among samples of land snails from archeological sites at Fort Hood, in central Texas. They determined that the effects of systematic errors in racemization rates could not be quantitively distinguished but that independent contextual data, such as landscape position, depositional processes, evidence of disturbance, or surface fire, did affect the A/I ratios of individual shells. Although my A/I ratios were determined from freshwater shells, all of the above contextual factors could have affected the thermal history of my shells and altered their racemization rates. Therefore, some of my sites may have been thermally affected by landscape position, depositional processes, disturbances, or fire and may have caused variation in A/I values of shells in one bed or variations among shells of different beds.

Sampling Strategy. As previously mentioned in Chapter 2, the most significant factor affecting the rate of racemization is temperature. To minimize the effects of seasonal temperature fluctuations, samples must be collected at sufficient depth where the amplitude of the temperature wave is less than ~6°C (Miller and Brigham-Grette, 1989). Although the depth at which this damping is attained varies with specific sediment factors, shells should be retained at least 1 m below the sediment surface throughout their depositional history (Miller and Brigham-Grette, 1989).

About 90% of my samples were collected 1 m below the surface. All were from at least 0.5 m below the surface. However, ~50% of my samples were collected above a depth of 3 m where seasonal variations in temperature may alter the racemization rates in fossil shells. Because all of my sites are in basins at similar elevations in northwest Nevada and southeast Oregon, they probably experienced similar seasonal temperature variations. However, it is possible that the thermal histories of some sites may have been affected by other processes. The Great Basin is geologically active. Shells buried in the Lahontan and Chewaucan basins may have been close enough to hot springs to be thermally affected. Because the mean annual temperature of shallow lake water is typically higher than the adjacent air temperature, a site that has been underwater for a longer period of time would have experienced a higher average temperature than one that was emerged longer. Therefore, I conclude that different thermal histories at different sites may be responsible for some of the variability in the racemization rates, specifically, the differences between stratigraphic units at different sites believed to be approximately the same age.

Reworking

Reworking of older shells into younger deposits may explain the differences in A/I values among individual shells in a single bed. Actually, differences in amino acid ratios among shells from the same bed are often used as evidence for reworking (Murray-Wallace and others, 1993; Wehmiller and others, 1995). Goodfriend and Stanley (1996) suggested that two processes could be involved in reworking: (1) *in situ* mixing by burrowing activity, and (2) redeposition from older sediment. Many of my sites show evidence of reworking by redeposition from older sediment. Other than A/I values showing a wide range, the evidence for redeposition includes: (1) broken shell concentrations, (2) shell concentrations consisting of similarly sized shells, and (3) the presence of shell concentrations in beach deposits. Therefore, the variability in A/I ratios among shells in a single bed is probably in part due to reworking.

Taxonomic Variation

The reliability of different genera for amino acid geochronology is known to vary (Miller and Brigham-Grette, 1989). The C.V. is typically below 10% for five well-preserved mollusc shells of a single population, although taxa with high natural variability may have a C.V. closer to 20% (Miller and Brigham-Grette, 1989).

To determine which genera produced the most consistent results, and if a particular genus was responsible for the variation in samples from the Lahontan and Chewaucan basins, I evaluated the C.V. for all of the genera analyzed for this study (Table 6). The C.V. ranged from 9 to 21% for the seven genera (Table 6). For genera with five or more A/I results, *Physa* produced the most consistent data with an average C.V. of 9.4%. *Lymnaea*, the most commonly used genus for geochronology, had a C.V. of 10.8%. *Vorticifex*, the principal genus used in this study, had an average C.V. of 11%, suggesting that the natural variability of this genus is not higher than other molluscs.

Summary

No single cause can be identified that accounts for all the variation in the data. I conclude that the variation in A/I ratios among shells at different sites, determined to be approximately the same age by radiocarbon dating, is probably due to differences in diagenetic and thermal histories among sites. However, it is impossible to determine to what extent each factor affected the A/I ratios in the fossils shells. More research is needed to address the physical and chemical processes that control racemization during fossil diagenesis.

Overall, however, the amino acid data from this study are reliable enough to separate the deposits of both Lake Lahontan and Lake Chewaucan into distinct relative-age groups that are probably separated by tens of thousands of years. Shells collected from sediments representing a distinct lake cycle have A/I ratios that cluster together and are distinguishable from shells with A/I ratios representing other lake cycles (discussed below). Despite the variability, lake cycles can be separated based on A/I ratios, and this allows the geochronology of Lake Lahontan and Lake Chewaucan to be determined.

LAKE LAHONTAN

In the Lahontan basin, at least five episodes of Quaternary lake expansion can be differentiated on the basis of stratigraphic position, previously published radiometric ages, and aminostratigraphy. A histogram of A/I ratios in *Vorticifex* and *Physa* shells in the Lahontan basin was plotted to assess the relative-age distribution of lake deposits (Figure 36a). Six clusters of A/I ratios are evident. These clusters, termed "aminozones" (Nelson, 1978) represent periods of lacustrine sedimentation, whereas the absence of A/I ratios is suggestive of periods of nondeposition during episodes low lake levels. In addition, the broad Eetza aminozone is separated into three subzones. These will be referred to as the late, middle, and early Eetza aminozones.

The six aminozones are mostly derived from sediments within the Carson Desert and Pyramid-Winnemuca subbasins. A crude hydrograph can be constructed for these two subbasins by plotting the elevation and mean A/I measured in *Vorticifex*, *Lymnaea*, *Physa*, and *Amnicola* and drawing a smooth curve connecting the upper elevations of the shells (Figure 37). The assumptions in this approach are that isostatic rebound was minimal, all the shells were collected from nearshore deposits, all sites experienced similar temperature histories, all the genera racemized at approximately the same rate, and gaps between clusters of A/I ratios indicate a lowering of the lake. I conclude from this figure that possibly six episodes of Quaternary lake expansion can be differentiated in the Lahontan basin. Also, the lacustrine history of both the Carson Desert and Pyramid-Winnemuca subbasins are similar.

Because the names Sehoo and Eetza have long been associated with the two latest lake episodes and alloformations (Morrison, 1965c, 1991), and because the general chronostratigraphy as originally presented is broadly consistent with mine, the names of these episodes and alloformations will be retained here as a first-order subdivision of lake deposits. However, these two alloformations may include deposits of multiple lake cycles. I will discuss the aminostratigraphy and assign each aminozone to a lake cycle. Then I will attempt to correlate each aminozone with previously determined lake cycles in the Bonneville basin.

Pre-Eetza Aminozone

The oldest lacustrine deposits found in this study are in a gravel pit southwest of Sehoo Mountain in western Wyemaha Valley at an elevation of ~1256 m (Site 7, Figure 2). This may be the same locality where Morrison and Frye (1965) found their "older pre-Lahontan" deposits and where McCoy (1981) found "pre-Eetza deposits." However, this is difficult to know because the pit has been excavated periodically since their studies. The old lake deposits consist of alternating beach and nearshore sediments overlain by colluvium (Figure 17). The A/I ratios in *Physa* shells in the nearshore sediment range from 0.766 to 0.839 (Table 3). McCoy (1981) measured similar ratios in the *Physa* shells that he collected near this location. Although these deposits were not overlain by Eetza deposits, the high A/I ratios indicate that they formed in a lake that occupied the Carson Sink subbasin prior to the Eetza lake cycle.

Eetza Aminozone

At least two and possibly three lake expansions during the Eetza lake episode are discernable on the basis of A/I ratios in fossil molluscs. Morrison (1991) found stratigraphic evidence for three episodes of expansion during the Eetza lake episode at the Rye Patch Dam area, ~50 km north of Lovelock, Nevada (Figure 2). Along the Truckee River, south of Nixon, Nevada, several outcrops extend as low as 1220 m elevation. Stratigraphic relations in these exposures indicate that the Eetza Alloformation represents at least six and possibly eight lake cycles (Morrison, 1991). However, neither the exposure at Rye Patch Dam or the sites along the Truckee River contained shells, so it is impossible to determine whether my three amino-based lake cycles are the same as Morrison's stratigraphically based cycles.

Deposits of the Eetza Alloformation are exposed at the Railroad Cut (Site 15, Figure 2). Morrison (1965c) originally assigned the beach sand and gravel at this site to the Eetza Alloformation. A collection of *Vorticifex* from near the top of the exposure yielded an A/I ratio of 0.278 ± 0.047 (UAL-2178) (Table 4). Two collections of *Vorticifex* shells from near the bottom of the exposure yielded A/I ratios of 0.390 ± 0.038 (UAL-1867) and 0.368 ± 0.031 (UAL-2179). These collection are separated by a gravel layer, which represents a lowered lake level, and their A/I ratios are distinct enough to be separated into two aminozones. I assign the upper portion to the late Eetza aminozone and the lower portion of this exposure to a middle Eetza aminozone, while recognizing that evidence for the middle Eetza aminozone is tentative.

Other evidence for a lake expansion late during the Eetza lake cycle is in the Carson Sink subbasin at the Wyemaha and the West Wyemaha Valley sites (Sites 5 and 6, Figure 2). The outcrop at Wyemaha Valley, at an elevation of ~1244 m, consists of deeper water sediment (fine sand and silt) than at the Railroad Cut site. *Vorticifex* shells collected from this site yielded an average A/I ratio of 0.321 ± 0.011 (UAL-2093). *Vorticifex* shells from

West Wyemaha Valley, at an elevation of ~1219, m yielded an average A/I ratio of 0.298 ± 0.013 (UAL-2195). The ratios from these two sites overlap at ± 1 SD, and both are distinct from those at the bottom of the Railroad Cut outcrop, evidence of a late Eetza lacustrine expansion in both the Carson Sink and Pyramid-Winnemuca subbasins.

Deposits of the oldest Eetza subzone were found at West Sehoo Mountain (Site 6, Figure 2) and South Sehoo Mountain (Site 8, Figure 2). Three collections of *Vorticifex* from nearshore deposits at West Sehoo Mountain yielded A/I ratios that all overlap at ± 1 SD (Table 3). These nearshore deposits also contain *Lymnaea* shells. Three collections yielded A/I ratios that overlap at ± 1 SD (Table 3). At South Sehoo Mountain, the A/I ratio in *Vorticifex* is indistinguishable from A/I ratios at the West Sehoo Mountain site. Because the A/I ratios at these two sites are distinctly higher (> 0.1) than the ratios from other units previously assigned to the Eetza Alloformation in both the Carson Sink and the Pyramid-Winnemuca subbasins, I assign these deposits to the early Eetza aminozone.

On the basis of A/I ratios of included shells, Eetza lake deposits can be clearly distinguished from older and younger lacustrine deposits. The Eetza lake episode seems to have been a period of fluctuating lake levels including intervals of deep-lake deposition in the Lahontan basin. Although the amino acid data indicate at least two and possibly three separate aminozones representing distinct lake cycles, the absence of a geosol between the aminozones indicates a lack of subaerial exposure. This might mean that Lake Lahontan was never below ~1220 m between maxima of the Eetza lake cycles.

Sehoo Aminozone

Sehoo lacustrine deposits represent the last deep-lake cycle in the Lahontan basin. Deposits of at least three lake-level oscillations have been recognized previously (e.g., Morrison 1991), but have not been characterized using amino acid analysis. Benson (1978, 1993), Benson and others (1995), and Benson and Thompson (1987) used radiocarbon dates to determine the history of the last rise and fall of Lake Lahontan. The last rise and fall correlates with Morrison's Sehoo Alloformation, although direct correlation between the radiocarbon chronology and the stratigraphic units has not been mentioned in the literature.

Sehoo lake deposits can be clearly distinguished from Eetza lake deposits on the basis of their A/I ratios in mollusc shells (Tables 4 and 5). However, only one episode of lake expansion can be discerned for the Sehoo age deposits with amino acid analysis. At the Railroad Cut site (Site 15), Morrison (1965c) separated deposits overlaying the Churchill geosol into the Lower Sehoo and Dendritic Sehoo members. However, the A/I ratios in fossils shells from these two units overlap slightly (0.113 ± 0.012 (UAL-2169); 0.140 ± 0.018 (UAL-2177/1866)) (Table 4). I was not able to find another stratigraphic section that Morrison had previously separated into multiple Sehoo members and in which there were shells. Older Sehoo deposits might be present at Upper Fallon Pit 3 (Site 12). *Vorticifex* shells from this site have A/I ratios of 0.177 ± 0.010 (UAL-2192) and 0.141 ± 0.010 (UAL-2193). However, there is no radiocarbon evidence to assess the possibility that these are older deposits of the Sehoo Alloformation.

A/I ratios in *Vorticifex* determined to be Sehoo in age by radiocarbon dating range from 0.083 to 0.252 (Tables 3 and 4). Ratios in other genera (*Lymnaea*, *Physa*, *Amnicola*, *Planorbella*) also radiocarbon-dated as Sehoo in age range from 0.071 to 0.223 (Tables 3 and 4). For some sites I cannot be confident that the amino acid analysis are on shells from the same beds that were radiocarbon-dated. However, where I am confident that I analyzed shells from the same unit, the correlation between radiocarbon age and A/I ratio is poor (Figure 38a). For example, three units at Sand Ramp (Site 1) were dated by AMS radiocarbon at ~13 ka (Table 2) and A/I ratios in shells collected from his outcrop range from 0.196 to 0.252 (Table 2). The reason for these discrepancies is unknown. Amino acid ratios did correlate with the radiocarbon ages from the Sehoo Alloformation at some sites. For example, shells at the Jessup site (Site 3) were dated at ~13 ka (Table 2), and A/I ratios in shells collected from the same beds ranged from 0.117 to 0.123 (Table 3). However, the overall variability of A/I ratios in shells of Sehoo age hampers attempts to subdivide the Sehoo aminozone.

Holocene Aminozone

The only evidence of a Holocene lake expansion that I found is from the shore of Pyramid Lake in the Pyramid-Winnemuca subbasin. At Blanc Tetons and Pelican Point (Sites 17 and 19), shells are encrusted in tufa mounds 10 to 15 m above the present 1156 m elevation of Pyramid Lake. The mean A/I ratios in *Vorticifex* from the Blanc Tetons are 0.068 ± 0.012 (UAL-1960) and 0.059 ± 0.029 (UAL-1957) at Pelican Point. Radiocarbon ages on tufa from Blanc Tetons range from ~9 to 20 ka and ~20 to 35 ka at Pelican Point (Benson and others, 1996). However, different parts of these tufa mounds are different ages, and the age relation of the tufa to the shells encrusted on the mounds is unknown. If the A/I ratios are age diagnostic, then they represent a minor (10 to 15 m above present) Holocene lake expansion confined to the Pyramid-Winnemuca subbasin.

Other apparently young shells were found at Pyramid Island (Site 14). They yielded an A/I ratio of 0.077 ± 0.030 (UAL-1978) and are probably Holocene shells reworked on the beaches of Pyramid Lake. Another possible Holocene site has a higher elevation and lower A/I ratios than the other sites. North Pyramid Lake (Site 13) at ~1190 m contains *Vorticifex* shells encrusted in a tufa mound. These shells yielded a mean ratio of 0.024 ± 0.003 (UAL-1848) and may represent an expansion of Pyramid Lake. This may be the same site where shells have been radiocarbon dated at ~19 ka (Benson, 1978). I could not be certain.

Morrison (1991) suggested that, during the Holocene, the Lahontan basin was dry or held temporary shallow lakes. During the early and late Holocene, shallow lakes existed in the Carson Desert, Humboldt, Pyramid, and Winnemuca Valleys (below 1200 m). Possibly Blanc Tetons, Pelican Point, and North Pyramid Lake sites represent a small lake expansion in the Pyramid Lake subbasin during the Holocene. These shells may be associated with the Fallon Formation, which records a lake rise in the Carson Desert to 1205 m at ~4 ka (Morrison, 1991).

LAKE CHEWAUCAN

In the Chewaucan basin, two episodes of Quaternary lake expansion can be differentiated on the basis of stratigraphic position, previously published radiometric ages, and aminostratigraphy. A/I measured in fossil *Vorticifex* from the Chewaucan basin can be subdivided into three aminozones (Figure 36b). Stratigraphic and geomorphic evidence for the most recent lake cycle in the Chewaucan basin is abundant. However, only two sites exhibit evidence for older lake cycles.

Older Aminozone

Definitive evidence for an early expansion of Lake Chewaucan occurs at Burrow Pit (Site 26) where A/I ratios in *Vorticifex* averaged 0.403 ± 0.036 (UAL-1933) (Table 5). *Vorticifex* shells from this bed were radiocarbon dated at ~22 ka (Table 2), which I interpret as a non-infinite, minimum age. Situated ~80 m above the Ana River section (see below), this site may record a higher, older lake level, which I assigm to the "older aminozone."

Ana River Aminozone

Evidence for another lake expansion is at two sites in the Chewaucan basin. At Ana River (Site 27), A/I ratios in *Vorticifex* averaged 0.270 ± 0.021 (UAL-1935). A thermoluminescence (TL) analysis on lake sediment 10 cm above these shells yielded an age of ~165 ka (Berger 1991; Table 2). These shells are also below what is interpreted as last-interglacial (stage 5) deposits (Davis, 1985). However, the lake deposits at this site may not record a deep lake throughout the Chewaucan basin. Davis (1985) suggested that the Chewaucan River, which now flows southeastward into Lake Abert, may have previously flowed northward into Summer Lake. If the Chewaucan River did flow into Summer Lake during earlier interpluvial periods, then a higher, permanent lake may have persisted there during those episodes.

Younger Aminozone

As previously mentioned, Allison (1982) found evidence for six fluctuations in the level of Lake Chewaucan. However, he did not interpret each fluctuation as a separate cycle because the chronology was too poorly known. Freidel (1993) proposed evidence for two episodes of lake expansion during the late Pleistocene (Figure 6). The youngest emerged lacustrine deposits in the Chewaucan basin can be clearly differentiated from the older deposit on the basis of A/I ratios in molluscs shells (Table 5). However, as with the Sehoo aminozone, the correlation between radiocarbon age and A/I ratios is weak (Figure 38b).

Evidence for one lake expansion is exhibited in the Lower Chewaucan Marsh subbasin. Fossil shells of *Vorticifex* from Tucker Hill (Site 28, Figure 3) were dated at ~12.1 ka (Table 2) and had an average A/I of 0.134 ± 0.006 (UAL-1714). Also, fossil shells of *Vorticifex* from Willow Creek (Site 29) were dated at ~11.9 ka (Table 2) and had an average A/I of 0.072 ± 0.003 (UAL-1936), significantly lower than ratios from the same genus at Tucker Hill.

Evidence for the same lake expansion is exhibited in the Lake Abert subbasin. Fossil shells of *Vorticifex* from Southeast Abert Lake (Site 30) were dated at ~11.5 ka (Table 2) and had an average A/I of 0.105 ± 0.011 (UAL-1930). Similarly, shells of *Vorticifex* from Northeast Abert Lake (Site 31) were dated at ~11.6 ka (Table 2). The average A/I in shells of *Vorticifex* from the upper two beds was 0.273 ± 0.014 (UAL-1928) and 0.152 ± 0.021 (UAL-1922) from the lower shell layer (Figure 39). However, there is a striking similarity between the unexpectedly high A/I ratios from the upper bed at this site (0.273 ± 0.014 (UAL-1928)) and the A/I ratios from the Ana River site (0.270 ± 0.021(UAL-1935)). This might indicate that the shells were reworked into the Abert shoreline deposits, but that they were formed at the same time as those in the Ana River section. However, a new radiocarbon analysis of *Amnicola* from the lower bed at Northeast Abert Lake (Site 31) indicates an age of ~12 ka (Table 2) and does not support this interpretation. Nonetheless, I tentatively identify the Ana River aminozone as represented by shells with A/I ratios between the younger aminozone and the older aminozone. This includes UAL-1928 from the Northeast Abert site.

CORRELATION OF LAHONTAN AND CHEWAUCAN BASINS

The extent of racemization in mollusc shells can be used to correlate lacustrine deposits between the Lahontan and Chewaucan basins. The direct correlation of A/I ratios between the two basins assumes that the two areas have experienced similar thermal histories. The present mean annual temperatures (MAT) of the Lahontan and Chewaucan basins are quite similar. The MAT of the Chewaucan basin is ~ 9.0°C (Freidel, 1993). The Lahontan basin has a MAT of ~ 9.5°C (data from Donald Jenson, Utah Climate Center). However, it is difficult to determine whether these two basins experienced similar average temperatures during the Quaternary. Although the Chewaucan basin is about 200 km north and 100 m higher than the Lahontan basin, their similar current MAT suggests that their climatic histories are sufficiently similar for this correlation.

The average A/I ratio in *Vorticifex* shells from the Sehoo aminozone (0.145 ± 0.039) overlap at ± 1 SD with the mean A/I ratio measured in *Vorticifex* shells from the younger aminozone found in the Chewaucan basin (0.118 ± 0.031) (Table 7). Also, radiocarbon ages from the Chewaucan basin (~13 to 11 ka) are bracketed by the ages of shells in the Sehoo Alloformation (~19 to 12 ka). The direct correlation of the Sehoo aminozone with deposits of the last lake cycle in the Chewaucan basin lends confidence to correlations among older aminozones in the two basins, if it is assumed that the temperatures in the Lahontan and Chewaucan basins fluctuated similarly through time.

Although I analyzed only two collections of shells from older lake deposits in the Chewaucan basin, the A/I ratios overlap with those from the Eetza aminozones in the Lahontan basin. *Vorticifex* samples from the middle Eetza aminozone average 0.379 ± 0.016 (Table 7), which overlaps the mean A/I in *Vorticifex* shells from the older aminozone (0.403 ± 0.035). Alternatively, the older aminozone may correlate with the early Eetza aminozone that contained *Vorticifex* shells averaging 0.459 ± 0.010 (Table 7). If the long-term MAT of the Chewaucan basin was lower than the Lahontan basin, then this correlation may be more likely. Also, the average A/I in *Vorticifex* shells within the tentative Ana River aminozone (0.272 ± 0.002) overlap with the average A/I from the late Eetza aminozone (0.299 ± 0.022). Presently, the data are too sparse to allow a secure conclusion for either of these correlations.

CORRELATION OF LAHONTAN AND BONNEVILLE BASINS

At its maximum elevation of 1552 m (Currey, 1982), Lake Bonneville covered about 51,700 km^2 (Morrison, 1965a) in the northwestern part of Utah during the late Pleistocene. The first systematic investigation of Lake Bonneville was by Gilbert (1890) whose interpretation of Lake Bonneville was based primarily on geomorphic and stratigraphic evidence. Several later workers produced significantly different interpretations of the history of the lake. Morrison (1965b) reviewed the investigations of Lake Bonneville. More recently, Scott and others (1983) presented their interpretation of

Quaternary lake cycles in the Bonneville basin, and Currey and Oviatt (1985) and Oviatt and others (1992) have further refined our understanding of the last lake cycle.

The study of Lake Bonneville most relevant to mine was by McCoy (1981, 1987). McCoy recognized at least four distinct deep-lake cycles of Pleistocene lakes in the Bonneville basin on the basis of isoleucine epimerization in fossil gastropod shells. Deposits of the earliest recognized cycle contain the Lava Creek tephra (~660 ka). Three younger lake cycles in the Bonneville basin are represented by lacustrine deposits of the Pokes Point (~200 ka), Little Valley (~140 ka), and Bonneville Alloformations (~25 to 11 ka).

To correlate lacustrine deposits between two basins by comparing unadjusted A/I ratios, the basins must have experienced similar thermal histories. The present MATs of the Lahontan and Bonneville basins are within 1°C. The Bonneville basin has a MAT of ~10.5°C (McCoy, 1987). The Lahontan basin has a MAT of ~ 9.5°C (data from Donald Jensen, Utah Climate Center). The basins may have experienced different temperatures in the past. However, if the temperatures were different, then clusters and gaps in the distribution of A/I data would be shifted, but still feasible to correlate. The mean A/I ratio in *Vorticifex* shells from the 35- to 12-ka Sehoo Alloformation (0.145 ± 0.039) overlap with the mean A/I ratio measured in *Lymnaea* shells by McCoy (1987) from the 25- to 11-ka Bonneville Alloformation (0.11 ± 0.03) (Figure 40a). The similarity in ratios is consistent with: (1) A/I ratios in *Amnicola* shells of the two alloformations that overlap between the two basins and (2) laboratory heating experiments and fossil evidence that demonstrate that shells of *Vorticifex* and *Lymnaea* racemize at similar rates (Chapter 2).

The correlation of Sehoo and Bonneville Alloformations lends confidence to correlations among older lake units in the two basins, if it is assumed that the temperatures in the Lahontan and Bonneville basins fluctuated equally through time. Differences between A/I ratios from the Eetza Alloformation suggest that it records two or three distinct lake cycles, an interpretation supported by previously reported stratigraphic evidence (Morrison, 1991). The mean A/I ratios from the late and early Eetza aminozones overlap with the mean A/I ratios from the Little Valley and Pokes Point Alloformations in the Bonneville basin, respectively (Figures 40b and 40c). Although McCoy (1987) measured A/I in *Lymnaea* shells in the Bonneville basin, my data show that *Lymnaea* shells racemize at a similar rate to *Vorticifex*. *Amnicola*, on the other hand, tend to racemize about 40% faster than *Lymnaea* (Light, 1997). Therefore, the overlap between A/I ratios in *Amnicola* from the Pokes Point Alloformation in the Bonneville basin and both *Lymnaea* and *Vorticifex* from the early Eetza aminozone in the Lahontan basin (Figure 40c) suggests that the Pokes Point Alloformation may be somewhat younger than the early Eetza aminozone or, alternatively, that Lahontan was somewhat warmer over the long term. However, the difference in A/I ratios between the Little Valley and Pokes Point Alloformations in the Bonneville basin is similar to the difference in A/I ratios between the late and early Eetza aminozones in the Lahontan basin. This similarity suggests correlative lacustrine histories between the two basins during this time period.

The middle Eetza aminozone in the Lahontan basin does not have a known correlative in the Bonneville basin. The middle Eetza may represent a lake oscillation only recorded in the Lahontan basin or it may not record a lake oscillation at all.

The high A/I ratios from the pre-Eetza deposits in the Carson subbasin suggest a correlation with the deep lake that occupied the Bonneville basin during the eruption of the Lava Creek tephra (Figure 40d). Two collections of *Lymnaea* shells in lacustrine sediments below this tephra in the Bonneville basin have an average A/I ratio of 0.81 ± 0.04 (McCoy, 1987). These results overlap the mean A/I ratios in three *Physa* shells from Southwest Sehoo Mountain (Site 7, Figure 2) in the Lahontan basin (0.813 ± 0.038; Table 7). *Lymnaea* and *Physa* shells found together in the same stratigraphic unit have yielded nearly identical ratios (Table 8, Figure 41). Because shells of *Vorticifex* and *Lymnaea* also racemize at the same rate (Chapter 2), it is significant that *Vorticifex* and *Physa* shells of the same age also yielded nearly identical ratios (Table 8, Figure 41). However, heating experiments should be done to further evaluate the difference in racemization rates between the two genera.

On the basis of these correlations between the Lahontan and Bonneville basins, I constructed a hydrograph for the Lahontan basin to compare with McCoy's (1987) hydrograph of the Bonneville basin (Figure 42). The similarity in aminostratigraphy indicates that the Lahontan and Bonneville basins experienced similar lake-level histories during the past ~660 ka.

AGES OF LAHONTAN BASIN LAKE CYCLES

To estimate the ages of Eetza deposits in the Lahontan basin, I calibrated the rate of amino acid racemization from eight *Vorticifex* collections whose ages were known: (1) modern shells with an average A/I ratio of 0.008 ± 0.001 (UAL-2062; Table 1), (2) shells from six radiocarbon-dated units listed in Table 2, and (3) shells from ~10 cm below a tephra with a thermoluminescence (TL) date of 165 ± 19 ka (Berger, 1991) at Ana River (Site 27, Figure 3). Further information on the dates from these sites is listed in Table 2.

I developed a calibration curve based on shells in the Chewaucan basin alone because: (1) there were more sites where I was sure that I collected shells at exactly the same places as those dated by radiocarbon, and (2) the use of shells from both basins might impose uncertainty if the two basins experienced different thermal histories.

Most kinetic models are based on reaction rates under constant temperature. Because fossil shells are invariably exposed to fluctuating temperatures, fossils of different ages have different EDT's and, therefore, the rate of racemization is not expected to conform to conventional first-order kinetic model. Instead, I used an empirical fit to the data, one based on a parabolic kinetic model (Mitterer and Kriausakul, 1989). This model closely fits my data, and yielded an r^2 of 0.850 (Figure 43). Linear regression yields the following age equation for *Vorticifex*:

$$t = (1450.177A/I - 46.441)^2 \tag{2}$$

where t is sample age in years. The associated age uncertainty is estimated from the 90% confidence envelope about the slope of the least-squares linear-regression line. The actual error should be least from age estimates between the calibration points, and becomes increasingly large as age estimates are extrapolated beyond the calibration points. Because my calibration points are not distributed evenly along the regression line, estimated error beyond the mean is somewhat exaggerated.

Holocene and Sehoo Aminozones

I have not attempted to estimate the ages of Holocene and Sehoo age deposits from the calibrated amino acid geochronology. Because the rate of isoleucine epimerization is relatively low and the ages of the deposits relatively young, the temporal resolution is not sufficient. Also, as previously mentioned, the data are too variable to attempt a reasonable age determination. Finally, the lake-level history of the last rise and fall of Lake Lahontan is already rather well known based on radiocarbon dating.

Late Eetza Aminozone

To estimate the age of the late Eetza aminozone, the average A/I ratio (0.299; Table 7) in shells of *Vorticifex* was applied to the calibration curve (Figure 43). The age estimate is 145 +95/-50 ka. The mean age is considered reasonable for several reasons: (1) Morrison (1991) suggested that the late Eetza lake cycle occurred ~200 to 150 ka on the basis of the presence of the poorly dated Wadsworth tephra, (2) Broecker and Kaufman (1965) developed a shell sample L-773L, which gave a U-Th age of 110 ± 15 ka from the Carson Desert, and (3) the A/I ratios overlap A/I ratios from the Little Valley Alloformation in the Bonneville basin, which has been correlated with marine oxygen-isotope stage 6 (~160 to 140 ka) by Scott and others (1983).

Early Eetza Aminozone

To estimate the age of the early Eetza aminozone, the average A/I ratio (0.459; Table 7) in *Vorticifex* was applied to the calibration curve (Figure 43). The age estimate is 385 + 270/- 160 ka. Again, the mean age is considered reasonable because: (1) the 400-ka Rockland tephra lies near the top of the Pauite Alloformation, which underlies the Eetza Alloformation (Morrison, 1991), (2) two U-Th dates on snail shells from the Eetza Alloformation gave ages of 215 +60/-45 ka and 288 +100/-70 ka (Morrison, 1991), and (3) the A/I ratios overlap with A/I ratios from the Pokes Point Alloformation in the Bonneville basin, which is estimated to be ~200 ka on the basis of amino acid ratios and the inferred age of the Little Valley Alloformation (McCoy, 1987).

If the average A/I ratio (0.379; Table 7) in *Vorticifex* shells for the middle Eetza aminozone were applied to the calibration curve, the age estimate would be between the estimates for the late and early Eetza aminozones. Together, the amino acid data indicate a prolonged Eetza lacustrine episode lasting from ~385 to 145 ka and including at least two lake cycles.

Pre-Eetza Aminozone

As previously discussed, *Physa* shells racemize at about the same rate as those of *Vorticifex* and *Lymnaea*. Therefore, to estimate the age of the pre-Eetza aminozone, the average A/I ratio (0.813; Table 7) in *Physa* was applied to equation 2. The age estimate is ~1250 +995/-645 ka. The mean estimate is highly speculative because of the increasingly large uncertainty as the calibration curve, developed mainly from late Quaternary data, is extrapolated to the middle Quaternary.

The A/I ratios in *Physa* shells from the oldest, pre-Eetza deposits overlap with those of *Lymnaea* shells from lake deposits that contain the Lava Creek tephra in the Bonneville basin. That tephra has been dated 660 ± 100 ka (Izett and others, 1992). If the 0.813 A/I ratios from the pre-Eetza deposits are ~660 ka, then either the calibration is in error or the EDT of the late Quaternary was considerably lower then during the middle Quaternary. The suggestion that the middle Quaternary was warmer than the late Quaternary is supported by evidence from a core from Owens Lake, a closed basin on the western edge of the Great Basin. A 323-m-long core, OL-92, from this lake represents ~800 ka of deposition (Smith and Bischoff, 1997). According to lithologies and fossil assemblages in OL-92, the period between 645 and 450 ka was more arid than from 450 to 10 ka (Smith and Bischoff, 1997). This period of aridity could be due to higher temperatures in the Great Basin that caused greater evaporation from lakes. Therefore, this warm period may have increased the EDT of the older shells in both the Bonneville and Lahontan basins.

I conclude that the 0.813 A/I ratios from the pre-Eetza deposits are ~660 ka and not ~1.2 Ma as suggested by the calibration curve. The calibration curve is uncertain beyond the control points. The correlation with ~660 ka deposits in the Bonneville basin seems secure because: (1) the sparse data show that *Physa* and *Lymnaea* shells racemize at similar rates, (2) the Bonneville and Lahontan basins probably experienced similar thermal histories during the Quaternary, and (3) independent data suggest that the middle Quaternary was warmer than the late Quaternary and may have increased the EDT of the older shells in both the Lahontan and Bonneville basins.

Morrison (1991) suggested that the Rye Patch Alloformation records a middle Pleistocene major lake cycle. The lower member of the formation contains the ~630 ka Rye Patch tephra and the upper member contains the 660-ka Lava Creek B tephra in the Humboldt Valley subbasin. These members record a lake rise above 1285 m (Morrison, 1991). Although Morrison believed that the Lava Creek B tephra was ~620 ka, Izett and others (1992) more recently dated the Lava Creek B tephra at ~660 ka. More work is needed to improve the age of the Rye Patch Alloformation.

An exposure of the Rye Patch Alloformation is also found in the Carson Desert subbasin where shells exposed at ~1220 m altitude gave two U-Th ages of 330 +110/-50 ka and 400 +200/-70 ka (Broecker and Kaufman, 1965). Although these ages are too young for the Rye Patch Alloformation based on tephrochronology, the last cited U-Th age is nearly correct. Because A/I ratios in *Physa* shells from pre-Eetza deposits overlap with A/I ratios in *Lymnaea* shells from lake deposits that contain the ~660 ka Lava Creek tephra in the Bonneville basin, I tentatively correlate the pre-Eetza aminozone with the Rye Patch Alloformation.

TABLE 6. COEFFICIENT OF VARIATION (C.V.) FOR SHELLS OF DIFFERENT GENERA ANALYZED IN THIS STUDY

Genus	Average C.V. (%)	N*
Vorticifex	11.0	54
Lymnaea	10.8	5
Amnicola	17.3	8
Physa	9.4	6
Psidium	4.5	1
Spherium	21.4	2
Planorbella	12.7	1
Average	12.4	Total 77

*N = number of samples

TABLE 7. MEAN A/I RATIOS FOR LAHONTAN AND CHEWAUCAN AMINOZONES

Aminozone	Genus	A/I	± 1 SD	N*
Lahontan basin				
Holocene	*Vorticifex*	0.057	0.023	4
Holocene	*Amnicola*	0.069	-	1
Sehoo	*Vorticifex*	0.145	0.039	30
Sehoo	*Amnicola*	0.127	0.026	3
Sehoo	*Physa*	0.078	0.009	2
Late Eetza	*Vorticifex*	0.299	0.022	3
Middle Eetza	*Vorticifex*	0.379	0.016	2
Early Eetza	*Vorticifex*	0.459	0.010	5
Early Eetza	*Lymnaea*	0.447	0.025	3
Pre-Eetza	*Physa*	0.813	0.038	4
Chewaucan basin				
Younger	*Vorticifex*	0.118	0.031	5
Younger	*Amnicola*	0.209	0.051	2
Younger	*Psidium*	0.183	0.101	3
Younger	*Spherium*	0.093	0.025	3
Ana River	*Vorticifex*	0.272	0.002	2
Older	*Vorticifex*	0.403	-	1

* N = number of samples; data listed in Tables 3 to 5

TABLE 8. A/I RATIOS MEASURED IN FOSSIL SHELLS OF DIFFERENT GENERA OF THE SAME AGE

Lab ID	*Lymnaea* A/I	*Vorticifex* A/I	*Physa* A/I	Location	Reference
AAL 889, 887	0.39		0.39	Searles Lake basin	McCoy (1987)
UAL 1748, 1747	0.028		0.025	Deseret	Oviatt (unpublished)
UAL 2203, 2204		0.113	0.084	Lahontan basin	This study
UAL 2200, 2206		0.083	0.071	Lahontan basin	This study

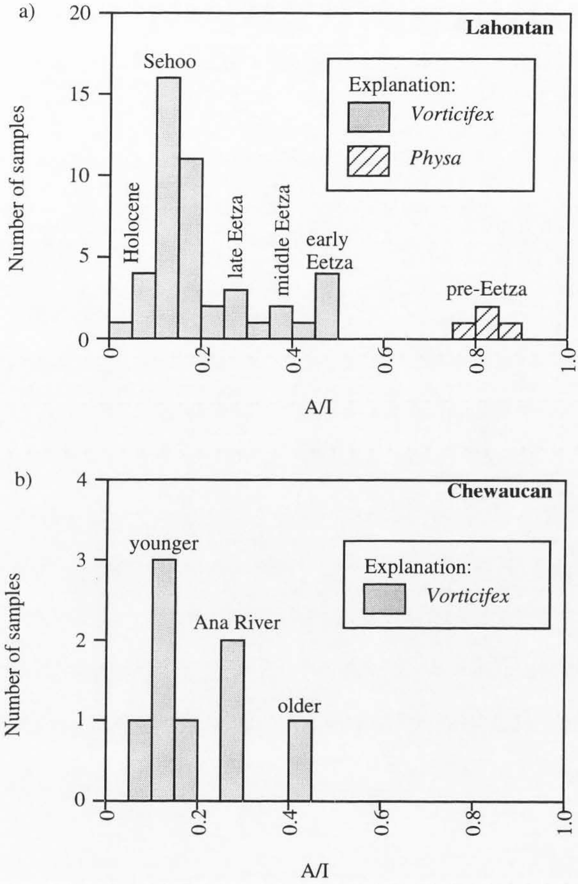

Figure 36. Frequency distribution of A/I measured in fossil shells collected from (a) the Lahontan basin, Nevada, and (b) the Chewaucan basin, Oregon. Data are listed in Tables 3 to 5.

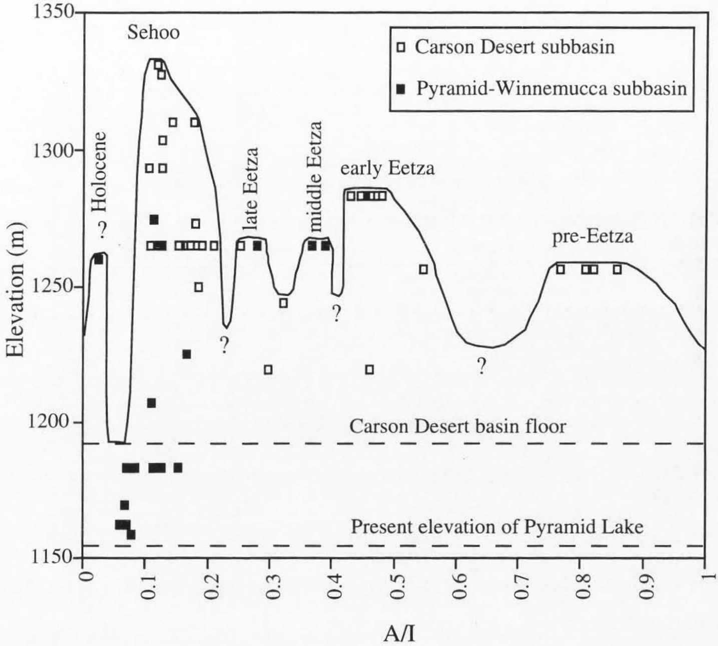

Figure 37. Elevation and A/I measured in *Vorticifex*, *Lymnaea*, *Physa*, and *Amnicola* from the Carson Desert and Pyramid-Winnemuca subbasins, Nevada. Solid line represents minimum lake levels interpreted from data and dashed line represents base level for each subbasin.

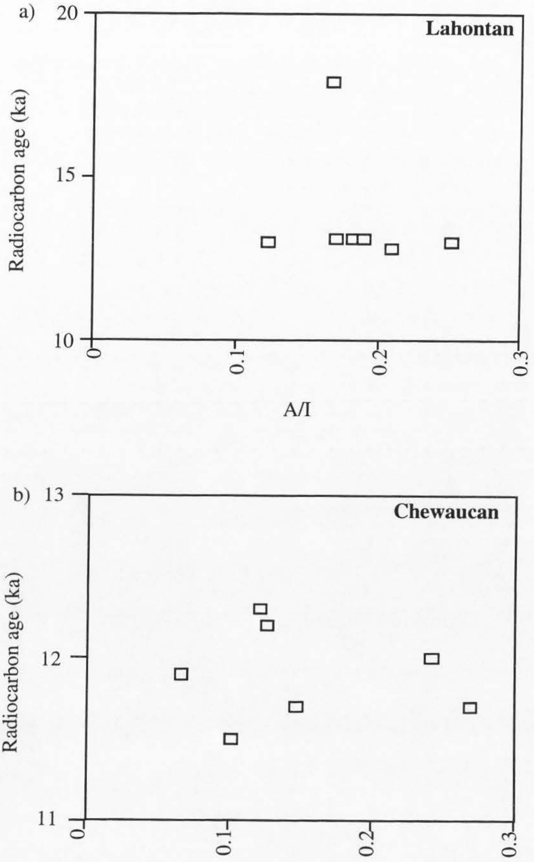

Figure 38. Comparison of radiocarbon ages and measured A/I in *Vorticifex* from (a) the Lahontan basin, Nevada, and (b) the Chewaucan basin, Oregon. Data are listed in Table 2.

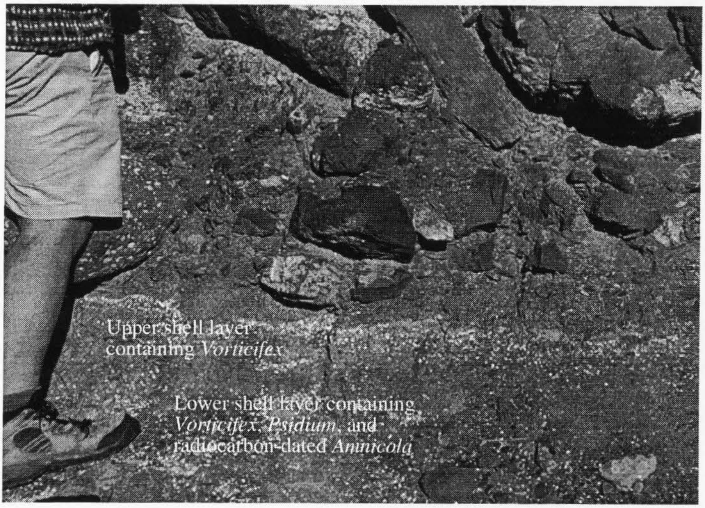

Figure 39. Exposure at Northeast Abert Lake (31), Oregon, exhibits two concentrated shell layers.

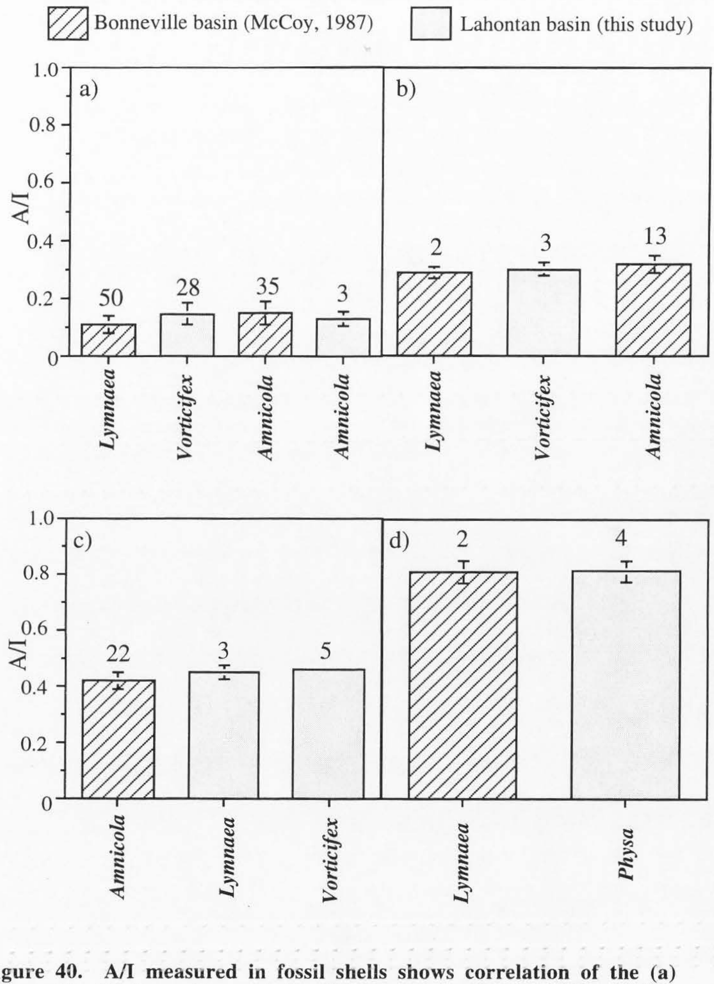

Figure 40. A/I measured in fossil shells shows correlation of the (a) Bonneville Alloformation and the Sehoo aminozone, (b) Little Valley Alloformation and the late Eetza aminozone, (c) Pokes Point Alloformation and the early Eetza aminozone, and (d) pre-Pokes Point deposits and the pre-Eetza aminozone. Numbers indicate number of samples. Bars indicate one standard deviation.

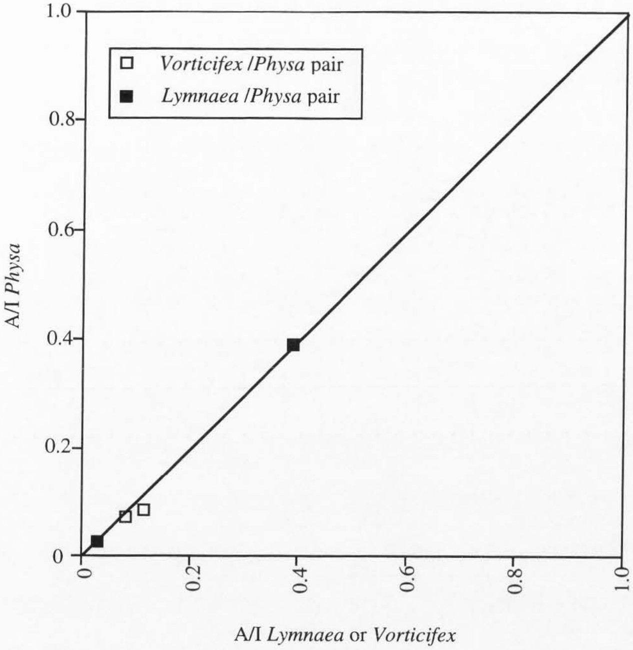

Figure 41. Relationship between A/I measured in fossil *Physa* and that in fossil *Lymnaea* and *Vorticifex*. Line shows 1:1 relationship.

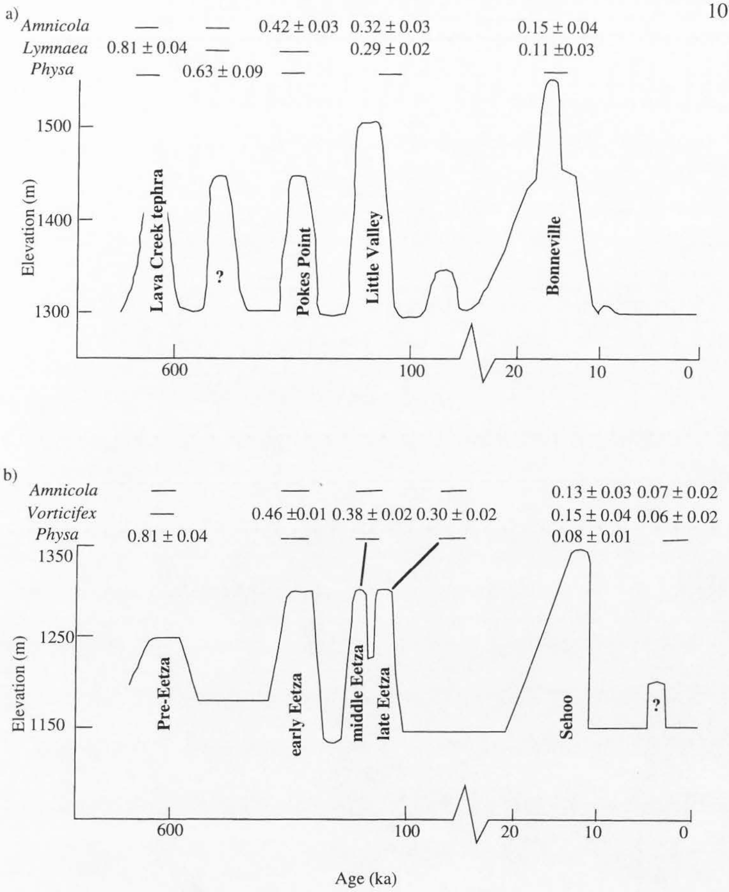

Figure 42. Comparison of hydrographs for: (a) Bonneville basin (McCoy, 1987) and (b) Lahontan basin based on A/I ratios from this study (Table 7).

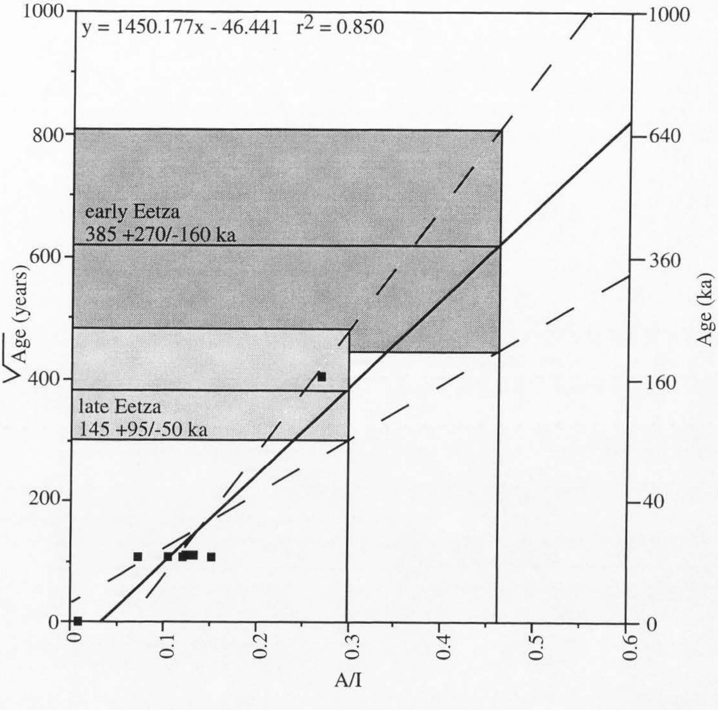

Figure 43. Amino acid calibration curve for *Vorticifex* from the Chewaucan basin, Oregon, providing the age of the late and early Eetza deposits. Dashed lines are 90% confidence limits for the linear regression. See text for explanation of calibration points.

CHAPTER 5

SUMMARY AND CONCLUSIONS

LAKE SUMMARY

The Quaternary lake-level history of Lake Lahontan includes evidence for five and possibly six lake cycles. Shells with the highest A/I ratios (~0.8) from the Carson Desert subbasin suggest a correlation with the deep lake that occupied the Bonneville basin during the eruption of the Lava Creek tephra ~660 ka. These old lake deposits might correlate with the Rye Patch Alloformation, named for deep-lake sediments deposited in the Lahontan basin ~660 ka. However, no shells were found in the type area of the Rye Patch Alloformation to test this correlation.

No lake deposits have been found in the age range of ~660 to 400 ka. The geological record is dominated by alluvium and eolian sand deposits and paleosols during this interval, which suggests low lake levels in the Lahontan basin (Morrison, 1991). The next younger lake deposits are ascribed to the Eetza Alloformation (Morrison, 1991). Based on amino acid data, the age of the early Eetza lake expansion was calculated to be 385 +270/-160 ka and the age of the late Eetza lake expansion was calculated to be 145 +95/-50 ka. The age estimate for the middle Eetza is between the estimates for the late and early Eetza lake expansions. Therefore, two and possibly three distinct lake expansions took place during the Eetza lacustrine episode. This determination agrees with Morrison's (1991) and McCoy's (1981) interpretations of a prolonged Eetza lacustrine episode. The amino acid data therefore indicate that the Eetza Alloformation includes deposits of at least two and possibly three lake cycles that lasted from ~385 to 145 ka.

The time between the formation of Eetza and the next younger Sehoo lacustrine deposits is represented by the Wyemaha Alloformation (Morrison, 1991). This formation includes subaerial and shallow-lake deposits. The age of the Sehoo Alloformation is determined from previous radiocarbon dates to be ~35 to 12 ka (e.g., Benson, 1996). Deposits of Sehoo age can be clearly differentiated from older lacustrine deposits on the basis of A/I ratios in mollusc shells. Although the amino acid data could not be used to subdivide the Sehoo into separate lake cycles, a more detailed geochronology of Sehoo lacustrine deposits that correlated tephras (Davis, 1978, 1983), U-series dates on snail shells (Morrison, 1965a), and radiocarbon dates on carbonates (e.g., Benson and others 1990) determined three episodes of lake expansion in deposits of the Sehoo Alloformation.

The only amino acid evidence for a Holocene lake expansion was in the Pyramid Lake subbasin. Shells encrusted in tufa mounds 10 to 15 m above the present 1156 m elevation of Pyramid Lake may represent a minor lake expansion during the Holocene. Shells encrusted in tufa at the North Pyramid Lake site at ~1190 m may represent a higher subsequent lake expansion during the late Holocene. Those higher-than-present lake deposits may be associated with Fallon Alloformation, which was deposited in shallow lakes during the Holocene (Morrison, 1991).

The Quaternary lake-level history of the Chewaucan basin includes evidence for at least two major lake episodes. The younger deposits can be clearly differentiated from older lacustrine deposits on the basis of A/I ratios in mollusc shells. They are similar in radiocarbon ages and A/I ratios as deposits of the Sehoo Alloformation in the Lahontan basin. The amino acid data differentiate only one lake expansion during the late Wisconsin, even though Freidel (1993) found evidence for two. However, I probably sampled only one of the two units that have been described in the basin.

Although the amino acid data are sparse, there were probably at least one and possibly two earlier lake expansions in the Chewaucan basin. Evidence for the oldest high lake is found at Burrow pit (Site 26) where the A/I ratios are similar to A/I ratios from the middle or early Eetza lake expansion in the Lahontan basin. A high stand of intermediate age is represented by ~165 ka shells at Ana River (Site 27) in the Summer lake subbasin, which are similar to A/I ratios from the late Eetza aminozone in the Lahontan basin. However, it is not clear that the deep lake in the Summer Lake subbasin extended throughout the Chewaucan basin.

In conclusion, this study has improved the understanding of the history of the Quaternary lakes in the Lahontan and Chewaucan basins. This is the first report of one and possibly two middle Pleistocene lake expansions in the Chewaucan basin. Although more research has been done in the Lahontan basin, this study has improved on the knowledge of the timing of lake expansions during the Eetza lacustrine episode. Although Morrison (1991) had independent evidence for more lake cycles during the Eetza lake episode than I found, the timing of the Eetza lake episode was not previuosly well understood.

CORRELATIONS BETWEEN BASINS

The amino acid data can be used to correlate deposits in the Lahontan basin with those in the Bonneville basin. The correlation of the Sehoo Alloformation with the Bonneville Alloformation using A/I ratios and radiocarbon dates of fossil shells (Figure 40a) lends confidence to correlations between older lake units in the two basins.

Although the correlations are crude, the amino acid data suggest that Lake Lahontan and Lake Bonneville experienced similar lake-level histories through the past ~660 ka. The late and early aminozones within the Eetza Alloformation in the Lahontan basin correlate, respectively, with amino acid data (McCoy, 1987) from the Little Valley and Pokes Point Alloformations in the Bonneville basin (Figure 42). The high A/I ratios from the Carson subbasin in the Lahontan basin suggest a correlation with the deep lake that occupied the Bonneville basin during the eruption of the Lava Creek tephra. This correlation assumes that *Lymnaea* and *Physa* shells racemize at similar rates and that the Bonneville and Lahontan basins experienced similar thermal histories during the Quaternary.

CLIMATE IMPLICATIONS

The amino acid calibration curve estimates the age of the pre-Eetza aminozone to be over 1 Ma, even though the amino acid data suggest that it correlates with lake deposits that contain the Lava Creek tephra (~660 ka) in the Bonneville basin. One explanation for this discrepancy is that the pre-Eetza deposits experienced a higher EDT than the younger shells that were used to develop the calibration curve. Because the calibration curve assumes isothermal conditions through time, it is possible that EDT of the late Quaternary was considerably lower than during the middle Quaternary. This possibility is supported by a core from Owens Lake, in which the period between 645 and 450 ka was interpreted as more arid than from 450 to 10 ka (Smith and Bischoff, 1997). This period of increased aridity probably coincides with higher temperatures in the Great Basin during which the EDT in both the Lahontan and Bonneville basins was higher than subsequent interglaciations.

Although lake levels in closed basins fluctuate with climate, the type of climate changes that caused fluctuations in Great Basin lakes is not yet clear. Lakes could have fluctuated in response to many combinations of precipitation, cloudiness, temperature changes, and to changes in basin geography and tectonics. The apparent similarities in the lake-level histories of the Bonneville and Lahontan basins indicate that they responded to similar global or at least hemispheric changes in climate (e.g., Oviatt, 1997). The important question, then, is what caused the climate changes during the past 660 ka recorded by both the Lahontan and Bonneville lake-level histories?

One contribution to these climate changes may have been the effect of the Laurentide ice sheet on atmospheric-circulation patterns. Although the Laurentide ice sheet responded to global and other changes in climate, the size of the ice sheet affected hemispheric and regional climate (e.g., Thompson and others, 1993). The Laurentide ice sheet's most pronounced influence on atmospheric circulation in the General Circulation

Models (GCMs) is that it splits the jet stream into a north and south branch, or at least displaces the jet stream southward (Thompson and others, 1993). Evidence for the displaced jet stream is found in the ancient lakes, such as Lake Lahontan and Lake Bonneville, in the Great Basin. These lakes existed in now-arid areas. They may represent greater precipitation and cooler temperatures than present brought on by the southward-displaced jet stream (Benson, 1993).

Lake Lahontan experienced large and abrupt rises at 23.5 and 15.5 ka (Benson and others, 1995). The lake-level rise at 23.5 ka may record the passage of the jet stream southward during the expansion of the Laurentide ice sheet, and the lake-level rise at 15.5 ka may indicate the passage of the jet steam northward during the contraction of the ice sheet (Benson and others, 1995). Because Lake Lahontan seems to have had rather brief highstands, the core of the southern branch of the jet stream may have remained only briefly over the Lahontan basin. Although the general chronologies of the lake cycles of Lake Bonneville and Lake Lahontan are similar, the precise timing of particular fluctuations probably differs by some length of time. The varied hydrologic responses between these two basins would be expected due to a wandering jet stream and the effects of regional processes on climate patterns.

During the last highstand, surface areas of Lake Bonneville and Lake Lahontan increased by a factor of ~10, whereas surface areas of Lake Russell and Lake Searles increased by a factor of ~4 to 6 (Benson and others, 1990). It is possible that the mean track of the jet stream passed over Lake Bonneville and Lake Lahontan but passed north of Lake Russell and Lake Searles (Benson and other, 1990). Although the use of lake levels as evidence for changes in climate is complicated by lake/atmospheric feedback processes (Hostetler and others, 1994) and the effects of spills across adjoining subbasins, the differences in effective wetness may have been due to the locations of the basins relative to the position of the jet stream. However, by 11 to 10 ka, the effect of the ice sheet on the wind field had diminished and the position of the jet stream was much like that of today (Thompson and others, 1993). This may explain the rapid lowering of Lake Lahontan and Lake Bonneville during this time period (Benson and others, 1990).

Middle Pleistocene expansions and contractions of ice sheets and their effects on atmospheric circulation in North America may explain the older fluctuations in the Lahontan and Bonneville basins as well. The marine oxygen-isotope record shows that global ice volume, and presumably the Laurentide ice sheet, was smaller during older glaciations. In contrast, Reheis and Morrison (1997) suggested that older lakes in the Lahontan basin were much larger and deeper. Because the ice sheet was smaller, the jet stream may not have been displaced as far south and instead was positioned directly over the Lahontan basin for a longer period of time. They also suggest that the uplift of the Sierra Nevada increased the rain shadow through time, and/or drainage captures reduced the size of the Lahontan drainage basin to cause the reduction of successive lake levels in the Lahontan basin.

FUTURE WORK

As previously mentioned, the aspect of the amino acid data most difficult to reconcile is the variation in A/I ratios among shells determined to be approximately the same age. Although it is beyond the scope of this thesis, I found no single cause that accounts for all of the variation in the data. I believe that most of the variation is due to reworking of the shells, differences in diagenetic histories, or differences in sampling. It is impossible to determine to what extent each of these factors affected the A/I ratios in the fossil shells. More research is needed to address the physical and chemical processes that control racemization during fossil diagenesis. This research probably should concentrate on heating experiments of modern shells to induce racemization. These shells should be heated at different temperatures and in different sediment types to determine what environmental differences cause changes in A/I ratios in the shells. More specifically for my study, further heating experiments need to be done on shells of *Lymnaea*, *Vorticifex*, and *Physa* for longer durations to evaluate the differences or similarities among the rates of racemization for these three genera.

Further research should also be done on the middle to early Pleistocene deposits of the Lahontan basin. The lake-level history of the last rise and fall of Lake Lahontan is relatively well understood. Not well understood is the lake-level history of the Lahontan basin before the last lake cycle. One problem is the lack of exposures of older deposits. Discovery of new exposures with shells and tephra that could be correlated and dated would greatly contribute to our understanding of the lacustrine history of the Lahontan basin. Although some U-Th dates on tufa and shells from the Lahontan basin determined to be early Wisconsin in age are discussed by Oviatt and McCoy (1992), Lao and Benson (1988), and Broecker and Kaufman (1965), the geochronology of these older deposits needs to be improved. Radiocarbon analysis of Holocene shells and those thought to be early Sehoo in age based on amino acid data, and microprobe analysis of tephra found in my sections, could improve the geochronology of Lake Lahontan. Also, the use of new dating techniques at exposures where there are no tephras or fossils for age control could also improve the lake-level chronology of Lake Lahontan and other ancient Great Basin lakes. Cosmogenic isotope dating and TL are just two of many dating techniques that may be helpful in this area. This could improve the geochronology and help to better correlate and compare the lacustrine history of the Lahontan basin with other paleoclimate data, such as packrat middens, glacial distribution, and deep-sea cores.

REFERENCES CITED

Abelson, P.H., 1954, Organic constituents of fossils: Carnegie Institute Washington Yearbook, v. 53, p. 97-101.

Adams, K.D., 1997, Late Quaternary pluvial history, isostatic reboound, and active faulting in the Lake Lahontan basin, Nevada and California [Ph.D. dissertation]: Reno, University of Nevada, 169 p.

Allison, I.S., 1982, Geology of pluvial Lake Chewaucan, Lake County, Orgeon: Studies in Geology No. 11. Corvallis, Oregon State University Press, 79 p.

Bada, J.L., 1982, Racemization of amino acids in nature: Interdisciplinary Science Reviews, v. 7, p. 30-46.

Bada, J.L. and Schroeder, R.A., 1975, Amino acid racemization reactions and their geochemical implications: Naturwissenschaften, v. 62, p. 71-79.

Benson, L.V., 1978, Fluctuation in the level of pluvial Lake Lahontan during the last 40,000 years: Quaternary Research, v. 9, p. 300-318.

Benson, L.V., 1993, Factors affecting ^{14}C ages of lacustrine carbonates: Timing and duration of the last highstand lake in the Lahontan Basin: Quaternary Research, v. 39, p. 163-174.

Benson, L.V., 1994, Carbonate deposition, Pyramid Lake subbasin, Nevada: 1. Sequence of formation and elevational distribution of carbonate deposits (tufas): Paleogeography, Paleoclimatology, Paleoecology, v. 109, p. 55-87.

Benson, L.V., and Thompson, R.S., 1987, The physical record of lakes in the Great Basin, *in* Ruddiman, W.F., and Wright, H.E., Jr., eds., North America and adjacent oceans during the last deglaciation: Boulder, Geological Society of America, The Geology of North America, v. K-3, p. 241-260.

Benson, L.V., Currey, P.R., Dorn, R.I., Lajoie, K.R., Oviatt, C.G., Robinson, S.W., Smith, G.I., and Stine, S., 1990, Chronology of expansion and contraction of four Great Basin lake systems during the past 35,000 years: Paleogeography, Paleoclimatology, Paleoecology, v. 78, p. 241-286.

Benson L., Currey, D., Lao, Y., and Hostetler, S., 1992, Lake-size variations in the Lahontan and Bonneville basins between 13,000 and 9,000 ^{14}C yr B.P.: Paleogeography, Paleoclimatology, Paleoecology, v. 95, p.19-32.

Benson L.V., Kasgarian, M., and Meyer, R., 1995, Carbonate deposition, Pyramid lake subbasin, Nevada: 2. Lake levels and polar jet stream positions reconstructed from radiocarbon ages and elevations of carbonate (tufas) deposited in the Lahontan basin: Paleogeography, Paleoclimatology, Paleoecology, v. 117, p. 1-30.

Benson, L.V., White, L.D., and Rye, R., 1996, Carbonate deposition, Pyramid Lake subbasin, Nevada: 4. Comparison of the stable isotope values of carbonate deposits (tufas) and the Lahontan lake-level record: Paleogeography, Paleoclimatology, Paleoecology, v. 122, p. 45-76.

Benson, L.V., Smoot, J.P., Kashgarian, M., Sarna-Wojcicki, A.M., and Burdett, J.W., 1997, Radiocarbon ages and environments of deposition of the Wono and Trego Hot Springs tephra layers in the Pyramid Lake subbasin, Nevada: Quaternary Research, v. 47, p. 251-260.

Berger, G.W., 1991, The use of glass for dating volcanic ash by thermoluminescence: Journal of Geophysial Research, v. 96, p. 19,705-19,720.

Bradley, R.S., 1985, Quaternary paleoclimatology: New York, Chapman Hall, 472 p.

Broecker, W.S., and Kaufman, A., 1965, Radiocarbon chronology of Lake Lahontan and Lake Bonneville II, Great Basin: Geological Society of America Bulletin, v. 76, p. 537-566.

Broecker, W.S., and Orr, P.C., 1958, Radiocarbon chronology of Lake Lahontan and Lake Bonneville: Bulletin of the Geological Society of America, v. 69, p. 1009-1032.

Broecker, W.S., and Walton, A.F., 1959, Reevaluation of the salt chronology of several Great Basin lakes: Bulletin of the Geological Society of America, v. 70, p. 601-618.

Currey, D.R., 1982, Lake Bonneville: Selected features of relevance to neotectonic analysis: U.S. Geological Open File Report 82-1070.

Currey, D.R., and Oviatt, C.G., 1985, Durations, average rates, and probable causes of Lake Bonneville expansions, stillstands, and contractions during the last deep-lake cycle: 32,000 to 10,000 years ago: Geographical Journal of Korea 10, p. 1085-1099.

Cupp, K., 1997, Pluvial history of late Pleistocene Lake Lahontan and isostatic rebound of the Fernley Sink subbasin: Churchill, Lyon, and Washoe counties, Nevada [Masters thesis]: Reno, University of Nevada, 128 p.

Davis, J.O., 1978, Quaternary tephrochronology of the Lake Lahontan area, Nevada and California: Nevada Archeological Survey Research Paper 7, 137 p.

Davis, J.O., 1983, Level of Lake Lahontan during deposition of the Trego Hot Springs tephra about 23,400 years ago: Quaternary Research, v. 19, p. 312-324.

Davis, J.O., 1985, Correlation of Late Quaternary tephra layers in a long pluvial sequence near Summer Lake, Oregon: Quaternary Research, v. 23, p. 38-53.

Ellis, G.L., Goodfriend, G.A., Abbott, J.T., Hare, P.E., and Von Endt, D.W., 1996, Assessment of integrety and geochronology of archeological sites using amino acid racemization in land snail shells: Examples from Cental Texas: Geoarcheology, v. 11, no.3, p. 189-213.

Fenneman, N.M., 1930, Physical divisions of the United States: U.S. Geological Survey Map, scale 1:7 million.

Freidel, D.E., 1993, Chronology and climatic controls of Late Quaternary lake-level flucuations in Chewaucan, Fort Rock, and Alkali basins, south-central Oregon [Ph.D. Dissertation]: Eugene, University of Oregon, 244 p.

Gilbert, G.K., 1890, Lake Bonneville: United States Geological Survey Monograph 1, 439 p.

Goodfriend, G.A., and Stanley, D.J., 1996, Reworking and discontinuities in Holocene sedimentation in the Nile Delta: documentation from amino acid racemization and stable isotopes in mollusk shells: Marine Geology, v. 129, p. 271-283.

Hare, P.E., and Abelson, P.H., 1968, Racemization of amino acids in fossil shells: Carnegie Institute Washington Yearbook, v. 66, p. 526-528.

Hare, P.E., and Mitterer, R.M., 1967, Nonprotein amino acids in fossil shells: Carnegie Institute Washington Yearbook, v. 65, p. 362-364.

Hare, P.E., and Mitterer, R.M., 1969, Laboratory simulation of amino diagenesis in fossils: Carnegie Institute Washington Yearbook, v. 67, p. 205-210.

Hoering, T.C., 1980, The organic constituents of fossil molluscs shells, *in* Hare, P.E., Hoering, T.C., and King, K., eds., Biogeochemistry of amino acids, New York, John Wiley and Sons, p. 193-201.

Hostetler, S.W., Giorgi, F., Bates, G.T., and Bartlein, P.J., 1994, Lake-atmosphere feedbacks associated with paleolakes Bonneville and Lahontan: Science, v. 263, p. 665-668.

Ingraham, N.L., and Taylor, B.E., 1989, The effect of snowmelt on the hydrogen isotope ratios of creek discharge in Surprise Valley, California: Journal of Hydrology, v. 106, p. 233-244.

Izett, G.A., Pierce, K.L., Naeser, N.D., and Jaworski, C., 1992, Isotopic dating of Lava Creek B tephra in terrace deposits along the Wind River, Wyoming: Implications for post 0.6 Ma uplift of the Yellowstone hotspot: GSA Abstracts with Programs 24, n. 7, p. A102.

Light, A., 1996, Amino acid paleotemperature reconstruction and radiocarbon shoreline chronology of the Lake Bonneville basin, USA [Masters thesis]: Logan, Utah State University, 142 p.

Lao, Y., and Benson, L., 1988, Uranium-Series Estimates and Paleoclimatic Significance of Pleistocene tufas from the Lahontan Basin, California and Nevada: Quaternary Research, v. 30, p. 165-176.

McCoy, W.D., 1981, Quaternary aminostratigraphy of the Bonneville and Lahontan basins, western U.S., with paleoclimatic implications [Ph.D. Dissertation]: University of Colorado, Boulder 181 p.

McCoy, W.D., 1987, Quaternary aminostratigraphy of the Bonneville Basin, western United States: Geological Society of America, v. 98, 0. 99-112.

Miller, G.H., and Brigham-Grette, J., 1989, Amino acid geochronology--Resolution and precision in carbonate fossils: Quaternary International, v. 1, p. 111-128.

Miller G.H., and Hare, P.E., 1980, Amino acid geochronology: integrity of the carbonate matrix and potential of molluscan fossils, *in* Hare, P.E., Hoering, T.C., and King, K.Jr., eds., Biogeochemistry of amino acids: New York, John Wiley and Sons, p. 415-443.

Mitterer, R.M., 1993, The diagenesis of proteins and amino acids in fossil shells, *in* Engel, M.H. and Macko, S.A., eds., Organic geochemistry: New York, Plenum Press, p. 739-753.

Mitterer, R.M., and Kriausakul, N., 1989, Calculation of amino acid racemization ages based on apparent parabolic kinetics: Quaternary Science reviews, v. 8, p. 853-857.

Morrison, R.B., 1964, Lake Lahontan: Geology of southern Carson Desert, Nevada: U.S. Geological Survey Professional Paper 401, 156 p.

Morrison, R.B., 1965a, Quaternary geology of the Great Basin, *in* Wright, H.E., Jr., and Frey, D.G., eds., The Quaternary of the United States: Princeton, New Jersey, Princeton University Press, p. 265-285.

Morrison, R.B., 1965b, New evidence on Lake Bonneville stratigraphy and history from southern Promontory Point, Utah: U.S. Geological Survey Professional Paper 525-C, p. 110-119.

Morrison, R.B., 1965c, Six guidebook articles; General features and stratigraphy of the Lake Lahontan area; Wave-built bars near Fallon turnoff (Eetza bar); South overlook; Railroad cut; Middle Overlook; North overlook, *in* International Association of Quaternary Research (INQUA), 7th Congress, Guidebook for Field Conference I (Northern Great Basin and California): Lincoln, Nebraska Academy of Science, p. 18-24, 33-35, 44-48.

Morrison, R.B., 1991, Quaternary stratigraphic, hydrologic, and climate history of the Great Basin, with emphasis on Lakes Lahontan, Bonneville, and Tecopa, *in* Morrison, R.B., ed., Quaternary non-glacial geology; conterminous U.S.: Boulder, Geological Society of America, The Geology of North America, v. K-2, p. 283-320.

Morrison, R.B., and Frye, J.C., 1965, Correlation of the middle and late Quaternary successions of the Lake Lahontan, Lake Bonneville, Rocky Mountain (Wasatch Range), southern Great Plains, and eastern Midwest areas: Nevada Bureau of Mines Report 9, 45 p.

Muller, P.J., 1984, Isoleucine epimerization in Quaternary planktonic Foraminifera: Effects of diagenetic hydrolysis and leaching, and Atlantic-Pacific intercore correlations: "Meteor" Forschungsergeb. Reihe C, v. 38, p. 25-47.

Murray-Wallace, C.V., Belperio, A.P, Gostin, V.A., and Cann, J.H., 1993, Amino acid racemization and radiocarbon dating of interstadial marine strata (oxygen isotope stage 3), Gulf St. Vincent, South Australia: Marine Geology, v. 110, p. 83-92.

Negrini, R.M., and Davis, J.O., 1992, Dating late Pleistocene pluvial events and tephras by correlating paleomagnetic secular variation records from the western Great Basin: Quaternary Research, v. 38, p. 46-59.

Negrini, R.M., Erbes, D.B., Roberts, A.P., Verosub, K.L., Sarna-Wojcicki, A.M., and Meyer, C.E., 1994, Repeating waveform initiated by a 180-190 ka geomagnetic excursion in western North America: Implications for field behaivor during polarity transitions and subsequent secular variation: Journal of Geophysical Research, v. 99, n. B12, p. 105-124.

Nelson, A.R., 1978, Quaternary glacial and marine stratigraphy of the Qivitu Peninsula, northern Cumberland Peninsula, Baffin Island, Canada [Ph.D. thesis]: Boulder, University of Colorado, 297 p.

Oviatt, C.G., 1997, Lake Bonneville flucuations and global climate change: Geology, v. 25, p. 155-158.

Oviatt, C.G., and McCoy, W.D., 1992, Early Wisconsin lakes and glaciers in the Great Basin, U.S.A., *in* Clark, P.U. and Lea, P.D., eds., The last interglacial-glacial transition in North America: Boulder, Colorado, Geological Society of America Special Paper 270, p. 279-287.

Oviatt, C.G., Currey, D.R., and Sack, D., 1992, Radiocarbon chronology of Lake Bonneville, eastern Great basin, USA: Paleogeography, Paleoclimatology, Paleoecology, v. 99, p. 225-241.

Reheis, M.C., and Morrison, R., 1997, High, old pluvial lakes of western Nevada: BYU Geological Studies, v. 42, Part I, p. 459-492.

Roberts, A.P., Verosub, K.L., and Negrini, R.M., 1994, Middle/Late Pleistocene relative paleointensity of the geomagnetic fields from lacustrine sediments, Lake Chewaucan, western United States: Geophysical Journal International, v. 118, p.101-110.

Russell, I.C., 1885, Geological history of Lake Lahontan: U.S. Geological Survey Monogram 11, 288 p.

Schroeder, R.A., and Bada, J.L., 1976, A review of the geochemical applications of the amino acid racemization reaction: Earth Science Reviews, v. 12, p. 347-391.

Scott, W.E., McCoy, W.D., Schroba, R.R., and Rubin, M., 1983, Reinterpretation of the exposed record of the last two lake cycles of Lake Bonneville, Western United States: Quaternary Research, v. 20, p. 261-285.

Sejrup H.P. and Haugen, J., 1994, Amino acid diagenesis in the marine bivalve *Arctica Islandica* Linne from northwest European sites--only time and temperature?: Journal of Quaternary Science, v. 9, p. 301-309.

Smith G.I., and Bischoff, J.L., 1997, An 800,000-year Paleoclimatic record from Core OL-92, Owens Lake, Southeast California: Geological Society of America Special Paper 317, 165 p.

Snyder, C.T., Hardman, G., and Zdenek, F.F., 1964, Pleistocene lakes in the Great Basin: U.S. Geological Survey Miscellaneous Geologic Map I-416, scale 1:5 million.

Thompson, R.S., Whitlock, C., Bartlein, P.J., Harrison, S.P., and Spaulding, W.G., 1993, Climatic changes in western United States since 18,000 yr B.P., *in* Wright, H.E., Jr., Kutzbach, J.E., Webb, T., Ruddiman, W.F., Street-Perrott, F.A., and Bartlein, P.J., eds., Global Climates since the last glacial maximum: Minneapolis, University of Minnesota Press, p. 514-523.

Wehmiller, J.F., 1980, Intergeneric differences in apparent racemization kinetics in molluscs and foraminifera; Implications for models of diagenetic racemization, *in* Hare, P.E., Hoering, T.C., and King, K., Jr., eds., Recent advances in biogeochemistry of amino acids: New York, John Wiley and Sons, p. 341-355.

Wehmiller, J.F., 1984, Interlaboratory comparison of amino acid enantiomeric ratios in fossil Pleistocene molluscs: Quaternary Research, v. 22, p. 109-120.

Wehmiller, J.F., 1993, Application of organic geochemistry for Quaternary research: Aminostratigraphy and aminochronology, *in* Engel, M.H. and Macko, S.A., eds., Organic geochemistry: New York, Plenum Press, p. 755-783.

Wehmiller, J.F., York, L.L., and Bart, M.L., 1995, Amino acid geochronology of reworked Quaternary mollusks on U.S. Atlantic coast beaches: implications for chronostratigraphy, taphonomy, and coastal sediment transport: Marine Geology, v. 124, p. 303-337.

Zar, J.H., 1984, Biostatistical analysis: Englewood Cliffs, New Jersey, Prentice-Hall, 718 p.

APPENDIX

TABLE A1. A/I DATA FOR MOLLUSCS HEATED AT 120°C

		aIle/Ile (A/I)								
UAL-	Genus	a	b	c	d	e	Mean	± 1 SD	C.V.	Time (days)
2062 A	*Vorticifex*	0.007	0.010				**0.009**	**0.002**	**25.0**	0
2062 B	*Vorticifex*	0.006	0.007				**0.007**	**0.001**	**10.9**	
2062 C	*Vorticifex*	0.008	0.009				**0.009**	**0.001**	**8.3**	
2062 D	*Vorticifex*	0.007	0.008				**0.008**	**0.001**	**9.4**	
2062 E	*Vorticifex*	0.007	0.008				**0.008**	**0.001**	**9.4**	
2062 F	*Vorticifex*	0.007	0.007				**0.007**	**0.000**	**0.0**	
2062 G	*Vorticifex*	0.008	0.007				**0.008**	**0.001**	**9.4**	
							0.008	**0.001**	**9.7**	
2063 A	*Vorticifex*	0.114	0.097	0.105			**0.105**	**0.009**	**8.1**	5
2063 B	*Vorticifex*	0.075	0.074				**0.075**	**0.001**	**0.9**	
2063 C	*Vorticifex*	0.075	0.071				**0.073**	**0.003**	**3.9**	
2063 D	*Vorticifex*	0.084	0.098				**0.091**	**0.010**	**10.9**	
2063 E	*Vorticifex*	0.073	0.068				**0.071**	**0.004**	**5.0**	
							0.083	**0.015**	**18.0**	
2064 A	*Vorticifex*	0.164	0.167				**0.166**	**0.002**	**1.3**	12
2064 B	*Vorticifex*	0.159	0.157				**0.158**	**0.001**	**0.9**	
2064 C	*Vorticifex*	0.167	0.164				**0.166**	**0.002**	**1.3**	
2064 D	*Vorticifex*	0.174	0.165				**0.170**	**0.006**	**3.8**	
							0.165	**0.005**	**2.9**	
2065 A	*Vorticifex*	0.299	0.277	0.289			**0.288**	**0.011**	**3.8**	23
2065 B	*Vorticifex*	0.280	0.263	0.275			**0.273**	**0.009**	**3.2**	
2065 C	*Vorticifex*	0.292	0.275	0.287			**0.285**	**0.009**	**3.1**	
2065 D	*Vorticifex*	0.299	0.276	0.279			**0.285**	**0.013**	**4.4**	
							0.283	**0.007**	**2.4**	
2066 A	*Vorticifex*	0.378	0.352				**0.365**	**0.018**	**5.0**	37
2066 B	*Vorticifex*	0.409	0.381	0.409			**0.400**	**0.016**	**4.0**	
2066 C	*Vorticifex*	0.427	0.401	0.419			**0.416**	**0.013**	**3.2**	
2066 D	*Vorticifex*	0.413	0.370	0.393			**0.392**	**0.022**	**5.5**	
2066 E	*Vorticifex*	0.477	0.441	0.452			**0.457**	**0.018**	**4.0**	
							0.406	**0.034**	**8.3**	
2067 A	*Lymnaea*	0.007	0.008	0.007			**0.007**	**0.001**	**7.9**	0
2067 B	*Lymnaea*	0.007	0.008				**0.008**	**0.001**	**9.4**	
2067 C	*Lymnaea*	0.008	0.007				**0.008**	**0.001**	**9.4**	
2067 E	*Lymnaea*	0.009	0.011	0.008			**0.009**	**0.002**	**16.4**	
							0.008	**0.001**	**12.0**	

2068 A	*Lymnaea*	0.087	0.085			**0.086**	**0.001**	**1.6**	5
2068 B	*Lymnaea*	0.097	0.099			**0.098**	**0.001**	**1.4**	
2068 C	*Lymnaea*	0.093	0.089			**0.091**	**0.003**	**3.1**	
2068 D	*Lymnaea*	0.091	0.103			**0.097**	**0.008**	**8.7**	
2068 E	*Lymnaea*	0.094	0.104			**0.099**	**0.007**	**7.1**	
2068 F	*Lymnaea*	0.100	0.103			**0.102**	**0.002**	**2.1**	
						0.095	**0.006**	**6.1**	
2069 A	*Lymnaea*	0.196	0.193			**0.195**	**0.002**	**1.1**	12
2069 B	*Lymnaea*	0.204	0.202			**0.203**	**0.001**	**0.7**	
2069 C	*Lymnaea*	0.204	0.198			**0.201**	**0.004**	**2.1**	
2069 D	*Lymnaea*	0.170	0.171			**0.171**	**0.001**	**0.4**	
2069 E	*Lymnaea*	0.166	0.170			**0.168**	**0.003**	**1.7**	
						0.187	**0.017**	**9.0**	
2070 A	*Lymnaea*	0.299	0.287			**0.293**	**0.008**	**2.9**	23
2070 B	*Lymnaea*	0.255	0.277	0.271		**0.268**	**0.011**	**4.2**	
2070 C	*Lymnaea*	0.274	0.299	0.288		**0.287**	**0.013**	**4.4**	
2070 D	*Lymnaea*	0.259	0.274			**0.267**	**0.011**	**4.0**	
2070 E	*Lymnaea*	0.285	0.288			**0.287**	**0.002**	**0.7**	
						0.280	**0.012**	**4.4**	
2071 A	*Lymnaea*	0.433	0.436			**0.435**	**0.002**	**0.5**	37
2071 C	*Lymnaea*	0.474	0.466			**0.470**	**0.006**	**1.2**	
2071 D	*Lymnaea*	0.462	0.440	0.427	0.404	**0.433**	**0.024**	**5.6**	
2071 E	*Lymnaea*	0.496	0.464	0.462		**0.474**	**0.019**	**4.0**	
						0.453	**0.022**	**4.9**	

TABLE A2. RESULTS OF AMINO ACID ANALYSIS OF FOSSIL SHELLS FROM LAHONTAN AND CHEWAUCAN BASINS

			aIle/Ile (A/I)							
UAL-	Field-ID	Genus	a	b	c	d	e*	Mean	± 1 SD	C.V.
1848 A	JB96-13A	*Vorticifex*	0.022	0.032	0.024			**0.026**	**0.005**	**20.4**
1848 B	JB96-13A	*Vorticifex*	0.026	0.027	0.028			**0.027**	**0.001**	**3.7**
1848 D	JB96-13A	*Vorticifex*	0.022	0.022				**0.022**	**0.000**	**0.0**
1848 E	JB96-13A	*Vorticifex*	0.021	0.023				**0.022**	**0.001**	**6.4**
								0.024	**0.003**	**10.8**
1864 A	JB96-1B	*Vorticifex*	0.134	0.133	0.133			**0.133**	**0.001**	**0.4**
1864 B	JB96-1B	*Vorticifex*	0.172	0.166	0.161	0.163		**0.166**	**0.005**	**2.9**
1864 C	JB96-1B	*Vorticifex*	0.138	0.147	0.143	0.138		**0.142**	**0.004**	**3.1**
1864 D	JB96-1B	*Vorticifex*	0.109	0.110	0.100	0.099		**0.105**	**0.006**	**5.6**
1864 E	JB96-1B	*Vorticifex*	0.134	0.146	0.143	0.147		**0.143**	**0.006**	**4.2**
								0.137	**0.022**	**16.0**
1865 A	JB96-2A	*Vorticifex*	0.225	0.198				**0.212**	**0.019**	**9.0**
1865 B	JB96-2A	*Vorticifex*	0.179	0.195				**0.187**	**0.011**	**6.1**
1865 D	JB96-2A	*Vorticifex*	0.151	0.159				**0.155**	**0.006**	**3.6**
								0.185	**0.028**	**15.4**
1866 A	JB96-15A	*Vorticifex*	0.149	0.159				**0.154**	**0.007**	**4.6**
1866 D	JB96-15A	*Vorticifex*	0.161	0.158				**0.160**	**0.002**	**1.3**
1866 E	JB96-15A	*Vorticifex*	0.135	0.148				**0.142**	**0.009**	**6.5**
								0.152	**0.009**	**6.1**
1867 A	JB96-15D	*Vorticifex*	0.392	0.398				**0.395**	**0.004**	**1.1**
1867 B	JB96-15D	*Vorticifex*	0.364	0.346				**0.355**	**0.013**	**3.6**
1867 C	JB96-15D	*Vorticifex*	0.457	0.438				**0.448**	**0.013**	**3.0**
1867 D	JB96-15D	*Vorticifex*	0.449	0.395	0.350			**0.398**	**0.050**	**12.5**
1867 E	JB96-15D	*Vorticifex*	0.360	0.351				**0.356**	**0.006**	**1.8**
								0.390	**0.038**	**9.8**
1868 A	JB96-15G	*Vorticifex*	0.341	0.326				**0.334**	**0.011**	**3.2**
1868 B	JB96-15G	*Vorticifex*	0.356	0.339	0.354			**0.350**	**0.009**	**2.7**
1868 C	JB96-15G	*Vorticifex*	0.363	0.425				**0.394**	**0.044**	**11.1**
1868 D	JB96-15G	*Vorticifex*	0.428	0.437				**0.433**	**0.006**	**1.5**
1868 E	JB96-15G	*Vorticifex*	0.411	0.428				**0.420**	**0.012**	**2.9**
								0.386	**0.043**	**11.2**
1869 A	JB96-7A	*Physella*	0.858	0.816				**0.837**	**0.030**	**3.5**
1869 B	JB96-7A	*Physella*	0.915	0.901				**0.908**	**0.010**	**1.1**
1869 C	JB96-7A	*Physella*	0.702	0.877				**0.790**	**0.124**	**15.7**
1869 D	JB96-7A	*Physella*	0.904	0.879				**0.892**	**0.018**	**2.0**
								0.857	**0.054**	**6.3**
1921 A	JB96-32A	*Vorticifex*	0.242	0.241				**0.242**	**0.001**	**0.3**
1921 B	JB96-32A	*Vorticifex*	0.248	0.236	0.241			**0.242**	**0.006**	**2.5**
1921 C	JB96-32A	*Vorticifex*	0.236	0.231				**0.234**	**0.004**	**1.5**
1921 D	JB96-32A	*Vorticifex*	0.239	0.239				**0.239**	**0.000**	**0.0**
1921 E	JB96-32A	*Vorticifex*	0.211	0.203	0.208			**0.207**	**0.004**	**1.9**
								0.233	**0.015**	**6.2**
1922 B	JB96-31B	*Vorticifex*	0.152	0.156	0.161			**0.156**	**0.005**	**2.9**
1922 C	JB96-31B	*Vorticifex*	0.171	0.178	0.176			**0.175**	**0.004**	**2.1**

1922 D	JB96-31B	*Vorticifex*	0.122	0.126	0.126	**0.125**	**0.002**	**1.9**
1922 E	JB96-31B	*Vorticifex*	0.139	0.141	0.173	**0.151**	**0.019**	**12.6**
						0.152	**0.021**	**13.7**
1923 B	JB96-31B	*Amnicola*	0.253	0.248		**0.251**	**0.004**	**1.4**
1923 C	JB96-31B	*Amnicola*	0.247	0.248	0.247	**0.247**	**0.001**	**0.2**
1923 D	JB96-31B	*Amnicola*	0.242	0.260		**0.251**	**0.013**	**5.1**
1923 E	JB96-31B	*Amnicola*	0.236	0.225		**0.231**	**0.008**	**3.4**
						0.245	**0.010**	**4.0**
1924 A	JB96-31B	*Psidium*	0.300	0.293		**0.297**	**0.005**	**1.7**
1924 B	JB96-31B	*Psidium*	0.285	0.291		**0.288**	**0.004**	**1.5**
1924 C	JB96-31B	*Psidium*	0.290	0.285		**0.288**	**0.004**	**1.2**
1924 D	JB96-31B	*Psidium*	0.317	0.322		**0.320**	**0.004**	**1.1**
1924 E	JB96-31B	*Psidium*	0.297	0.312		**0.305**	**0.011**	**3.5**
						0.299	**0.013**	**4.5**
1927 A	JB96-1B	*Vorticifex*	0.190	0.187		**0.189**	**0.002**	**1.1**
1927 B	JB96-1B	*Vorticifex*	0.177	0.175		**0.176**	**0.001**	**0.8**
1927 D	JB96-1B	*Vorticifex*	0.170	0.166		**0.168**	**0.003**	**1.7**
1927 E	JB96-1B	*Vorticifex*	0.181	0.183		**0.182**	**0.001**	**0.8**
						0.179	**0.009**	**4.9**
1928 A	JB96-31A	*Vorticifex*	0.276	0.279		**0.278**	**0.002**	**0.8**
1928 B	JB96-31A	*Vorticifex*	0.267	0.253		**0.260**	**0.010**	**3.8**
1928 C	JB96-31A	*Vorticifex*	0.301	0.287		**0.294**	**0.010**	**3.4**
1928 D	JB96-31A	*Vorticifex*	0.273	0.268		**0.271**	**0.004**	**1.3**
1928 E	JB96-31A	*Vorticifex*	0.269	0.257		**0.263**	**0.008**	**3.2**
						0.273	**0.014**	**5.0**
1930 A	JB96-30A	*Vorticifex*	0.096	0.116		**0.106**	**0.014**	**13.3**
1930 B	JB96-30A	*Vorticifex*	0.088	0.095		**0.092**	**0.005**	**5.4**
1930 C	JB96-30A	*Vorticifex*	0.126	0.112		**0.119**	**0.010**	**8.3**
1930 D	JB96-30A	*Vorticifex*	0.119	0.089		**0.104**	**0.021**	**20.4**
						0.105	**0.011**	**10.7**
1931 A	JB96-30A	*Spherium*	0.109	0.122		**0.116**	**0.009**	**8.0**
1931 B	JB96-30A	*Spherium*	0.125	0.115		**0.120**	**0.007**	**5.9**
1931 C	JB96-30A	*Spherium*	0.115	0.122		**0.119**	**0.005**	**4.2**
1931 D	JB96-30A	*Spherium*	0.109	0.161		**0.135**	**0.037**	**27.2**
1931 E	JB96-30A	*Spherium*	0.112	0.121		**0.117**	**0.006**	**5.5**
						0.121	**0.008**	**6.6**
1933 A	JB96-26A	*Vorticifex*	0.362	0.362		**0.362**	**0.000**	**0.0**
1933 B	JB96-26A	*Vorticifex*	0.398	0.392		**0.395**	**0.004**	**1.1**
1933 C	JB96-26A	*Vorticifex*	0.461	0.440		**0.451**	**0.015**	**3.3**
1933 D	JB96-26A	*Vorticifex*	0.437	0.416		**0.427**	**0.015**	**3.5**
1933 E	JB96-26A	*Vorticifex*	0.382	0.377		**0.380**	**0.004**	**0.9**
						0.403	**0.036**	**8.9**
1935 A	JB96-27A	*Vorticifex*	0.301	0.282		**0.292**	**0.013**	**4.6**
1935 B	JB96-27A	*Vorticifex*	0.274	0.280		**0.277**	**0.004**	**1.5**
1935 C	JB96-27A	*Vorticifex*	0.236	0.240		**0.238**	**0.003**	**1.2**
1935 D	JB96-27A	*Vorticifex*	0.278	0.285		**0.282**	**0.005**	**1.8**

1935 E	JB96-27A	*Vorticifex*	0.257	0.268			**0.263**	**0.008**	**3.0**
							0.270	**0.021**	**7.7**
1936 A	JB96-29A	*Vorticifex*	0.069	0.069			**0.069**	**0.000**	**0.0**
1936 B	JB96-29A	*Vorticifex*	0.072	0.072			**0.072**	**0.000**	**0.0**
1936 C	JB96-29A	*Vorticifex*	0.074	0.074			**0.074**	**0.000**	**0.0**
							0.072	**0.003**	**3.5**
1937 A	JB96-6C	*Lymnaea*	0.442	0.447			**0.445**	**0.004**	**0.8**
1937 C	JB96-6C	*Lymnaea*	0.492	0.334			**0.413**	**0.112**	**27.1**
							0.429	**0.022**	**5.2**
1938 A	JB96-6C	*Vorticifex*	0.515	0.543			**0.529**	**0.020**	**3.7**
1938 B	JB96-6C	*Vorticifex*	0.399	0.400			**0.400**	**0.001**	**0.2**
1938 C	JB96-6C	*Vorticifex*	0.458	0.439			**0.449**	**0.013**	**3.0**
1938 D	JB96-6C	*Vorticifex*	0.418	0.433		*0.487*	**0.426**	**0.011**	**2.5**
1938 E	JB96-6C	*Vorticifex*	0.406	0.456	0.424		**0.429**	**0.025**	**5.9**
							0.446	**0.049**	**11.1**
1939 A	JB96-6B	*Vorticifex*	0.496	0.498			**0.497**	**0.001**	**0.3**
1939 B	JB96-6B	*Vorticifex*	0.462	0.450			**0.456**	**0.008**	**1.9**
1939 C	JB96-6B	*Vorticifex*	0.485	0.417	0.423		**0.442**	**0.038**	**8.5**
1939 D	JB96-6B	*Vorticifex*	0.504	0.478		*0.544*	**0.491**	**0.018**	**3.7**
							0.471	**0.027**	**5.7**
1941 A	JB96-3C	*Vorticifex*	0.128	0.126		*0.143*	**0.127**	**0.001**	**1.1**
1941 B	JB96-3C	*Vorticifex*	0.133	0.131			**0.132**	**0.001**	**1.1**
1941 C	JB96-3C	*Vorticifex*	0.113	0.115			**0.114**	**0.001**	**1.2**
1941 D	JB96-3C	*Vorticifex*	0.109	0.114			**0.112**	**0.004**	**3.2**
1941 E	JB96-3C	*Vorticifex*	0.133	0.129		*0.143*	**0.131**	**0.003**	**2.2**
							0.123	**0.010**	**7.9**
1942 A	JB96-3A	*Vorticifex*	0.125	0.127			**0.126**	**0.001**	**1.1**
1942 B	JB96-3A	*Vorticifex*	0.121	0.119			**0.120**	**0.001**	**1.2**
1942 C	JB96-3A	*Vorticifex*	0.119	0.118			**0.119**	**0.001**	**0.6**
1942 D	JB96-3A	*Vorticifex*	0.102	0.102			**0.102**	**0.000**	**0.0**
							0.117	**0.010**	**8.8**
1955 A	JB96-20A	*Vorticifex*	0.102	0.140			**0.121**	**0.027**	**22.2**
1955 B	JB96-20A	*Vorticifex*	0.089	0.080			**0.085**	**0.006**	**7.5**
1955 C	JB96-20A	*Vorticifex*	0.118	0.091			**0.105**	**0.019**	**18.3**
1955 D	JB96-20A	*Vorticifex*	0.130	0.131			**0.131**	**0.001**	**0.5**
1955 E	JB96-20A	*Vorticifex*	0.129	0.123			**0.126**	**0.004**	**3.4**
							0.113	**0.019**	**16.6**
1956 A	JB96-19A	*Amnicola*	0.077	0.116			**0.097**	**0.028**	**28.6**
1956 B	JB96-19A	*Amnicola*	0.066	0.071			**0.069**	**0.004**	**5.2**
1956 C	JB96-19A	*Amnicola*	0.057	0.062			**0.060**	**0.004**	**5.9**
1956 D	JB96-19A	*Amnicola*	0.069	0.071			**0.070**	**0.001**	**2.0**
1956 E	JB96-19A	*Amnicola*	0.050	0.051			**0.051**	**0.001**	**1.4**
							0.069	**0.017**	**25.0**
1957 A	JB96-19A	*Vorticifex*	0.037	0.037			**0.037**	**0.000**	**0.0**
1957 B	JB96-19A	*Vorticifex*	0.091	0.090			**0.091**	**0.001**	**0.8**

1957 C	JB96-19A	*Vorticifex*	0.086	0.087			**0.087**	**0.001**	**0.8**
1957 D	JB96-19A	*Vorticifex*	0.028	0.027			**0.028**	**0.001**	**2.6**
1957 E	JB96-19A	*Vorticifex*	0.064	0.043			**0.054**	**0.015**	**27.8**
							0.059	**0.029**	**48.3**
1958 B	JB96-18A	*Vorticifex*	0.090	0.095			**0.093**	**0.004**	**3.8**
1958 C	JB96-18A	*Vorticifex*	0.124	0.130			**0.127**	**0.004**	**3.3**
							0.110	**0.024**	**22.2**
1960 A	JB96-17A	*Vorticifex*	0.087	0.083			**0.085**	**0.003**	**3.3**
1960 B	JB96-17A	*Vorticifex*	0.067	0.064			**0.066**	**0.002**	**3.2**
1960 D	JB96-17A	*Vorticifex*	0.060	0.052			**0.056**	**0.006**	**10.1**
1960 E	JB96-17A	*Vorticifex*	0.064	0.069			**0.067**	**0.004**	**5.3**
							0.068	**0.012**	**17.8**
1961 A	JB96-16A	*Vorticifex*	0.155	0.177	0.172		**0.168**	**0.012**	**6.9**
1961 B	JB96-16A	*Vorticifex*	0.176	0.174			**0.175**	**0.001**	**0.8**
1961 C	JB96-16A	*Vorticifex*	0.159	0.157			**0.158**	**0.001**	**0.9**
							0.167	**0.009**	**5.1**
1962 A	JB96-10B	*Vorticifex*	0.184	0.188			**0.186**	**0.003**	**1.5**
1962 B	JB96-10B	*Vorticifex*	0.177	0.181			**0.179**	**0.003**	**1.6**
1962 C	JB96-10B	*Vorticifex*	0.152	0.159			**0.156**	**0.005**	**3.2**
1962 E	JB96-10B	*Vorticifex*	0.163	0.163			**0.163**	**0.000**	**0.0**
							0.171	**0.014**	**8.2**
1966 A	JB96-1E	*Vorticifex*	0.158	0.157			**0.158**	**0.001**	**0.4**
1966 B	JB96-1E	*Vorticifex*	0.174	0.175			**0.175**	**0.001**	**0.4**
1966 C	JB96-1E	*Vorticifex*	0.192	0.195			**0.194**	**0.002**	**1.1**
1966 D	JB96-1E	*Vorticifex*	0.222	0.216			**0.219**	**0.004**	**1.9**
1966 E	JB96-1E	*Vorticifex*	0.206	0.208			**0.207**	**0.001**	**0.7**
							0.190	**0.025**	**13.0**
1967 B	JB96-1D	*Vorticifex*	0.221	0.199	0.215		**0.212**	**0.011**	**5.4**
1967 C	JB96-1D	*Vorticifex*	0.256	0.263			**0.260**	**0.005**	**1.9**
1967 D	JB96-1D	*Vorticifex*	0.275	0.302	0.282		**0.286**	**0.014**	**4.9**
1967 E	JB96-1D	*Vorticifex*	0.254	0.249			**0.252**	**0.004**	**1.4**
							0.252	**0.031**	**12.2**
1968 A	JB96-1C	*Vorticifex*	0.190	0.229	0.195	0.182	**0.199**	**0.021**	**10.4**
1968 B	JB96-1C	*Vorticifex*	0.209	0.213	0.209		**0.210**	**0.002**	**1.1**
1968 C	JB96-1C	*Vorticifex*	0.208	0.210	0.202		**0.207**	**0.004**	**2.0**
1968 D	JB96-1C	*Vorticifex*	0.211	0.226			**0.219**	**0.011**	**4.9**
1968 E	JB96-1C	*Vorticifex*	0.216	0.216			**0.216**	**0.000**	**0.0**
							0.210	**0.008**	**3.7**
1975 A	JB96-1A	*Vorticifex*	0.177	0.153	0.198		**0.176**	**0.023**	**12.8**
1975 C	JB96-1A	*Vorticifex*	0.183	0.177			**0.180**	**0.004**	**2.4**
1975 D	JB96-1A	*Vorticifex*	0.160	0.159			**0.160**	**0.001**	**0.4**
1975 E	JB96-1A	*Vorticifex*	0.151	0.146	0.148		**0.148**	**0.003**	**1.7**
							0.166	**0.015**	**8.9**
1976 A	JB96-25C	*Lymnaea*	0.216	0.206			**0.211**	**0.007**	**3.4**
1976 B	JB96-25C	*Lymnaea*	0.253	0.251	0.262		**0.255**	**0.006**	**2.3**

1976 C	JB96-25C	*Lymnaea*	0.236	0.242	0.247			**0.242**	**0.006**	**2.3**
1976 D	JB96-25C	*Lymnaea*	0.182	0.172	0.187			**0.180**	**0.008**	**4.2**
1976 E	JB96-25C	*Lymnaea*	0.227	0.218	0.232			**0.226**	**0.007**	**3.1**
								0.223	**0.029**	**13.0**
1977 A	JB96-23B	*Vorticifex*	0.231	0.231			*0.137*	**0.231**	**0.000**	**0.0**
1977 B	JB96-23B	*Vorticifex*	0.217	0.222			*0.174*	**0.220**	**0.004**	**1.6**
1977 C	JB96-23B	*Vorticifex*	0.186	0.192			*0.157*	**0.189**	**0.004**	**2.2**
1977 D	JB96-23B	*Vorticifex*	0.183	0.194			*0.178*	**0.189**	**0.008**	**4.1**
1977 E	JB96-23B	*Vorticifex*	0.207	0.208			*0.186*	**0.208**	**0.001**	**0.3**
								0.207	**0.019**	**9.0**
1978 A	JB96-14A	*Amnicola*	0.048	0.048				**0.048**	**0.000**	**0.0**
1978 B	JB96-14A	*Amnicola*	0.045	0.046				**0.046**	**0.001**	**1.6**
1978 C	JB96-14A	*Amnicola*	0.110	0.106				**0.108**	**0.003**	**2.6**
1978 D	JB96-14A	*Amnicola*	0.079	0.078				**0.079**	**0.001**	**0.9**
1978 E	JB96-14A	*Amnicola*	0.104	0.103				**0.104**	**0.001**	**0.7**
								0.077	**0.030**	**38.6**
2091 A	JB96-23A	*Vorticifex*	0.210	0.229	0.200		*0.075*	**0.213**	**0.015**	**6.9**
2091 B	JB96-23A	*Vorticifex*	0.192	0.194	0.207			**0.198**	**0.008**	**4.1**
2091 C	JB96-23A	*Vorticifex*	0.196	0.179	0.164	0.185		**0.181**	**0.013**	**7.4**
2091 D	JB96-23A	*Vorticifex*	0.183	0.218	0.161	0.187		**0.187**	**0.023**	**12.5**
2091 E	JB96-23A	*Vorticifex*	0.179	0.182	0.184			**0.182**	**0.003**	**1.4**
								0.192	**0.013**	**7.0**
2092 B	JB96-25B	*Planorbella*	0.076	0.077				**0.077**	**0.001**	**0.9**
2092 C	JB96-25B	*Planorbella*	0.109	0.082	0.091			**0.094**	**0.014**	**14.6**
2092 D	JB96-25B	*Planorbella*	0.102	0.102	0.098			**0.101**	**0.002**	**2.3**
2092 E	JB96-25B	*Planorbella*	0.086	0.079	0.079			**0.081**	**0.004**	**5.0**
								0.088	**0.011**	**12.7**
2093 A	JB96-4A	*Vorticifex*	0.256	0.396	0.336			**0.329**	**0.070**	**21.3**
2093 B	JB96-4A	*Vorticifex*	0.312	0.312				**0.312**	**0.000**	**0.0**
2093 C	JB96-4A	*Vorticifex*	0.296	0.327				**0.312**	**0.022**	**7.0**
2093 D	JB96-4A	*Vorticifex*	0.321	0.354				**0.338**	**0.023**	**6.9**
2093 E	JB96-4A	*Vorticifex*	0.304	0.330				**0.317**	**0.018**	**5.8**
								0.321	**0.011**	**3.6**
2094 A	JB96-29A	*Spherium*	0.108	0.109				**0.109**	**0.001**	**0.7**
2094 B	JB96-29A	*Spherium*	0.071	0.081	0.077			**0.076**	**0.005**	**6.6**
2094 C	JB96-29A	*Spherium*	0.054	0.054	0.049			**0.052**	**0.003**	**5.5**
2094 D	JB96-29A	*Spherium*	0.055	0.052				**0.054**	**0.002**	**4.0**
								0.073	**0.026**	**36.2**
2165 B	JB97-10A	*Vorticifex*	0.115	0.122				**0.119**	**0.005**	**4.2**
2165 C	JB97-10A	*Vorticifex*	0.097	0.098				**0.098**	**0.001**	**0.7**
2165 D	JB97-10A	*Vorticifex*	0.094	0.096				**0.095**	**0.001**	**1.5**
2165 E	JB97-10A	*Vorticifex*	0.111	0.112				**0.112**	**0.001**	**0.6**
								0.106	**0.011**	**10.6**
2166 A	JB97-1C	*Vorticifex*	0.153	0.155				**0.154**	**0.001**	**0.9**
2166 B	JB97-1C	*Vorticifex*	0.154	0.144				**0.149**	**0.007**	**4.7**
2166 D	JB97-1C	*Vorticifex*	0.136	0.151	0.159			**0.149**	**0.012**	**7.9**

2166 E	JB97-1C	*Vorticifex*	0.161	0.166		**0.164**	**0.004**	**2.2**
						0.154	**0.007**	**4.5**
2167 A	JB97-1D	*Vorticifex*	0.185	0.190		**0.188**	**0.004**	**1.9**
2167 B	JB97-1D	*Vorticifex*	0.188	0.189		**0.189**	**0.001**	**0.4**
2167 C	JB97-1D	*Vorticifex*	0.182	0.183		**0.183**	**0.001**	**0.4**
2167 E	JB97-1D	*Vorticifex*	0.168	0.173		**0.171**	**0.004**	**2.1**
						0.182	**0.008**	**4.5**
2168 A	JB97-15A	*Vorticifex*	0.095	0.094		**0.095**	**0.001**	**0.7**
2168 B	JB97-15A	*Vorticifex*	0.141	0.133		**0.137**	**0.006**	**4.1**
2168 C	JB97-15A	*Vorticifex*	0.109	0.115		**0.112**	**0.004**	**3.8**
						0.115	**0.021**	**18.7**
2169 A	JB97-15B	*Vorticifex*	0.114	0.109		**0.112**	**0.004**	**3.2**
2169 B	JB97-15B	*Vorticifex*	0.118	0.114		**0.116**	**0.003**	**2.4**
2169 C	JB97-15B	*Vorticifex*	0.101	0.097		**0.099**	**0.003**	**2.9**
2169 D	JB97-15B	*Vorticifex*	0.111	0.104		**0.108**	**0.005**	**4.6**
2169 E	JB97-15B	*Vorticifex*	0.132	0.132		**0.132**	**0.000**	**0.0**
						0.113	**0.012**	**10.8**
2177 A	JB97-15C	*Vorticifex*	0.123	0.151	0.133	**0.136**	**0.014**	**10.5**
2177 B	JB97-15C	*Vorticifex*	0.115	0.116		**0.116**	**0.001**	**0.6**
2177 C	JB97-15C	*Vorticifex*	0.153	0.156		**0.155**	**0.002**	**1.4**
2177 D	JB97-15C	*Vorticifex*	0.143	0.146		**0.145**	**0.002**	**1.5**
2177 E	JB97-15C	*Vorticifex*	0.084	0.083		**0.084**	**0.001**	**0.8**
						0.127	**0.028**	**22.2**
2178 A	JB97-15D	*Vorticifex*	0.232	0.229		**0.231**	**0.002**	**0.9**
2178 B	JB97-15D	*Vorticifex*	0.277	0.280		**0.279**	**0.002**	**0.8**
2178 C	JB97-15D	*Vorticifex*	0.324	0.326		**0.325**	**0.001**	**0.4**
						0.278	**0.047**	**17.0**
2179 A	JB97-15E	*Lymnaea*	0.358	0.340		**0.349**	**0.013**	**3.6**
2179 B	JB97-15E	*Vorticifex*	0.429	0.405		**0.417**	**0.017**	**4.1**
2179 C	JB97-15E	*Vorticifex*	0.340	0.332		**0.336**	**0.006**	**1.7**
2179 D	JB97-15E	*Vorticifex*	0.372	0.374		**0.373**	**0.001**	**0.4**
2179 E	JB97-15E	*Vorticifex*	0.364	0.366		**0.365**	**0.001**	**0.4**
						0.368	**0.031**	**8.4**
2180 A	JB97-7H	*Physa*	0.833	0.826		**0.830**	**0.005**	**0.6**
2180 B	JB97-7H	*Physa*	0.885	0.900		**0.893**	**0.011**	**1.2**
2180 C	JB97-7H	*Physa*	0.678	0.720		**0.699**	**0.030**	**4.2**
						0.807	**0.099**	**12.2**
2181 A	JB97-6A	*Vorticifex*	0.423	0.444	0.448	**0.438**	**0.013**	**3.1**
2181 B	JB97-6A	*Vorticifex*	0.466	0.496	0.515	**0.492**	**0.025**	**5.0**
2181 C	JB97-6A	*Vorticifex*	0.463	0.502	0.516	**0.494**	**0.027**	**5.6**
2181 D	JB97-6A	*Vorticifex*	0.400	0.415	0.422	**0.412**	**0.011**	**2.7**
2181 E	JB97-6A	*Vorticifex*	0.430	0.466	0.473	**0.456**	**0.023**	**5.1**
						0.459	**0.035**	**7.7**
2182 A	JB97-6B	*Vorticifex*	0.475	0.480		**0.478**	**0.004**	**0.7**
2182 B	JB97-6B	*Vorticifex*	0.460	0.458		**0.459**	**0.001**	**0.3**

2182 C	JB97-6B	*Vorticifex*	0.471	0.470		**0.471**	**0.001**	**0.2**
2182 D	JB97-6B	*Vorticifex*	0.426	0.442		**0.434**	**0.011**	**2.6**
						0.460	**0.019**	**4.1**
2183 A	JB97-6B	*Lymnaea*	0.466	0.470		**0.468**	**0.003**	**0.6**
2183 B	JB97-6B	*Lymnaea*	0.512	0.542	0.493	**0.516**	**0.025**	**4.8**
2183 C	JB97-6B	*Lymnaea*	0.448	0.490	0.429	**0.456**	**0.031**	**6.9**
						0.480	**0.032**	**6.6**
2184 A	JB97-6C	*Lymnaea*	0.433	0.430		**0.432**	**0.002**	**0.5**
2184 B	JB97-6C	*Lymnaea*	0.461	0.475		**0.468**	**0.010**	**2.1**
2184 C	JB97-6C	*Lymnaea*	0.518	0.500		**0.509**	**0.013**	**2.5**
2184 D	JB97-6C	*Lymnaea*	0.414	0.401		**0.408**	**0.009**	**2.3**
2184 E	JB97-6C	*Lymnaea*	0.467	0.585	0.467	**0.506**	**0.068**	**13.5**
						0.464	**0.045**	**9.7**
2185 A	JB97-7A	*Amnicola*	0.404	0.461	0.406	**0.424**	**0.032**	**7.6**
2185 B	JB97-7A	*Amnicola*	0.653	0.560	0.720	**0.644**	**0.080**	**12.5**
2185 C	JB97-7A	*Amnicola*	0.597	0.555	0.577	**0.576**	**0.021**	**3.6**
						0.548	**0.113**	**20.6**
2189 A	JB97-7A	*Physa*	0.772	0.671	0.805	**0.749**	**0.070**	**9.3**
2189 B	JB97-7A	*Physa*	0.782	0.682	0.664	**0.709**	**0.064**	**9.0**
2189 C	JB97-7A	*Amnicola*	0.847	0.843		**0.845**	**0.003**	**0.3**
2189 D	JB97-7A	*Amnicola*	0.758	0.761		**0.760**	**0.002**	**0.3**
						0.766	**0.057**	**7.5**
2190 A	JB97-7E	*Physa*	0.806	0.842		**0.824**	**0.025**	**3.1**
2190 B	JB97-7E	*Physa*	0.816	0.790		**0.803**	**0.018**	**2.3**
2190 C	JB97-7E	*Physa*	0.803	0.840		**0.822**	**0.026**	**3.2**
2190 D	JB97-7E	*Physa*	0.811	0.852		**0.832**	**0.029**	**3.5**
						0.820	**0.012**	**1.5**
2191 A	JB97-11A	*Vorticifex*	0.126	0.135		**0.131**	**0.006**	**4.9**
2191 B	JB97-11A	*Vorticifex*	0.124	0.126		**0.125**	**0.001**	**1.1**
2191 C	JB97-11A	*Vorticifex*	0.123	0.125		**0.124**	**0.001**	**1.1**
2191 D	JB97-11A	*Vorticifex*	0.118	0.126		**0.122**	**0.006**	**4.6**
2191 E	JB97-11A	*Vorticifex*	0.127	0.130		**0.129**	**0.002**	**1.7**
						0.126	**0.003**	**2.7**
2192 A	JB97-12A	*Vorticifex*	0.172	0.168		**0.170**	**0.003**	**1.7**
2192 B	JB97-12A	*Vorticifex*	0.154	0.172		**0.163**	**0.013**	**7.8**
2192 C	JB97-12A	*Vorticifex*	0.166	0.190		**0.178**	**0.017**	**9.5**
2192 D	JB97-12A	*Vorticifex*	0.173	0.199		**0.186**	**0.018**	**9.9**
2192 E	JB97-12A	*Vorticifex*	0.161	0.214		**0.188**	**0.037**	**20.0**
						0.177	**0.010**	**5.9**
2193 A	JB97-12B	*Vorticifex*	0.153	0.157		**0.155**	**0.003**	**1.8**
2193 B	JB97-12B	*Vorticifex*	0.139	0.141		**0.140**	**0.001**	**1.0**
2193 C	JB97-12B	*Vorticifex*	0.145	0.141		**0.143**	**0.003**	**2.0**
2193 D	JB97-12B	*Vorticifex*	0.131	0.121		**0.126**	**0.007**	**5.6**
2193 E	JB97-12B	*Vorticifex*	0.141	0.137		**0.139**	**0.003**	**2.0**
						0.141	**0.010**	**7.4**

2194 A	JB97-22A	*Vorticifex*	0.111	0.121				**0.116**	**0.007**	**6.1**
2194 B	JB97-22A	*Vorticifex*	0.121	0.138				**0.130**	**0.012**	**9.3**
2194 C	JB97-22A	*Vorticifex*	0.121	0.128				**0.125**	**0.005**	**4.0**
2194 D	JB97-22A	*Vorticifex*	0.122	0.123				**0.123**	**0.001**	**0.6**
2194 E	JB97-22A	*Vorticifex*	0.102	0.096				**0.099**	**0.004**	**4.3**
								0.118	**0.012**	**10.0**
2195 A	JB97-5A	*Vorticifex*	0.349	0.292	0.353	0.242	*0.348*	**0.309**	**0.053**	**17.0**
2195 B	JB97-5A	*Vorticifex*	0.317	0.298	0.266	0.318		**0.300**	**0.024**	**8.1**
2195 C	JB97-5A	*Vorticifex*	0.325	0.285	0.289			**0.300**	**0.022**	**7.4**
2195 D	JB97-5A	*Vorticifex*	0.320	0.307	0.292			**0.306**	**0.014**	**4.6**
2195 E	JB97-5A	*Vorticifex*	0.248	0.294	0.287			**0.276**	**0.025**	**9.0**
								0.298	**0.013**	**4.3**
2196 A	JB97-8A	*Vorticifex*	0.517	0.527				**0.522**	**0.007**	**1.4**
2196 B	JB97-8A	*Vorticifex*	0.461	0.493	0.459			**0.471**	**0.019**	**4.1**
2196 C	JB97-8A	*Vorticifex*	0.535	0.600	0.529			**0.555**	**0.039**	**7.1**
								0.461	**0.114**	**24.7**
2197 A	JB97-10A	*Vorticifex*	0.113	0.115				**0.114**	**0.001**	**1.2**
2197 B	JB97-10A	*Vorticifex*	N/D	N/D						
2197 C	JB97-10A	*Vorticifex*	N/D	N/D						
2197 D	JB97-10A	*Vorticifex*	0.054	0.055				**0.055**	**0.001**	**1.3**
2197 E	JB97-10A	*Vorticifex*	0.171	0.133	0.135			**0.146**	**0.021**	**14.6**
								0.105	**0.047**	**44.4**
2198 A	JB97-10B	*Vorticifex*	0.148	0.141				**0.145**	**0.005**	**3.4**
2198 B	JB97-10B	*Vorticifex*	0.140	0.140				**0.140**	**0.000**	**0.0**
2198 C	JB97-10B	*Vorticifex*	0.120	0.119				**0.120**	**0.001**	**0.6**
2198 D	JB97-10B	*Vorticifex*	0.110	0.110				**0.110**	**0.000**	**0.0**
2198 E	JB97-10B	*Vorticifex*	0.118	0.125				**0.122**	**0.005**	**4.1**
								0.127	**0.015**	**11.5**
2199 A	JB97-24C	*Vorticifex*	0.126	0.124				**0.125**	**0.001**	**1.1**
2199 B	JB97-24C	*Vorticifex*	0.157	0.133	0.128			**0.139**	**0.016**	**11.1**
2199 C	JB97-24C	*Vorticifex*	0.133	0.131				**0.132**	**0.001**	**1.1**
2199 D	JB97-24C	*Vorticifex*	0.142	0.131				**0.137**	**0.008**	**5.7**
2199 E	JB97-24C	*Vorticifex*	0.104	0.101				**0.103**	**0.002**	**2.1**
								0.127	**0.015**	**11.6**
2200 A	JB97-21B	*Vorticifex*	0.061	0.068	0.063			**0.064**	**0.004**	**5.6**
2200 B	JB97-21B	*Vorticifex*	0.080	0.081				**0.081**	**0.001**	**0.9**
2200 C	JB97-21B	*Vorticifex*	0.247	0.254				**0.251**	**0.005**	**2.0**
2200 D	JB97-21B	*Vorticifex*	0.093	0.095				**0.094**	**0.001**	**1.5**
2200 E	JB97-21B	*Vorticifex*	0.092	0.094				**0.093**	**0.001**	**1.5**
								0.083	**0.014**	**16.9**
2201 A	JB97-24A	*Amnicola*	0.111	0.108				**0.110**	**0.002**	**1.9**
2201 B	JB97-24A	*Amnicola*	0.094	0.091				**0.093**	**0.002**	**2.3**
2201 C	JB97-24A	*Amnicola*	0.110	0.110				**0.110**	**0.000**	**0.0**
2201 D	JB97-24A	*Amnicola*	0.114	0.113				**0.114**	**0.001**	**0.6**
2201 E	JB97-24A	*Amnicola*	0.093	0.088				**0.091**	**0.004**	**3.9**
								0.102	**0.012**	**11.5**

2202 A	JB97-9A	*Vorticifex*	0.187	0.173		**0.180**	**0.010**	**5.5**
2202 B	JB97-9A	*Vorticifex*	0.175	0.190		**0.183**	**0.011**	**5.8**
2202 C	JB97-9A	*Vorticifex*	0.191	0.190		**0.191**	**0.001**	**0.4**
2202 D	JB97-9A	*Vorticifex*	0.161	0.166		**0.164**	**0.004**	**2.2**
2202 E	JB97-9A	*Vorticifex*	0.193	0.188		**0.191**	**0.004**	**1.9**
						0.179	**0.011**	**6.3**
2203 A	JB97-21A	*Vorticifex*	0.122	0.112		**0.117**	**0.007**	**6.0**
2203 B	JB97-21A	*Vorticifex*	0.109	0.114		**0.112**	**0.004**	**3.2**
2203 C	JB97-21A	*Vorticifex*	0.106	0.116		**0.111**	**0.007**	**6.4**
2203 D	JB97-21A	*Vorticifex*	0.110			**0.110**		
2203 E	JB97-21A	*Vorticifex*	0.113	0.116		**0.115**	**0.002**	**1.9**
						0.113	**0.003**	**2.8**
2204 A	JB97-21A	*Physa*	0.070	0.075		**0.073**	**0.004**	**4.9**
2204 B	JB97-21A	*Physa*	0.090	0.091		**0.091**	**0.001**	**0.8**
2204 C	JB97-21A	*Physa*	0.091	0.090		**0.091**	**0.001**	**0.8**
2204 D	JB97-21A	*Physa*	0.100	0.097		**0.099**	**0.002**	**2.2**
2204 E	JB97-21A	*Physa*	0.072	0.074		**0.073**	**0.001**	**1.9**
						0.084	**0.013**	**15.5**
2205 A	JB97-21A	*Amnicola*	0.131	0.128		**0.130**	**0.002**	**1.6**
2205 B	JB97-21A	*Amnicola*	0.135	0.137		**0.136**	**0.001**	**1.0**
2205 C	JB97-21A	*Amnicola*	0.124	0.123		**0.124**	**0.001**	**0.6**
2205 D	JB97-21A	*Amnicola*	0.112	0.114		**0.113**	**0.001**	**1.3**
2205 E	JB97-21A	*Amnicola*	0.127	0.129		**0.128**	**0.001**	**1.1**
						0.127	**0.010**	**7.7**
2206 A	JB97-21B	*Physa*	0.065	0.060		**0.063**	**0.004**	**5.7**
2206 B	JB97-21B	*Physa*	0.079	0.082		**0.081**	**0.002**	**2.6**
2206 C	JB97-21B	*Physa*	0.059	0.066		**0.063**	**0.005**	**7.9**
2206 D	JB97-21B	*Physa*	0.076	0.078	*0.122*	**0.077**	**0.001**	**1.8**
2206 E	JB97-21B	*Physa*	0.061	0.065		**0.063**	**0.003**	**4.5**
						0.071	**0.009**	**13.2**
2207 A	JB97-21B	*Amnicola*	0.159	0.163		**0.161**	**0.003**	**1.8**
2207 A	JB97-21B	*Amnicola*	0.118	0.115		**0.117**	**0.002**	**1.8**
2207 C	JB97-21B	*Amnicola*	0.153	0.160		**0.157**	**0.005**	**3.2**
2207 D	JB97-21B	*Amnicola*	0.138	0.141		**0.140**	**0.002**	**1.5**
2207 E	JB97-21B	*Amnicola*	0.193	0.194		**0.194**	**0.001**	**0.4**
						0.153	**0.033**	**21.5**
2208 A	JB97-24B	*Amnicola*	0.123	0.129		**0.126**	**0.004**	**3.4**
2208 B	JB97-24B	*Amnicola*	0.117	0.119		**0.118**	**0.001**	**1.2**
2208 C	JB97-24B	*Amnicola*	0.149	0.143		**0.146**	**0.004**	**2.9**
2208 D	JB97-24B	*Amnicola*	0.135	0.137		**0.136**	**0.001**	**1.0**
						0.132	**0.012**	**9.2**

*Italicized numbers indicate ratios not used for this study